AN INVESTIGATION OF ACOUSTICAL EFFECTS ON THE LOW HEAT-FLUX REGION OF NUCLEATE POOL BOILING

By

KAM WU LI

Bachelor of Science in Mechanical Engineering
Chu Hai College
Hong Kong
1957

Master of Mechanical Engineering
Colorado State University
Fort Collins, Colorado
1961

Submitted to the Faculty of the Graduate School of
the Oklahoma State University
in partial fulfillment of the requirements
for the degree of
DOCTOR OF PHILOSOPHY
May, 1965

AN INVESTIGATION OF ACOUSTICAL EFFECTS ON THE LOW HEAT-FLUX REGION OF NUCLEATE POOL BOILING

Thesis Approved:

Gerald D. Parker
Thesis Adviser

D. R. Haworth

G. W. Gumaer

Robert Hultgren

J. H. Boggs
Dean of the Graduate School

ACKNOWLEDGEMENT

The author wishes to express his deep gratitude to the National Aeronautics and Space Administration for the financial assistance without which this work would not have been completed.

The author also appreciates the fact that he has been financially supported by the School of Mechanical Engineering, while doing his doctoral study at Oklahoma State University.

The guidance and instructive assistance of his adviser, Dr. Jerald D. Parker, are sincerely appreciated. Thanks are also due to Dr. Richard L. Lowery and Professor Faye C. McQuiston for their invaluable counsel in the present study. A special mention should be given to Mr. O'Neill Burchett who gave many suggestions in the construction and operation problems. The services of Mr. J. A. McCandless and Mr. G. M. Cooper, the laboratory technicians, are greatly acknowledged. The author would also like to express his appreciation to Mrs. Betty Stewart for her careful typing of this thesis.

Finally, the author is appreciative of the opportunity that he was given to study and to pursue a career of his own choice in this country, the United States of America.

TABLE OF CONTENTS

LIST OF FIGURES

LIST OF TABLES

CHAPTER I

INTRODUCTION

During the last two decades, the industrial application of acoustical energy has stimulated a great interest among engineers and much progress has been made. For applications such as flaw detection, thickness gauging, agglomeration of aerosols, cleaning of small metals parts, cutting and grinding, acoustical energy has been successfully applied on a commercial scale. There are also many other applications which are still in the research stage.

A primary interest to thermal engineers is the effect of acoustical energy upon heat transfer rates. Some research has been carried out to determine how the mechanical or acoustical vibration affects the heat transfer in convection. Generally speaking, the present knowledge in this field is limited and still mostly in the experimental stage. The mechanism of interaction between acoustical vibration and heat transfer by convection is still not thoroughly understood. The general mathematical equations relating to acoustical vibration and heat transfer are still not completely solved.

An investigation of the effects of acoustical energy on nucleate boiling has a practical significance. It seems, however, that there has been very little work done in this area since Isacoff's work (1)[1]

[1]Numbers in parentheses refer to sources listed in the bibliography.

was published in 1956. Isacoff indicated that there is a pronounced effect of acoustical energy on the critical heat flux in nucleate boiling. However, there are some problems yet to be answered and investigated. These are, for example, how would the variation of acoustical power under a certain frequency affect the heat transfer rate in the low heat flux region of nucleate boiling and the incipient point of boiling. It is the objectives of this investigation, therefore, to cast some light on this area and also to find out whether there exists a critical value of acoustical power at a certain frequency beyond which the heat transfer rate would not be altered and whether the surface temperature of the heater can be reduced in the presence of a sound field while the heat transfer rate remains constant.

This investigation may help to further the application of acoustical energy in nucleate boiling. It is also hoped that the results of this work would lead to a better understanding of the mechanism of nucleate boiling which is still one of the unsolved problems in this field.

CHAPTER II

LITERATURE SURVEY

Very little information has been found in the literature about the effects of acoustic waves on boiling heat transfer. This literature survey, therefore, includes some background material which will be useful to the present investigation. The materials presented here represent the published information on nucleate boiling heat transfer and the effects of acoustic waves on convective heat transfer and nucleate boiling.

Nucleate Boiling Heat Transfer

In general, boiling heat transfer can be classified as follows:

A. According to the liquid bulk temperature

1. subcooled liquid boiling
2. superheated liquid boiling
3. saturated liquid boiling

B. According to the relative motion between liquid and heating surface

1. pool boiling (boiling without forced convection)
2. boiling with forced convection

C. According to the mechanism of heat transfer between liquid and heating surface

1. nucleate boiling
2. transitional boiling
3. film boiling

D. According to the method of heat supply

1. surface-heated boiling
2. volume-heated boiling

Ever since 1934 when Shiro Nukigama (2) published his famous paper, there has been much research work carried out in this field. The development of this subject is characterized by the fact that the experimental investigation always preceeds the analytical. So far, the analytical attacks have not been completely successful. In this part of the literature survey, more attention is directed to the analytical aspect. It is also restricted to the nucleate boiling from a submerged heater.

Some Factors Affecting the Nucleate Boiling Heat Transfer

Various factors affecting the nucleate boiling heat transfer have been found experimentally by many investigators and have been excellently summarized by Westwater (3). For completeness, these factors are listed in the following:

1. Properties of liquid
2. Properties of heating surface
3. Surface conditions
4. Geometric arrangement of the heating surface
5. Pressure in the system
6. Surface tension of liquid
7. Degree of agitation
8. Impurities in liquid
9. Short-wave irradiation

It should be noticed that some of these effects are only qualitatively understood. Much work, both experimental and analytical, still needs to be done before a complete picture of nucleate boiling can be formed.

Mechanism of Nucleate Boiling

In a study of the mechanism of nucleate boiling, Jakob (4) stated that two conditions must be fulfilled before the vapor bubble formation on the heating surface can occur. That is, the liquid surrounding the heating surface must be superheated and nuclei must exist, for instance,

some tiny gas bubbles or small solid particles. It was found that only a small portion of the heat produced by the heating surface is directly transferred to the bubbles themselves, while the larger part of heat is transferred to the liquid. The agitation or microconvection produced by these vapor bubbles is mainly responsible for the high heat transfer rate in nucleate boiling.

Rohsenow and Clark (5) carried out a series of experiments with the aid of a high-speed camera on surface boiling with forced convection. It was found that the bubbles themselves are insiginificant carriers of energy, if compared with the total energy introduced by the heating surface. The high heat transfer rate obtained in their experiments can be explained as follows: the bubbles are generated from the heating surface and then produce a strong agitation in the quiescent regions of liquid adjacent to the heating surface. It is these strong agitations which cause an increase in the heat transfer rate.

Gunther and Kreith (6) conducted a photographic study of bubbles formation in heat transfer to subcooled water and showed that the latent heat transport accounts for only 2 per cent of the total heat flux. Also the pictures indicated that there exists a vigorous circulation pattern in both the horizontal and vertical directions. Obviously their experimental results support the mechanism of nucleate boiling proposed by Rohsenow and Clark.

Although the microconvection model, or so-called stirring mechanism, has been widely accepted, there is still a lack of some conclusive evidences to prove this hypothesis as stated by Sabersky and Snyder (7). Forster and Greif (8) pointed out that the microconvection model is

incompatible with some experimental findings because it fails to yield an explanation for the insensitivity of boiling heat flux to the level of subcooling, and also for the effect of forced convection on nucleate boiling.

Edward (9) proposed a mechanism of mass transfer. He stated that although the heat flux carried by latent heat is quite small, this heat flux can be increased by assuming additional heat flux through the bubbles by mass transfer. However, this proposed mechanism, as mentioned by Snyder (7), has not been verified experimentally. In general, it is not widely accepted.

Sabersky and Mulligan (10) suggested another mechanism for nucleate boiling with forced convection. By this mechanism, the bubble would increase the heat transfer rate and pressure drop in the same manner as the roughness of surface. Again Forster and Grief (8) pointed out that the result predicted by this mechanism is not in agreement with the experimental findings.

To explain a remarkable increase in the heat transfer rate for nucleate boiling, the vapor-liquid exchange mechanism was proposed by Forster and Grief (8). They considered that, in addition to the latent heat transport, the bubbles also transfer heat during their growth by pushing a quantity of hot liquid from the heating surface into the cooler region and during their collapse by bringing a volume of cold liquid into contact with the heating surface. Based upon this concept, they arrived at an equation for the heat transfer rate in nucleate boiling as shown later. Forster and Grief claimed that this vapor-liquid exchange mechanism can explain why they boiling heat flux is

insensitive to the level of subcooling and why the boiling heat flux remains insensitive to the degree of forced convection.

Zuber (11) took a new approach to the problem of nucleate boiling. Supported by various investigators (12, 13, 14), he conceived that there are two regions in nucleate boiling. The first is called the region of isolated bubbles where the active site density is small and no interference among bubbles would occur. This region corresponds to low heat flux. As the heat transfer rate is increased, the process of vapor removal from the heating surface changes from an intermittent to a continuous one as the isolated bubbles change to continuous vapor columns. In the second region, the site density is large if compared with that in the first region, and the mutual influence between bubbles becomes significant as the critical condition is approached. This "two-regions" concept is very important, because it indicates that there is so much difference in these two regions that a single analytical model can hardly describe the entire nucleate boiling process.

In his thesis, Zuber (11) found that the bubble formation at an orifice and bubble formation in nucleate boiling are closely similar to each other. Using this similarity, Zuber derived an expression for the product of bubble diameter and frequency of bubble emission in nucleate boiling. The derived expression is in good agreement with experimental data. Zuber also found a similarity between nucleate boiling and the bubbling of a gas from a perforated surface. Based upon this similarity, he showed that the critical heat flux is a hydrodynamic phenomenon known as "flooding." That is, the maximum heat flux would occur when the steady flow of the liquid column towards the heating surface is interrupted by the surrounding vapor columns.

Review of Previous Correlations

Many formulae for nucleate boiling heat transfer have been established in the light of experimental results during the last decade. Some of these formulae are entirely empirical and valid only for some special cases. Some others, described here as the semitheoretical ones, are mostly based upon a simplified model and are designed to be applicable in a broaden range. In general, these semitheoretical formulae always involve one or two constants which have to be determined experimentally.

Rohsenow (16) assumed that the heat transfer coefficient of nucleate boiling can be represented in a form similar to the Nusselt Equation for forced convection and introduced a relation between the bubble Nusselt and bubble Reynolds Number. The equation most convenient for the correlation of experimental data is given as

$$\frac{C_\ell \, \Delta T}{\lambda \, Pr^{1.7}} = \text{const} \left[\frac{q}{\lambda \, \mu_\ell} \left(\frac{g_c \, \sigma}{g \, (\rho_\ell - \rho_v)} \right)^{\frac{1}{2}} \right]^{0.33} \tag{1}$$

or

$$h = \text{const} \; \frac{g^{0.5} \, \Delta T^{2.03} \, K^{5.15} \, (\rho_\ell - \rho_v)^{0.5}}{g_c^{0.5} \, \sigma^{0.5} \, \lambda^{2.03} \, C_\ell^{2.12} \, \mu_\ell^{4.15}} \tag{2}$$

where the constant depends upon the liquid - surface combination and the liquid properties are evaluated at the saturated temperature corresponding to the local pressure. Equation (1) applies only to the clean surface. For other surface conditions, both the constant and the exponent of Prandtl Number would change, while 0.33, exponent of the bubble Reynolds Number, appears to be unaltered.

With the aid of the bubble-growth theory developed by Forster and Zuber (17) and by Plesset and Zwick (18), Levy (19) obtained a generalized equation for nucleate boiling shown in the following

$$q = \frac{K\, C_\ell\, \rho_\ell^{\,2}\, (\Delta T)^3}{B_\ell\, \sigma\, t_s\, (\rho_\ell - \rho_v)} \tag{3}$$

or in the following form

$$h = \text{const}\, \frac{K\, C_\ell\, \rho_\ell^{\,2} (\Delta T)^2}{\sigma\, t_s\, (\rho_\ell - \rho_v)} \tag{4}$$

where B_ℓ is a function $\lambda\, \rho_v$ and determined in experiments. Levy claimed that Equation (3) is valid for various pressure and the heating surface - liquid combination. The validity of Equation (3) has been tested for a large number of liquids.

Chang and Snyder (20) divided the nucleate boiling region into two parts: feeble nucleate boiling and vigorous nucleate boiling. Starting from the equations of momentum and energy, they derived an expression for the heat transfer in vigorous nucleate boiling. This equation is

$$q = \text{const}\, \frac{K\, \Delta P^{1.4}\, (\Delta T)}{\sigma\, (\rho_v \lambda)^{0.8}} \left[C_\ell\, t_s\, (\rho_\ell - \rho_v) \right]^{0.4} \tag{5}$$

or

$$h = \text{const}\, \frac{K\, \Delta P^{1.4}}{\sigma\, (\rho_v \lambda)^{0.8}} \left[C_\ell\, t_s\, (\rho_\ell - \rho_v) \right]^{0.4} \tag{6}$$

where the constant in Equation (5) is determined in experiments. For instance, when this constant is equal to 4×10^{-4}, Equation (6) will

correlate well the experimental data of previous investigations. (21) (22)

For the estimation of heat flux at feeble boiling where both the natural convection and bubble agitation exist, Chang and Snyder also obtained an equation which is shown as Equation (20) in their paper (20).

Forster and Grief (8) proposed a semitheoretical formula shown as Equation (7) and stated that the validity of Equation (7) has been tested for a number of liquids at atmospheric pressure and for water at 1.0 and 50 atmospheres.

$$q = \text{const} \frac{K}{\sigma} \Delta P \left(\frac{A^2}{\nu} \right)^{0.2} Pr^{\frac{1}{3}} \Delta T \tag{7}$$

where

$$A = \frac{\left[\pi K C_\ell \rho_\ell \right]^{0.5} \Delta P}{\left[\rho_v \lambda \right]^2}$$

For comparison, the Equation (7) can be rewritten as

$$h = \text{const} \frac{K^{0.86} \Delta P^{1.4} \rho_\ell^{0.4} \pi^{0.2} C_\ell^{0.53} \mu_\ell^{0.13}}{\sigma \lambda^{0.8} \rho_v^{0.8}} \tag{8}$$

It should be noticed that even among these four semitheoretical formulae, there are still some differences in such important parameters as the temperature potential and viscosity of liquids. So far as the temperature potential is concerned, Equation (2) and Equation (4) are almost identical to each other while ΔT disappears in Equation (6) and Equation (8). As for viscosity of liquids, it plays an important role in Equation (2) and a minor role in Equation (8) while it disappears in Equation (4) and Equation (6).

Nishikawa and Yamagata (23) recognized that the stirring effect of bubbles is the key factor controlling the heat transfer rate in nucleate boiling. Starting from an analysis of the elementary phenomena, they derived an equation for the heat transfer coefficient in nucleate boiling. After some algebraic manipulations, the equation can be shown in the following form,

$$h = \text{const} \frac{f_f f_p^2 C_\ell K^2 \rho_\ell^2 (\Delta T)^2}{\sigma \lambda \rho_v} \tag{9}$$

Nishikawa and Yamagata claimed that Equation (9) is also applicable to saturated or surface boiling with forced convection. Equation (9) is also independent of pressure and heating surface-fluid combination.

Recently, there appears a new development in the semitheoretical investigation. The semitheoretical correlation no longer involves the idea of a bubble Reynolds Number or bubble Nusselt Number. Instead of these, the general form of the equation for the heat transfer coefficient in nucleate boiling is

$$h = \text{const} \quad n^a \Delta T^b \tag{10}$$

where the exponents, a and b, are constants which depend upon experimental results.

In studying the phenomena of nucleate boiling, Hara (24) realized an existance of the nonreproducible character in the creation of bubble nuclei and set up a hydrodynamic model. In this model, it is supposed that the bubble once created would grow and rise from the heating surface. The liquid surrounding the bubble would be induced to move. The amount of heat carried by this induced motion of liquid to the heating

surface is equal to that transferred from the heating surface to the liquid and to the latent heat carried away by the bubbles. Based upon his hydrodynamic model, he derived an expression as follows

$$\Delta T = 0.114\, n^{-\frac{1}{4}}\, q^{\frac{2}{3}} \tag{11}$$

After some rearrangement, Equation (11) can be shown as

$$h = 18.6\, n^{0.376}\, (\Delta T)^{0.5} \tag{12}$$

It is interesting to note that Equation (11) is in a form similar to the empirical equation shown as Equation (16) in this thesis.

Tien (15) made use of his proposed hydrodynamic model as previously described and derived an equation for nucleate boiling as follows

$$h = \text{const.}\ K\, Pr^{0.33}\, n^{0.5} \tag{13}$$

where the constant is determined in experiments. Although Equation (13) is originally derived for the prediction of the heat transfer coefficient in a low heat-flux region, it might well serve as an approximation in the high heat-flux region. It is interesting to note that Equation (13) is similar to the empirical correlation of boiling data obtained by Kurihara and Meyers (25). This empirical correlation will be shown as Equation (15) in this section.

Recently Equation (13) was re-examined by Lienhard (26). Based upon the experimental results obtained by Benjamin and Westwater (27), Lienhard obtained Equation (14) which can correlate experimental data better than Equation (13).

$$h = \text{const}\ A^{\frac{1}{2}}\, K\, Pr^{\frac{1}{3}}\, \Delta T^{\frac{1}{4}}\, n^{\frac{1}{3}} \tag{14}$$

where

$$A = \frac{\left[\sigma\, g\, (\rho_v - \rho_\ell) \,/\, \rho_\ell^{\,2}\right]_{\text{liquid of interest}}}{\left[\sigma\, g\, (\rho_v - \rho_\ell) \,/\, \rho_\ell^{\,2}\right]_{\text{water}}}$$

the constant is determined in experiments.

It should be noted that the temperature potential, ΔT, plays a different role among the Equations (12), (13), and (14). Therefore, additional investigations are needed in this area.

For completeness, Kurihara's (25) empirical equation and Nishikawa's correlation are reproduced respectively in the following,

$$q = 820\, (h)^{-\frac{1}{3}} \left[K \left(\frac{\rho_v}{\mu_\ell} \right)^{\frac{1}{3}} Pr^{-0.89} \right] n^{\frac{1}{3}}\, \Delta T, \tag{15}$$

$$\Delta T = 0.448\, n^{-\frac{1}{6}}\, q^{\frac{2}{3}} \tag{16}$$

By rearranging, Equation (15) and Equation (16) can be shown respectively as

$$h = 152 \left[K \left(\frac{\rho_v}{\mu_\ell} \right)^{\frac{1}{3}} Pr^{-0.89} \right]^{\frac{3}{4}} n^{\frac{1}{4}} \tag{17}$$

$$h = 3.35\, n^{\frac{1}{4}}\, \Delta T^{\frac{1}{2}} \tag{18}$$

Effects of Acoustical Energy on Convective Heat Transfer

Since Fand and Kaye (28) have given an excellent summary in this subject, this part of the literature survey will only include a brief review of previous experimental investigation and various mechanisms of interaction between vibration and convective heat transfer.

Brief Review of Previous Experimental Investigations

It has been found experimentally that there exists a critical sound intensity. Only when the sound intensity is higher than the critical value will the increase in sound intensity increase the heat transfer coefficient. The critical value for sound intensity depends upon a number of variables such as the frequency of sound wave and the fluid properties.

Experimental investigations also revealed that the heat transfer coefficient can be increased by increasing either the amplitude or frequency of sound waves, or both at the same time. Beyond a certain value of sound intensity, however, the increase in heat transfer becomes less and less pronounced.

It is widely accepted that the effect of acoustic energy upon convective heat transfer would be related to the temperature difference between the heating surface and the fluid. In general, the greater the temperature difference is, the larger effect the acoustic energy has on convective heat transfer. It is expected because the boundary layer is more easily disturbed in a large temperature difference and it is easier for eddy motions to be generated.

Fand and Peeble (29) reported that the effect of acoustic waves upon convective heat transfer is found to be identical to that of mechanical vibration imposed on heating surfaces provided that the intensity of vibration is the same. In other words, the heat transfer correlations obtained for the case of acoustical vibration are also valid for the case of mechanical vibration. However, it should be noticed that this finding is, so far, only reported by Fand and Peeble.

Since many experiments were carried out by various investigators under different conditions, there is no attempt to make any quantitative comparison among them in this literature survey. It should be known that most experiments, to the writer's knowledge, are concerned only with air or water both in forced convection and in free convection.

On the Mechanism of Interaction Between Vibration and Heat Transfer

Various mechanisms have been proposed by some researchers and have been discussed by Fand (30). These mechanisms are mostly concerned with the interaction between the transverse horizontal vibration and free convection from a horizontal cylinder.

Westervelt (31) proposed that the increase in free convective heat transfer rate by sound waves is caused by a modification of the convective flow in the inner streaming boundary layer. In other words, at the critical sound intensity, the inner streaming boundary layer would collapse and be replaced by a vigorous and chaotic kind of motion which is responsible for the increase in heat transfer rate.

Based upon their own experimental results, Fand and Kaye (28), (30) suggested that the presence of thermoacoustic streaming, primarily through the action of the vortices which form above the cylinder, is the cause for an increase in heat transfer rate when the heated horizontal cylinder is subject to a strong sound field. However, the main reason for the increase of heat transfer rate on the lower half of cylinder is that some fluctuations are acoustically induced within the laminar boundary layer.

Sprout (32) and Holman (33) explained the mechanism in terms of the interaction of acoustical streaming with the boundary layer flow.

In their proposed mechanism, the increase in heat transfer rate is due to not only the collapse of the inner streaming boundary layer as said by Westervelt, but also the occurrence of flow separation and a circulatory motion on the upper half of the cylinder. These flow separations are caused by a superposition of isothermal streaming on the free convective flow. In the lower half of the cylinder, the direction of isothermal streaming is the same as that of free convective flow; and so, the thermal boundary layer thickness at that part of the cylinder is reduced. It is expected, therefore, that the higher heat transfer rate results.

It should be pointed out that for the case in which the heating cylinder is vertically vibrated, the increase in heat transfer rate is due to the vertically induced turbulence. This type of induced turbulence is entirely different from the thermoacoustic streaming found in the case in which the heating cylinder is in a transverse horizontal vibration.

It may be noticed that none of the mechanisms just mentioned above have led to the quantitative formulation of heat transfer prediction. In 1956, Chang (35) developed a wave theory for free convective heat transfer and boiling. He also claimed that this wave theory can serve to explain the phenomena that the heat transfer rate can be improved by acoustical vibration or mechanical vibration. The expression of heat transfer coefficient he derived for free convection from a horizontal flat plate can be shown as follows,

$$h = \frac{1}{2}\left(C_{\ell}\, \rho_{\ell}\, K\, f\right)^{0.5} \tag{19}$$

where $$f = \frac{4\alpha}{a^2} \tag{20}$$

Equation (19) can be rewritten as

$$h = \frac{C_\ell \rho_\ell}{4} a \cdot f \tag{21}$$

Equation (21) indicates that the heat transfer coefficient, h, is proportional to the product of frequency and amplitude of the wave. Unfortunately, there is no such experiment carried out as free convection from a horizontal flat plate subject to a strong sound field. Therefore, this theory can not be completely justified in the present time. For the case of a cylinder as the heating surface, however, it has been demonstrated experimentally (28), (36), (32) that the heat transfer coefficient of free convection can be increased by increasing the sound intensity, i.e., a · f. The general correlation found in experiments can be shown as follows,

$$h = \text{const } a^m \cdot f^n \tag{22}$$

where the constant and exponents are determined experimentally.

Effects of Acoustical Energy on Nucleate Boiling Heat Transfer

Isakoff (1) conducted a series of experiments and found that there was no effect of acoustic vibration on the low heat flux region in nucleate boiling when he applied the acoustic waves on the boiling water which was stored in a cylinder-shaped tank. The acoustic waves he used were generated and propagated from the bottom of the tank. The sound intensity and frequency at the oscillating diaphram were approximately 2 watts/cm^2 and 10 kc respectively. No measurement was made to determine

the actual sound intensity in the boiling water. Also no data were reported for other different conditions such as different frequency and sound intensity. However, Isakoff found that the presence of sound would increase the maximum heat transfer rate from an electrically heated platinum wire to boiling water by about 60 per cent over the values obtained in the absence of sound, when other conditions remained unaltered.

Kovalenko (37) found in his experiments that the mechanical vibration would not affect the boiling heat transfer. The frequency and amplitude of mechanical vibration at the vibrating diaphram were 700 or 3000 cpm and 0.15 or 0.35 mm respectively.

Romie (38) once intended to conduct a series of experiments to determine the effect of acoustic vibration upon the maximum heat flux in the flow system under an atmospheric condition. The water would flow in the direction of sound propagation within an annular flow channel bounded on the outside by a glass tube and on the inside by a stainless steel element with a heated length of 5 or 6 inches. The frequency and maximum acoustical power of waves he intended to use were 25 kc and approximately 300 watts, respectively. However, he did not carry out these experiments according to the author's correspondence from him.

CHAPTER III

ANALYTICAL ASPECTS OF THE PRESENT INVESTIGATION

The following analysis is intended to furnish the basis on which a mechanism is proposed to explain the experimental results obtained in this present investigation. At first, the analysis is carried out to estimate the effect of sound waves on the bubble growth in a superheated liquid and thus to estimate the stirring motion induced by the bubble growth in a liquid. This induced stirring motion will be related to the sound pressure and the frequency of sound. When a vapor bubble grows to such an extent that the bubble growth rate approaches zero, the bubble continues to experience a volume pulsation. The volume of the vapor bubble changes periodically in the sound field, even though the vapor bubble ceases to grow (i.e., the mean volume of vapor bubble remains unaltered). This kind of volume pulsation will be approximately expressed in terms of fluid properties, sound pressure and sound frequency. Finally, the radius of a vapor bubble departing from a heating surface under the influence of sound waves is approximately calculated and compared with that in the absence of sound.

Effects of Sound Waves on a Vapor Bubble Growth in a Superheated Liquid

A vapor bubble is generally initiated from a small gas-filled cavity or scratch on a solid surface when the surrounding liquid is

superheated to a certain degree. It is accepted that these two conditions are necessary but not sufficient for a bubble initiation. Before a vapor bubble starts to grow, it experiences a period called the waiting period. During the waiting period, the liquid surrounding the bubble nucleus is heated to a temperature equal to or above the temperature of the vapor in the bubble. Then the vapor bubble experiences the second period called the unbinding period. The unbinding period is characterized by the fact that the growth rate increases rapidly. The effects of surface tension and the inertia of liquid are not negligible. During this period, the momentum equation governs the motion of the bubble surface. After the unbinding period, the vapor bubble grows very fast in the third period called the growing period. During the growing period, the heat transfer process at the bubble surface is dominating. At that time the effects of liquid inertia and of surface tension can be neglected. The unbinding period is short compared with the other two periods.

The effects of sound waves on vapor bubble growth in superheated liquid will now be discussed. Attention is directed only to the growing period of a vapor bubble. For this purpose, the simple model is established and presented in Figure 1. The vaporization process by which the vapor bubble grows in a superheated liquid is maintained by the heat transferred to the vapor bubble from the surrounding liquid. For simplicity the initial temperature in the liquid surrounding the vapor bubble is assumed to be uniform throughout, while the temperature of the vapor inside the bubble is the saturation temperature corresponding to the vapor pressure. When the vapor bubble starts to grow in the superheated liquid under the influence of sound, the temperature of vapor

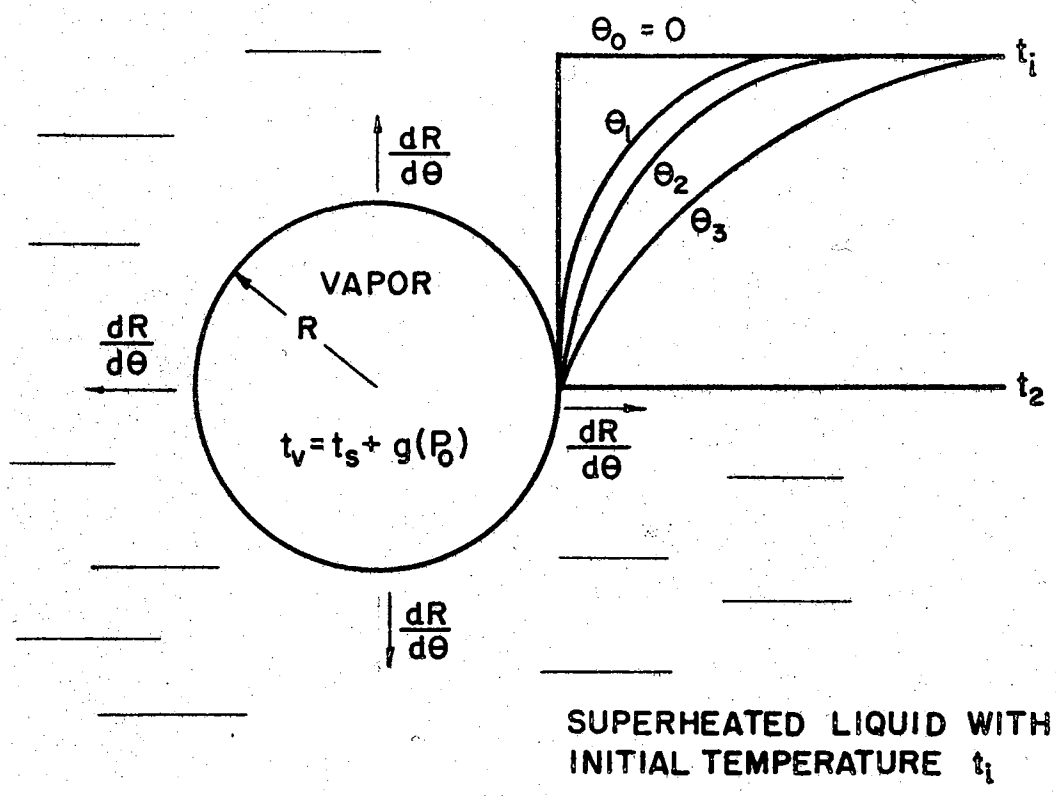

Figure 1. A Model for a Vapor Bubble Growing in Superheated Liquid With Initial Temperature t_i Under the Influence of Sound Waves.

inside the bubble is assumed to be the sum of the saturation temperature and the temperature fluctuation due to the presence of a sound field, i.e., $t_v = t_s + g(P_o)$ where the function $g(P_o)$ represents this temperature fluctuation. Since the bubble diameter encountered in nucleate boiling is generally far smaller than that of the wave length of an ultrasonic wave (the ratio of bubble diameter to the wave length is approximately equal to 0.01 for a vapor bubble of 0.03 inches in diameter in water for a sound field of 20,000 cycles/sec.), it can be assumed that the temperature and vapor pressure inside the vapor bubble are uniformly distributed. It might be noticed that when a vapor bubble grows, the vapor bubble would simultaneously experience a volume pulsation under the influence of a sound field. However this volume pulsation, as shown in the next section, is found to be somewhat proportional to the radius of a vapor bubble and this is very small during most of the growing period. Therefore, the volume pulsation of a vapor bubble during this period can be assumed to be negligibly small as compared with the effects of sound waves on the bubble growth. In addition, the following assumptions are also made:

1. The effects of liquid inertia and of surface tension on bubble growth are neglected.

2. The thermodynamic properties of the liquid and its vapor such as thermal conductivity and latent heat are independent of temperature and would not be altered in the presence of sound waves.

3. Since the radial velocity of the bubble surface is considered to be negligible in comparison with sonic velocity in either the liquid or vapor, the fluids will be assumed to be incompressible.

According to the model presented in Figure 1, the growth rate of a vapor bubble in the superheated liquid can be expressed as follows:

$$\lambda \rho_v \frac{dR}{d\theta} = K \left(\frac{\partial T}{\partial x}\right)_{x=0} \tag{23}$$

where $\left(\frac{\partial T}{\partial x}\right)_{x=0}$ is the temperature gradient at the bubble wall in the liquid. To determine this temperature gradient, the mathematical formulation can be expressed as follows:

$$\frac{\partial^2 T}{\partial x^2} = \frac{1}{\alpha} \frac{\partial T}{\partial \theta} \tag{24}$$

with the boundary and initial conditions

$$T(x,0) = T_i \tag{25}$$

$$T(0,\theta) = g(P_o) \tag{26}$$

$$T(\infty,\theta) = T_i \tag{27}$$

where $T = t - t_s$. It should be noticed that Equation (24) is formulated in the system of rectangular coordinates with the origin on the bubble surface. Obviously it is assumed that the problem can be treated to be one-dimensional. These can be justified, for the similar method was used to calculate the growth of a vapor bubble in the absence of a sound field and the results of calculation are agreeable qualitatively with experimental works (11). By Equation (24), the temperature distribution in the superheated liquid surrounding the vapor bubble can be obtained. The solution to Equation (24) and its boundary and initial conditions can be easily shown in Appendix A.

$$T(x,\theta) = T_i \operatorname{erf} \frac{x}{2(\alpha\theta)^{\frac{1}{2}}} + g(P_o) \operatorname{erfc} \frac{x}{2(\alpha\theta)^{\frac{1}{2}}} \tag{28}$$

The temperature gradient in the superheated liquid can be obtained by a differentation of Equation (28) with respect to x. That is:

$$\frac{\partial T(x,\theta)}{\partial x} = \frac{e^{\frac{-x^2}{4\alpha\theta}}}{(\pi\alpha\theta)^{\frac{1}{2}}} \left[T_i - g(P_o) \right] \tag{29}$$

The temperature gradient in the superheated liquid at the bubble surface therefore can be shown as:

$$\left(\frac{\partial T}{\partial x}\right)_{x=0} = \frac{T_i - g(P_o)}{(\pi\alpha\theta)^{\frac{1}{2}}} \tag{30}$$

A combination of Equation (23) and Equation (30) leads to an expression for the growth rate of a vapor bubble in a liquid with an initial uniform temperature. This expression is:

$$\frac{dR}{d\theta} = \frac{K}{\rho_v \lambda (\pi\alpha\theta)^{\frac{1}{2}}} \left[T_i - g(P_o) \right] \tag{31}$$

After an integration of Equation (31), the radius of a vapor bubble can be expressed as follows:

$$R - R_i = \frac{K}{\lambda \rho_v (\pi\alpha)^{\frac{1}{2}}} \left[2T_i \theta^{\frac{1}{2}} - \int_o^\theta \theta^{-\frac{1}{2}} g(P_o)\, d\theta \right] \tag{32}$$

where R_i is the initial radius.

It is shown that the expression for the bubble growth rate indicated in Equation (31) contains two terms. The first term is identical to that obtained by Zuber (11) for the case without sound waves. The second term is obviously due to the presence of sound waves and will vanish when no wave is present. A careful examination of the second term in Equation (31) indicates that the presence of sound waves would cause a fluctuation

in the growth rate of a vapor bubble and thus intensifies the stirring motion in the liquid surrounding the vapor bubble. For illustration, the function, $g(P_o)$, representing the temperature fluctuation inside the vapor bubble in the presence of sound waves, is assumed to be a sine function, i.e., $g(P_o) = t_o \sin \omega\theta$ and the following numerical values used.

$$K = 1.095 \times 10^{-4} \text{ Btu/sec. ft. F}$$

$$\rho_v = 0.0373 \text{ lbm/ft.}^3$$

$$\lambda = 970.3 \text{ Btu/lbm.}$$

$$\alpha = 0.182 \times 10^{-5} \text{ ft.}^2\text{/sec.}$$

$$T_i = 30^o \text{ F}$$

The growth rates of a bubble have been calculated under various conditions according to Equation (31) and are presented in Figure 2, Figure 3, and Figure 4.

Since the temperature fluctuation inside the vapor bubble is a function of sound pressure, the temperature amplitude, t_o, used in above numerical calculation is proportional to the sound pressure P_o. Therefore, it can be concluded from Figure 2 that an increase in sound pressure at a certain sound frequency would increase the fluctuation in the growth rate of a vapor bubble and thus would intensify the stirring motion in the liquid surrounding the vapor bubble. It is also indicated in Figure 3 and Figure 4 that different frequencies of sound waves would bring different degrees of stirring motion.

It might be noticed that the temperature fluctuation inside the vapor bubble in the presence of a sound field has been expressed by a function $g(P_o)$. There is no attempt at the present time to evaluate

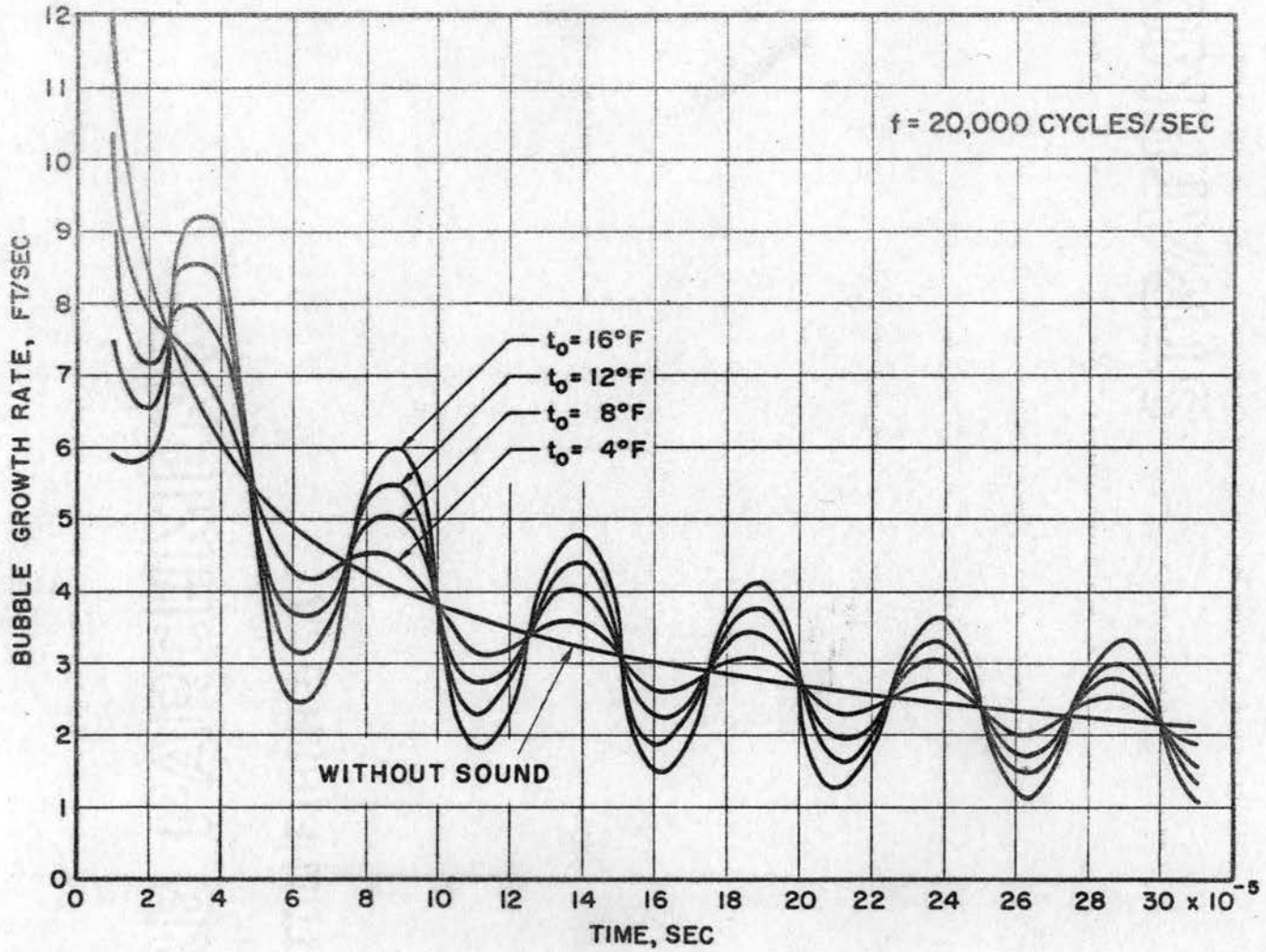

Figure 2. Effect of Sound Waves on the Vapor Bubble Growth Rate at the Constant Sound Frequency 20,000 Cycles/Sec.

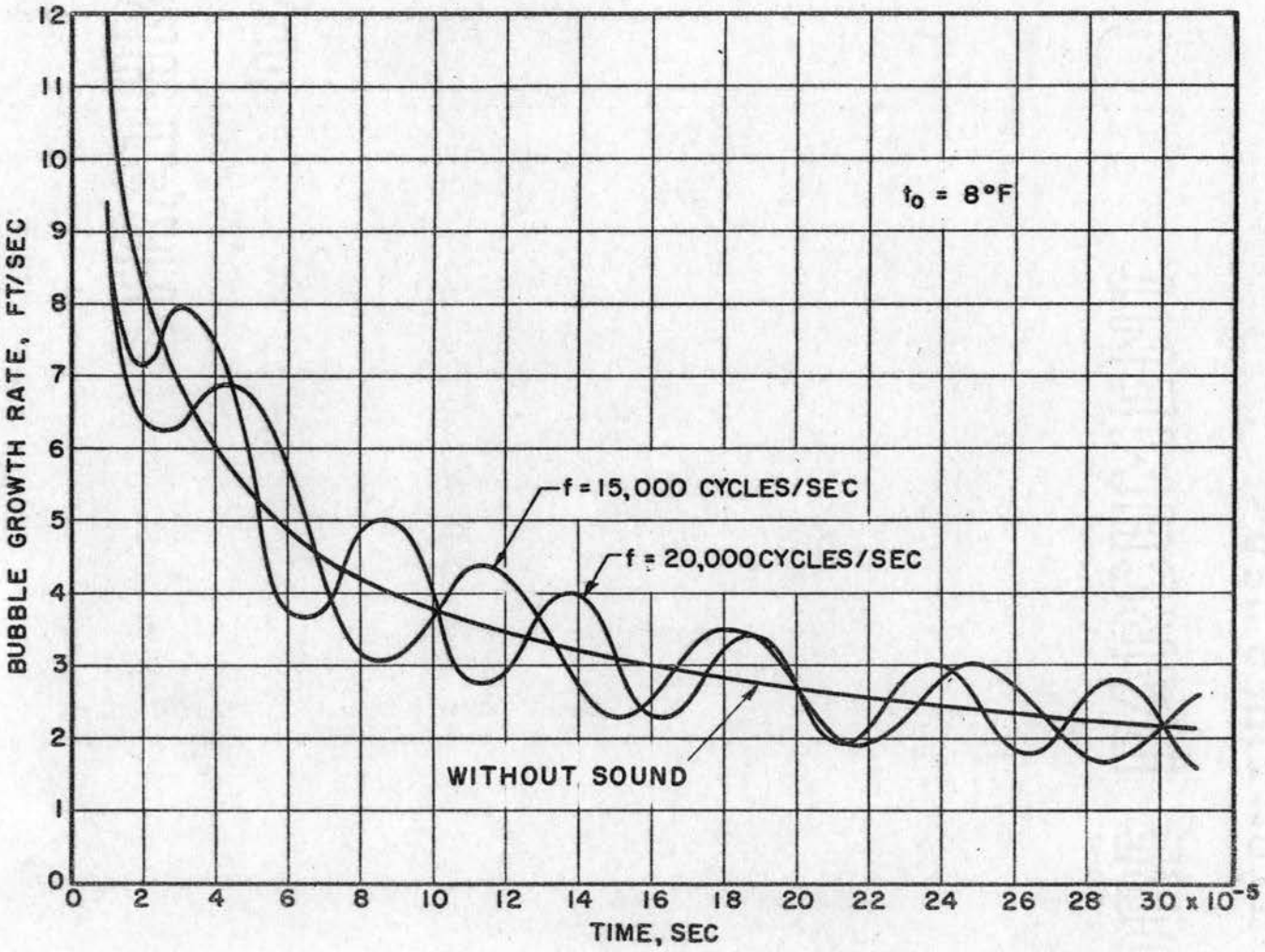

Figure 3. Effect of Sound Frequency on the Vapor Bubble Growth Rate at a Constant Sound Pressure, I.

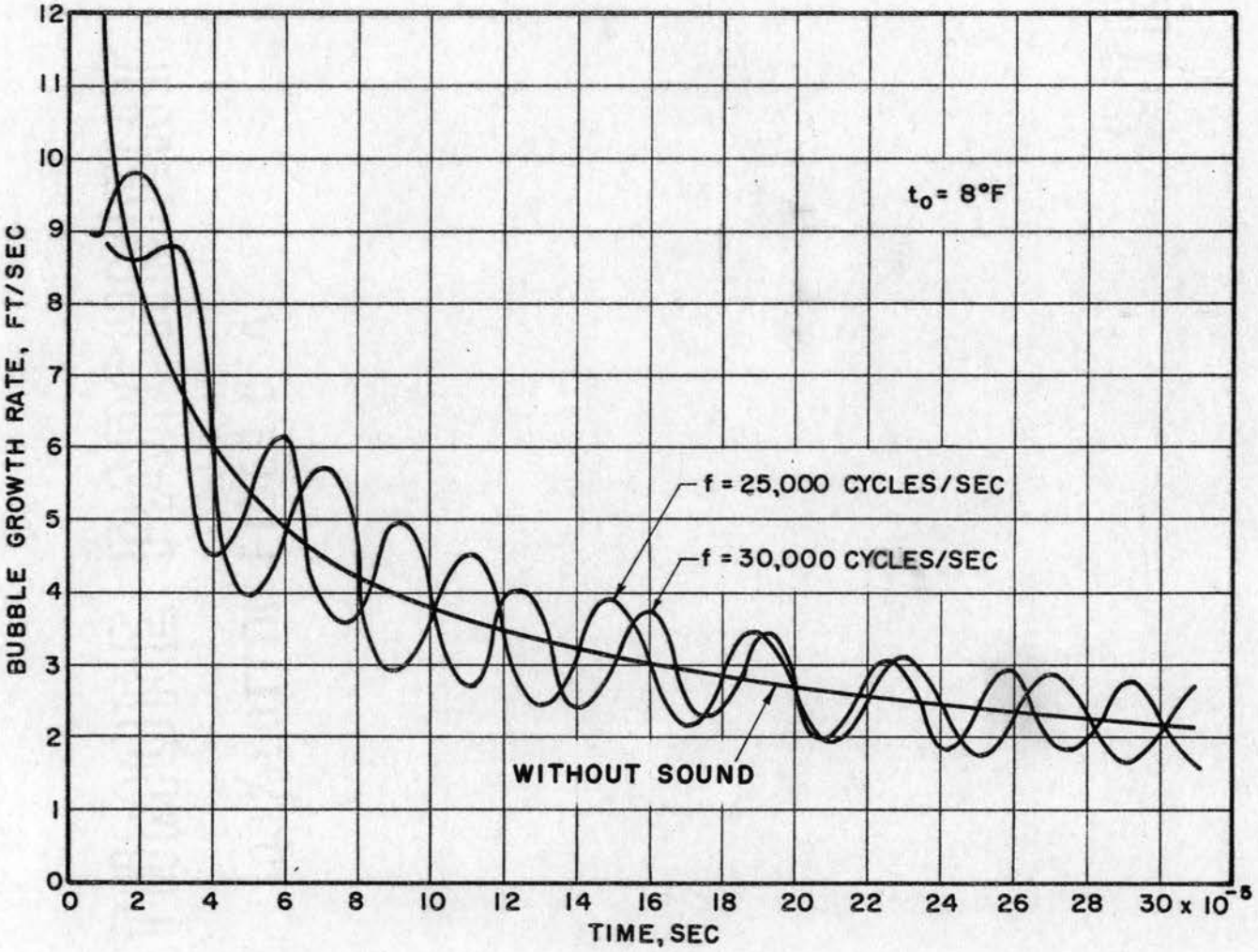

Figure 4. Effect of Sound Frequency on the Vapor Bubble Growth Rate at a Constant Sound Pressure, II.

this function and to show it in an explicit form. However, $g(P_o)$ is the periodic function with a phase angle between the temperature fluctuation and the sound pressure. Also there is no doubt that the amplitude of the function, $g(P_o)$, is somewhat proportional to the amplitude of the sound pressure.

Volume Pulsation of a Vapor Bubble in a Sound Field

When the vapor bubble in the superheated liquid grows to such an extent that the temperature gradient at the bubble wall approaches zero and thus the radial velocity of the bubble wall due to the evaporation process also approaches zero, it can be expected that the motion of the bubble wall is no longer governed by the heat transfer process as indicated in the last section. The volume pulsation which the vapor bubble experiences under an influence of a sound field will become pronounced at that time. If the viscosity and gravity effects can be ignored and the heat transfer process at the bubble wall is negligible, the radius of the vapor bubble in the liquid under an influence of sound field would satisfy the following equation.

$$R \frac{d^2R}{d\theta^2} + \frac{3}{2}\left(\frac{dR}{d\theta}\right)^2 = \frac{P_v - P_\ell}{\rho_\ell} - \frac{2\sigma}{\rho_\ell R} \tag{33}$$

where

$$P_v = \left(P_a + \frac{2\sigma}{R_m}\right) \frac{R_m^3}{R^3} \tag{34}$$

and

$$P_\ell = P_a - f(P_o) \tag{35}$$

with the initial condition

$$\frac{dR}{d\theta} = 0 \quad \text{at } \theta = 0 \tag{36}$$

$$R(\theta) = R_m \quad \text{at } \theta = 0 \tag{37}$$

Equation (33) is a nonlinear differential equation. Its solution cannot be directly obtained. However, if the instantaneous bubble volume V is used, then the modified equation is soluble mathematically.

Let $V = \frac{4}{3}\pi R^3$, (38)

then

$$\frac{dV}{d\theta} = 4\pi R^2 \frac{dR}{d\theta} \tag{39}$$

$$\frac{d^2V}{d\theta^2} = 8\pi R \left(\frac{dR}{d\theta}\right)^2 + 4\pi R^2 \left(\frac{d^2R}{d\theta^2}\right) \tag{40}$$

From Equation (39) and Equation (40), it can be shown

$$\frac{dR}{d\theta} = \frac{1}{4\pi R^2} \frac{dV}{d\theta} \tag{41}$$

$$\frac{d^2R}{d\theta^2} = \frac{1}{4\pi R^2} \frac{d^2V}{d\theta^2} - \frac{2}{16\pi^2 R^5} \left(\frac{dV}{d\theta}\right)^2 \tag{42}$$

Substituting Equation (41) and Equation (42) into Equation (33) would give

$$\frac{\rho_\ell}{4\pi R} \frac{d^2V}{d\theta^2} - \frac{\rho_\ell \left(\frac{dR}{d\theta}\right)}{8\pi R^2} \frac{dV}{d\theta} = P_v - P_\ell - \frac{2\sigma}{R} \tag{43}$$

Let $v = V - V_m$ and $v \ll V_m$. Equation (43) can be approximately expressed as

$$\frac{\rho_\ell}{4\pi R_m}\frac{d^2v}{d\theta^2} - \frac{\rho_\ell \dot{R}_m}{8\pi R_m^2}\frac{dv}{d\theta} + r\frac{P_{vm}}{V_m}v = P_{vm} - P_\ell - \frac{2\sigma}{R_m} \qquad (44)$$

Substituting Equation (34) and Equation (35) into Equation (44) would give

$$\frac{\rho_\ell}{4\pi R_m}\frac{d^2v}{d\theta^2} - \frac{\rho_\ell \dot{R}_m}{8\pi R_m^2}\frac{dv}{d\theta} + r\frac{P_{vm}}{V_m}v = f(P_o) \qquad (45)$$

with the initial condition

$$\dot{v}(\theta) = 0 \quad \text{at} \quad \theta = 0 \qquad (46)$$

$$v(\theta) = 0 \quad \text{at} \quad \theta = 0 \qquad (47)$$

Obviously Equation (45) indicates that the volume pulsation of a vapor bubble in a liquid under an influence of sound field would obey a standard second-order differential equation for a linear, forced oscillating system with inertial coefficient equal to $\frac{\rho_\ell}{4\pi R_m}$, resistive coefficient $\frac{-\rho_\ell \dot{R}_m}{8\pi R_m^2}$ and stiffness coefficient $\frac{rP_{vm}}{V_m}$.

It is found by an analysis of order of magnitude that the resistive coefficient is negligibly small as compared with the inertial coefficient. If it can be assumed that the function for the sound pressure, $f(P_o)$, is $P_o \sin \omega\theta$, Equation (45) would become

$$\frac{\rho_\ell}{4\pi R_m}\frac{d^2v}{d\theta^2} + \frac{3r}{4\pi R_m^3}\left(P_a + \frac{2\sigma}{R_m}\right)v = P_o \sin \omega\theta \qquad (48)$$

with the initial conditions

$$v(\theta) = 0 \quad \text{at} \quad \theta = 0 \tag{49}$$

$$\dot{v}(\theta) = 0 \quad \text{at} \quad \theta = 0 \tag{50}$$

The solution to Equation (48) and its initial conditions can be easily shown as

$$v(\theta) = \frac{4\pi R_m P_o / \rho_\ell}{\omega_m^2 - \omega^2} \left(\sin \omega \theta - \frac{\omega}{\omega_m} \sin \omega_m \theta\right) \tag{51}$$

where ω_m is the natural frequency of a vapor bubble of radius R_m in a liquid and is expressed as follows

$$\omega_m^2 = \frac{3r \left(P_a + \frac{2\sigma}{R_m}\right)}{\rho_\ell R_m^2} \tag{52}$$

It is seen in Equation (51) that the volume pulsation of a vapor bubble, $v(\theta)$, is somewhat proportional to the mean volume of the vapor bubble if the conditions in a sound field and fluid properties remain unaltered.

According to Equation (51) and the following numerical values

$$P_a = 2120 \quad \text{lbf/ft}^2$$

$$\sigma = 0.00383 \quad \text{lbf/ft}$$

$$R_m = 0.001 \quad \text{ft}$$

$$\rho_\ell = 59.7 \quad \text{lbm/ft}^3$$

the volume pulsations of a vapor bubble in the saturated water under the influence of sound have been calculated for various sound pressures and frequencies. The dimensionless form of the volume pulsation, v/V_m, is expressed as a function of time with sound frequency or sound pressure

as the parameter. These curves are shown in Figure 5 and Figure 6. It is seen in Figure 5 that this volume pulsation is very complicated in pattern and is not in the same phase as the sound pressure. However, the amplitude of volume pulsation is somewhat proportional to the amplitude of sound waves at a constant sound frequency. It can be concluded, therefore, that the stirring motion induced by this volume pulsation of a vapor bubble in its surrounding liquid will increase as the sound pressure increases at a certain sound frequency. It is indicated in Figure 6 that the sound waves of lower frequency would be more effective than that of higher frequency, as far as this production of the induced stirring in a liquid is concerned. It may be noticed, however, that the last statement would hold only if the statistically average radius of vapor bubbles, R_m, is 0.001 ft. (The natural frequency for a vapor bubble of radius 0.001 ft. is approximately equal to 11,000 cycles per second).

An Estimation of the Radius of a Vapor Bubble Departing From the Heating Surface

The radius of a vapor bubble leaving from the heating surface is one of the important items in the analysis of nucleate boiling. This radius is controlled by the buoyant force and the forces due to the surface tension between the vapor bubble, the liquid, and the heating surface. Under the influence of a sound field, however, the radius of a vapor bubble departing from a heating surface is no longer controlled by these factors, but probably by the natural frequency of the vapor bubble. That is, when the natural frequency of the vapor bubble coincides with the frequency of sound waves which are impressed on the vicinity of a bubble in liquid, the bubble may disappear with an explosion right on the heating surface.

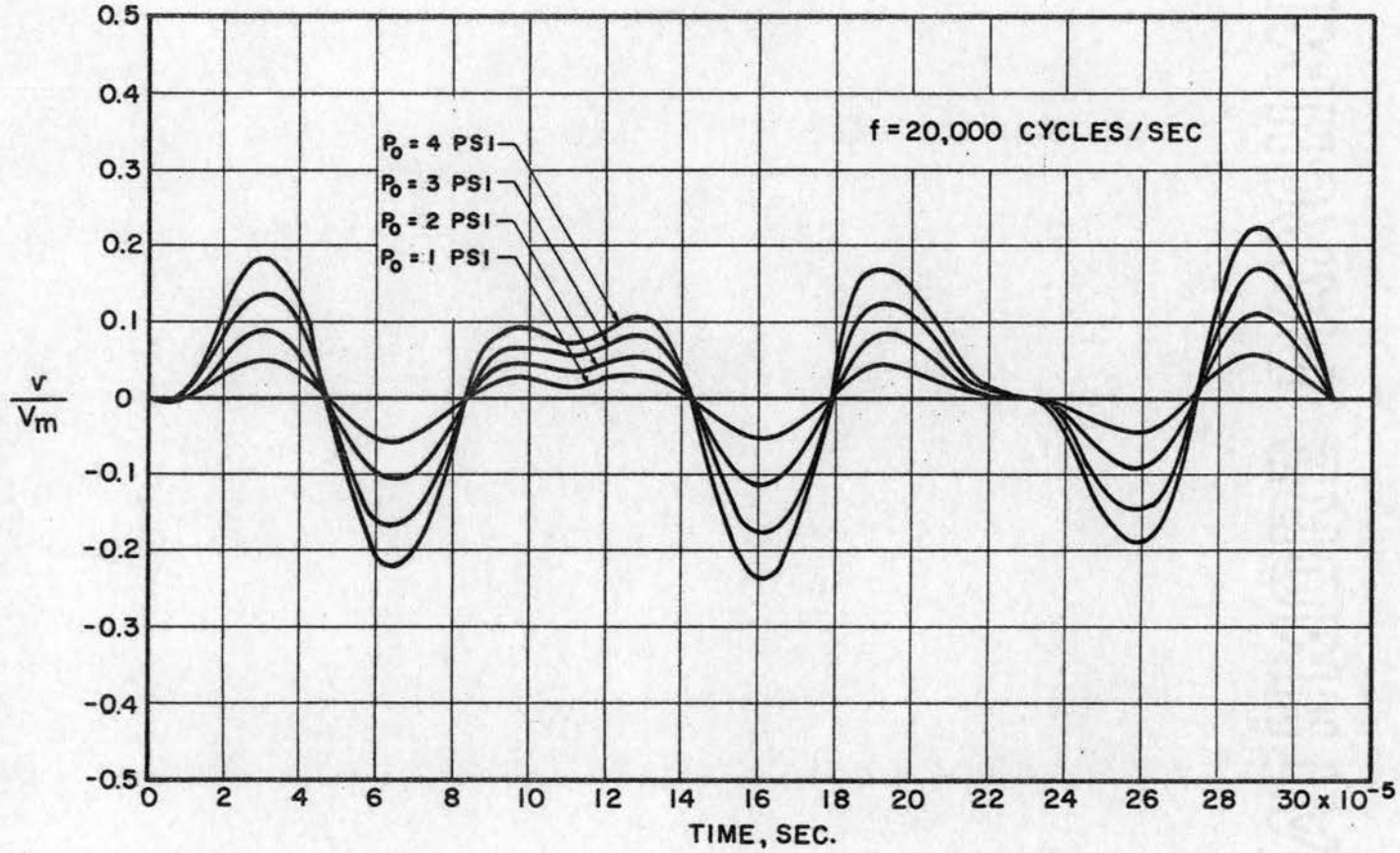

Figure 5. Effect of Sound Pressure on the Volume Pulsation of a Vapor Bubble at Constant Sound Frequency.

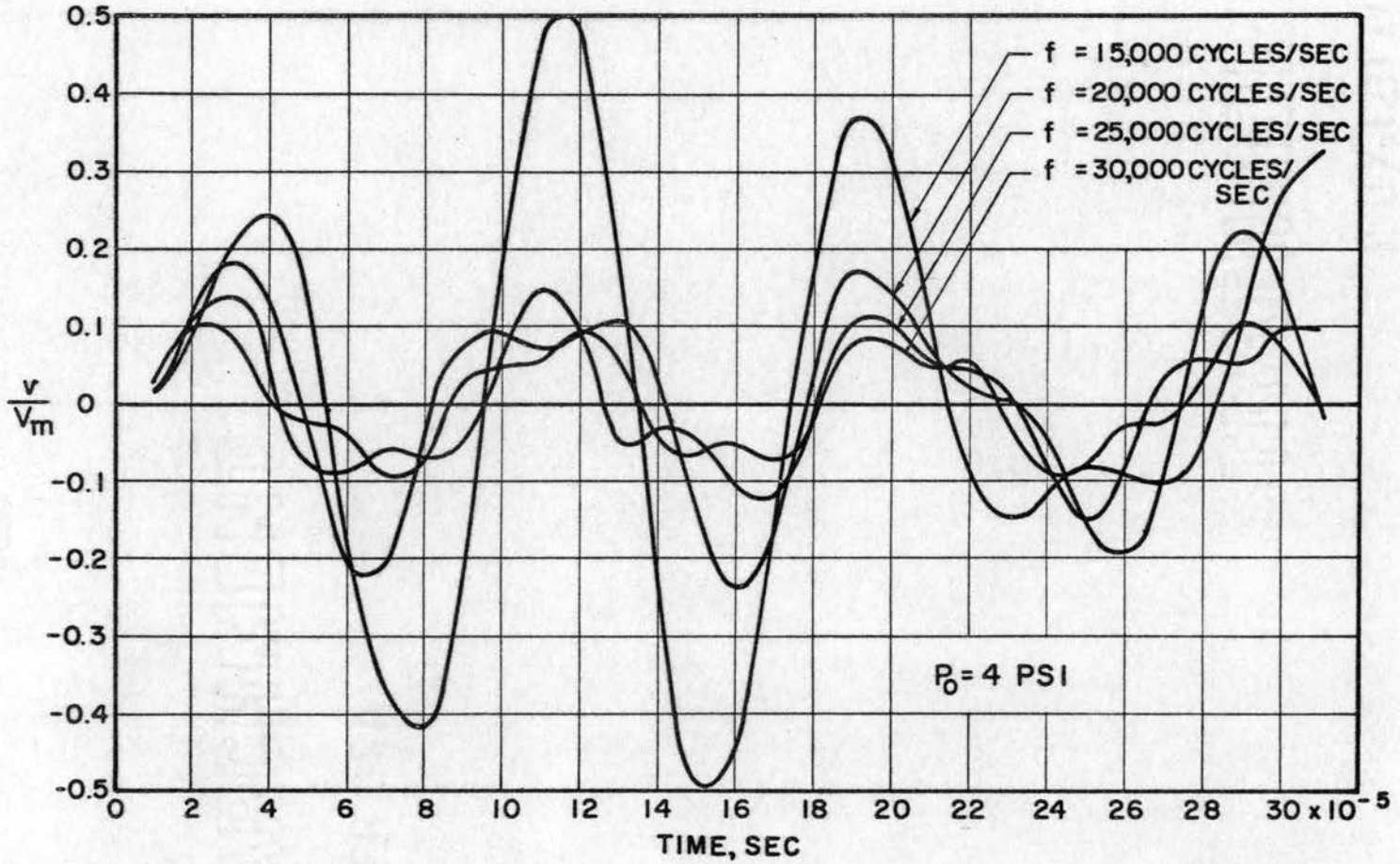

Figure 6. Effect of Sound Frequency on the Volume Pulsation of a Vapor Bubble at Constant Sound Pressure.

The relation between the resonant radius of a vapor bubble and its natural frequency has been derived in the last section and is reproduced as follows

$$\omega_n^2 = \frac{3r\left(P_a + \frac{2\sigma}{R_n}\right)}{\rho_\ell R_n^2} \tag{53}$$

It should be known that the derivation of Equation (53) has been based upon the following assumption. A vapor bubble is imagined to be in the fluid of infinite extent and is not influenced by an existence of the boundary. According to Equation (53) and with the following numerical value

$$r = 1.4$$

$$P_a = 2120 \text{ lbf/ft}^2$$

$$\sigma = 0.00383 \text{ lbf/ft}$$

$$\rho_\ell = 59.7 \text{ lbm/ft}^3$$

the resonant radius of a vapor bubble has been calculated for various sound frequencies and is shown in Figure 7.

The radius of a vapor bubble departing from a heating surface under no influence of sound can be approximately calculated through the equation derived by Fritz (39). For comparison, Fritz's equation is reproduced as follows

$$R_d = 0.0104\ \Phi \left[\frac{\sigma}{g(\rho_\ell - \rho_v)}\right]^{\frac{1}{2}} \tag{54}$$

where the contact angle Φ is measured in degree. According to Equation (54) and with the following data

$$\sigma = 0.00383 \text{ lbf/ft}$$

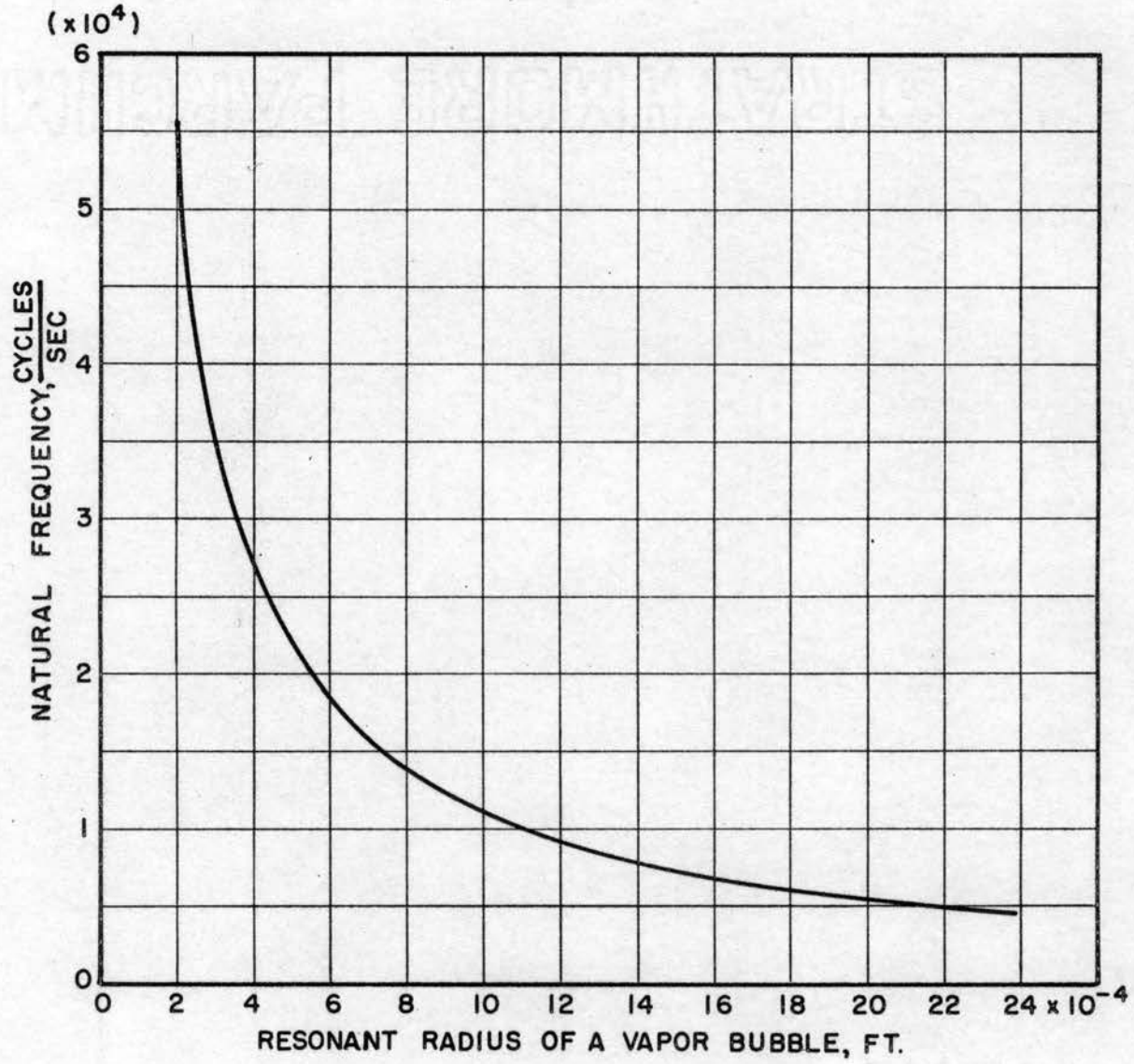

Figure 7. Natural Frequency of a Vapor Bubble Versus its Resonant Radius.

$$\rho_\ell = 59.7 \text{ lbm/ft}^3$$

$$\rho_v = 0.0373 \text{ lbm/ft}^3$$

$$g = 32.17 \text{ ft/sec}^2$$

the radius of a vapor bubble departing from the heating surface has been calculated for various contact angles and is shown in Figure 8.

It is seen in comparison between Figure 7 and Figure 8 that the resonant radius of a vapor bubble for sound waves of 20,000 cycles/sec is 5.6×10^{-4} ft., much smaller than the value obtained from Equation (54) for various contact angles. In other words, the vapor bubble may disappear with an explosion on the heating surface before it can grow to such an extent that the vapor bubble would depart from the heating surface on its own buoyant force. Thus it can be expected that the stirring motion due to the bubble departure from a heating surface would be greater in the sound field than in the case without sound. It is also seen in Figure 7 that the higher the frequency of sound, the smaller the resonant radius of the vapor bubble in the liquid.

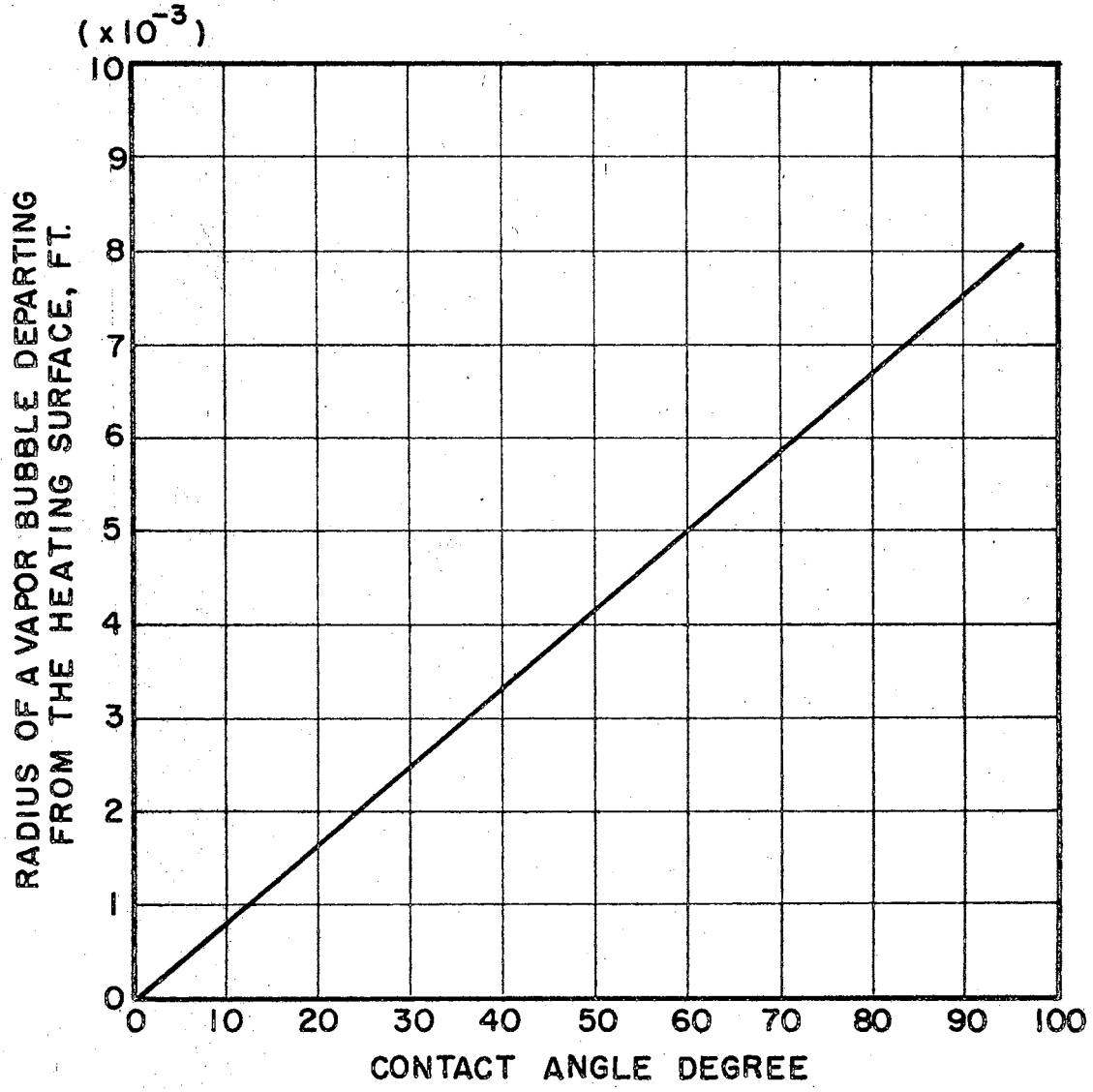

Figure 8. Radius of a Vapor Bubble Departing From the Heating Surface, According to Eq (54).

CHAPTER IV

DESCRIPTION OF APPARATUS

An apparatus was constructed to produce nucleate boiling water around the heating element and to measure the heat transfer coefficient and the temperature of the heating surface under various acoustical conditions and bulk temperatures of water. The apparatus consisted of two systems: (1) A system to measure the heat transfer coefficient on the heating surface under various acoustical conditions and different bulk temperatures of water; (2) A system of sound generation and the measurement of sound pressure in the vicinity of the heating surface.

Heat Transfer Measurement

A schematic diagram of the system for the heat transfer measurement is presented in Figure 9. Two rectangular tanks of different sizes (26" x 19" x 18") and (18" x 12" x 16"), were made of stainless steel. The tank of small size was supported by the big tank in such a way as shown in Figure 10, while the big tank rested on the floor. In operation, the two tanks were filled with the fresh water. The water level in the small tank was maintained at about 6 inches in height. Two heaters which were used to raise the water temperature to the desired level were installed near the bottom of the big tank. Because of this arrangement, the convective currents produced by the heaters would not

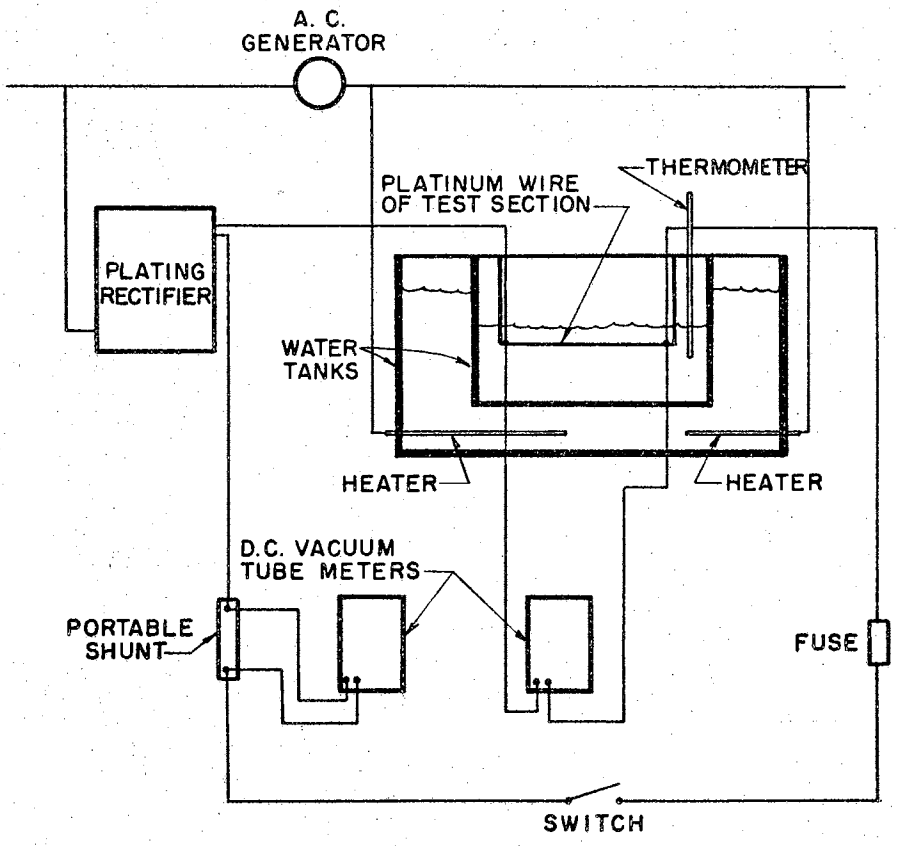

Figure 9. A Schematic Diagram of the System for Heat Transfer Measurement.

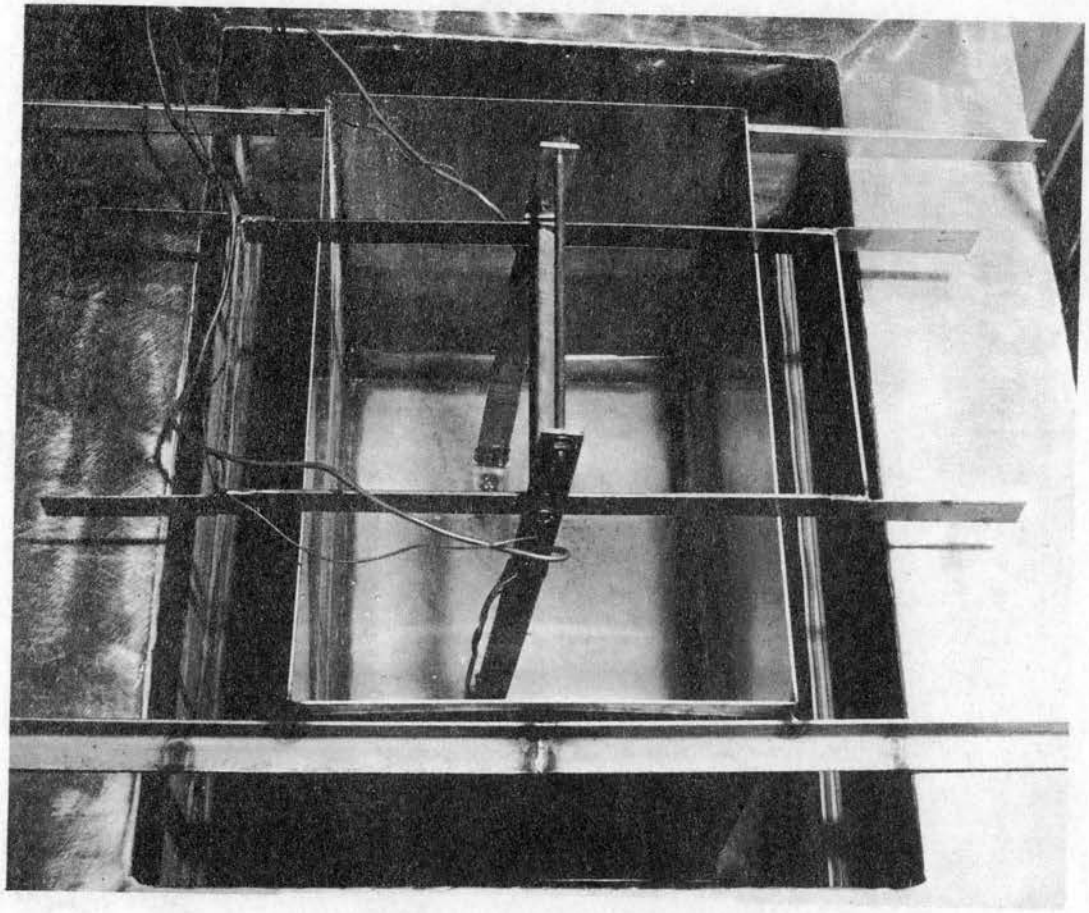

Figure 10 A Photograph of the Arrangement of the Two Water Tanks

enter into the water in the small tank; therefore, the temperature of the water in the tank could be uniformly maintained. The water level in the big tank was immaterial as long as it was high enough to cover the diaphrams of the magnetostrictive oscillators which were installed at both sides of the big tank. More description about the sound generation and its measurement will follow in a later section.

The heating surface on which the heat transfer rates were measured under various conditions consisted of a piece of platinum wire 0.008 inches in diameter and about 6 inches in length. During operation, the platinum wire was submerged under water in the small tank and about 1.5 inches from the bottom of the small tank. The platinum wire of the test section was suspended by the "hanger" in such a manner that the wire of the test section can be replaced after a certain time. This construction insured that the same surface condition could be expected during all runs of the experiments. A rectifier was used to transform the alternating current to the direct current which energized the circuit as shown in Figure 9. The power supplied by the rectifier could be adjusted by the rheostat installed inside the rectifier.

Direct current in the circuit was measured through the use of a portable shunt and a D-C vacuum-tube meter. The voltage drop across the wire of the test section was directly indicated on another D-C vacuum-tube meter. The bulk temperature of the water was obtained by two thermometers. The average value of two readings was used.

Measurement of the voltage drop across the platinum wire of the test section and the direct current through it provided enough data from which the temperature of the heating surface and heat transfer rate from it

could be calculated. Combined with measurement of bulk temperature of water, the above data were also used to calculate the heat transfer coefficient between the heating surface and its surrounding boiling water.

The data of fresh water used in the experiments were provided by the water plant of Stillwater, Oklahoma and presented in Appendix B.

Sound Measurement

The schematic diagram for a sound generation and its measurement is shown in Figure 11. The sound waves of 20,000 cycles/sec used in these experiments were generated by the several oscillators of magnetostriction-type. These oscillators were mounted on both sides of the tank as shown in Figure 12. It should be noticed, however, that the oscillators mounted on the bottom of the tank, as shown in Figure 12, were not used in any run of the present experiments. The power supplied to the oscillators mounted on both sides of the tank was provided by an ultrasonic generator manufactured by International Ultrasonic Company. Since there was only one set of oscillators available at that time, all sound waves in these experiments were of 20,000 cycles/sec while the acoustical energy input to water in the tank could be controlled in the ultrasonic generator. The console of the sound generator and the arrangement of the whole experimental setup are shown in Figure 13. In this experimental setup, it was expected that the pattern of sound waves in water would be very complicated because of a complete reflection at a water-air interface, a partial reflection at the wall of the tanks and an interaction among the sound waves.

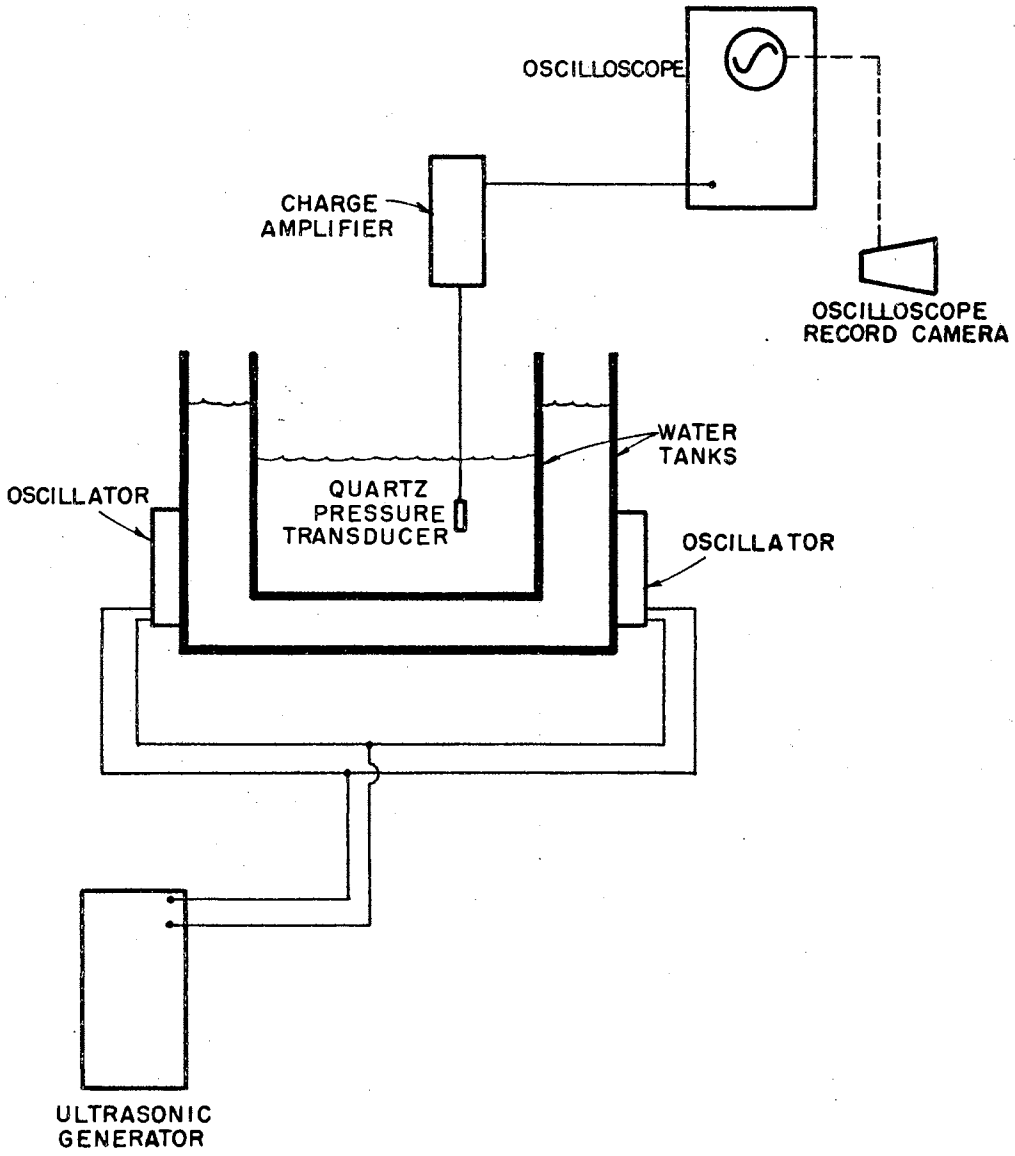

Figure 11. A Schematic Diagram of the System for the Sound Generation and its Measurements.

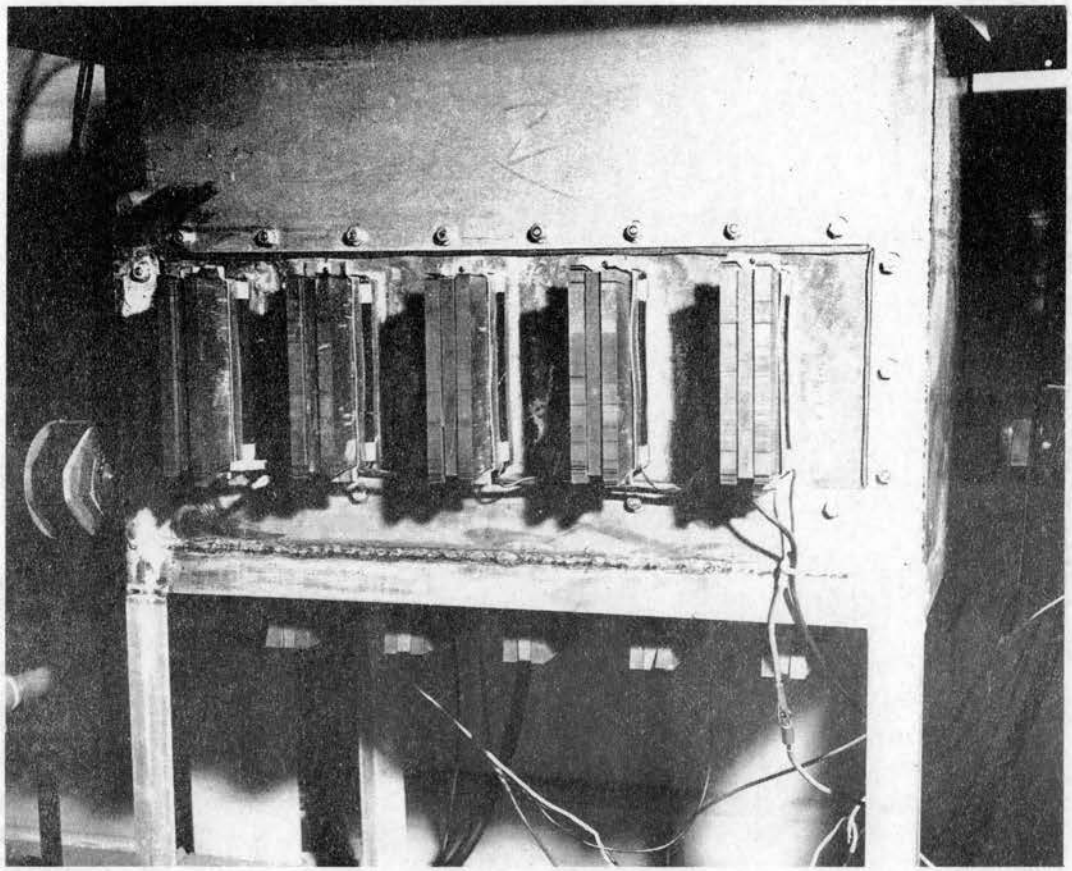

Figure 12 A Photograph of the Magnetostrictive Oscillators Mounted on Both Sides of the Water Tank

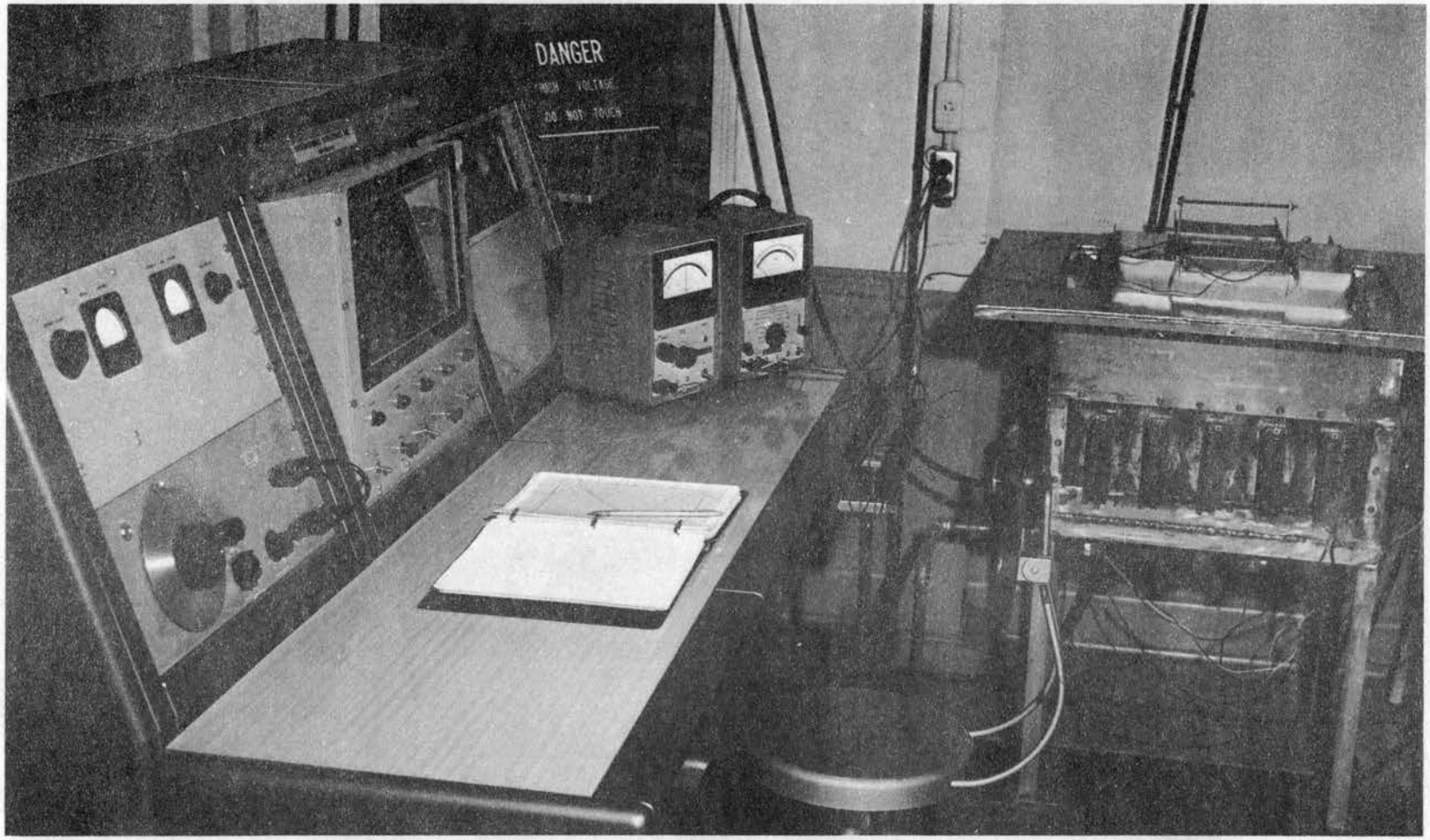

Figure 13 The Console of the Sound Generator and the Arrangement of the Present Apparatus

It was obvious that the sound intensity or sound pressure would not be uniformly distributed in the water. It, therefore, became necessary to measure the sound pressure in the water at the vicinity of the heating surface rather than to measure the acoustical energy input into the water.

To measure the sound pressure just mentioned above, a quartz pressure transducer was used and connected with an oscilloscope through a charge amplifier. An oscilloscope record camera was used to record the sound pressure at the location where the pressure transducer was placed. The photographs obtained in this way could also indicate the sound frequency in that location. The system of sound measurement had been thoroughly calibrated before it was used in the experiments.

A list of equipment used in the present investigation was presented in Appendix C.

CHAPTER V

EXPERIMENTAL PROCEDURES

During all experiments these water tanks were filled with the fresh water. In the small tank the water level was about 6 inches in height. In the big tank, which supports the small tank, the water level was high enough to cover the diaphrams of magnetostrictive oscillators. The water was heated to the desired level and maintained in an equilibrium condition by two submerged heaters before the experiments were started. (In one part of this experimental investigation, the temperature of the water was maintained in an equilibrium to the room temperature.) Then, the platinum wire of the test section was submerged into the water of the small tank and about 1½ inches from the bottom of the tank. The power supplied to the circuit shown in Figure 9 was provided and controlled by the rectifier. First, the nucleate boiling was produced under no influence of sound. During all experiments the power to the platinum wire of the test section was increased step by step. In other words, after a small increase in power, there would be no measurement of any type made unless the whole system was again in an equilibrium condition. In the present experimental setup, it took two minutes to reach this kind of equilibrium. In this manner, all heat transfer measurements were recorded. These procedures were repeated until the maximum power which could be obtained with the present setup was reached. Then the power was cut off and the platinum wire of the test section was replaced.

When the experiments were conducted under the influence of a sound field, the procedures in heat transfer measurements were the same as in the cases without the presence of sound. The sound measuring system had to be warmed up for 30 minutes before it was used. It was also necessary that the ultrasonic generator be warmed up for 15 minutes before it was coupled with oscillators and produced the waves in the water. At first, sound waves of low energy were produced and maintained while all heat transfer measurements were made in such a way as in the cases without sound. The same procedures were repeated to obtain the data for the cases with sound waves of high energy. In the ultrasonic generator used in the present investigation, the acoustic energy could be varied gradually at the sound frequency of 20,000 cycles/sec.

Since there were some unpredictable internal as well as external loss in the system, including sound generators, oscillators, and the path of propagation of sound waves in addition to the complexity of wave patterns in water at the vicinity of the heating element, it became necessary to measure the sound pressure in the vicinity of the platinum wire of the test section. During the experiments, the sound pressure signals received by the quartz pressure transducer obviously consisted of three parts: (1) the signals due to the sound waves produced by oscillators; (2) the signals due to the formation, growth and collapse of bubbles in the neighborhood of pressure transducers; and (3) the signals due to the existence of the heated platinum wire (40). It was believed that the signals of the second kind were far smaller than those of the first kind, and thus could be neglected. However, the signals of the third kind could not be neglected and had been known to depend upon the amount

of direct current through the platinum wire of the test section (40). To avoid these difficulties, the sound pressure was recorded when the power supplied to the platinum wire of the test section was cut off. This procedure was entirely justified as far as the purposes of present investigation were concerned. It was also expected that the sound pressure varied along the platinum wire. Therefore, three readings of sound pressure along the wire were recorded for each acoustic energy input. The average value of these three readings was used in the present investigation.

CHAPTER VI

EXPERIMENTAL RESULTS

Data of experiments which are considered to be reliable are tabulated in Appendix D. The surface temperature of the platinum wire of the test section, the heat transfer rate and heat transfer coefficient between the test section and its surrounding water, which were calculated from these experimental data, are also presented in Appendix D. It may be noticed that the experimental results presented here consists of two parts: one for the case in which the bulk temperature of water is around $85^{\circ}F$ (at that time, two submerged heaters were not used); another part for the case in which the bulk temperature of water is around $200^{\circ}F$. Based upon these experimental results, some curves are drawn and presented in this section to facilitate the discussion.

First, the experimental results for the case in which the bulk temperature of water is around $85^{\circ}F$ are presented. Figure 14 indicates that the heat transfer rate is affected in the presence of a sound field both in the free convective region and the nucleate boiling region. It is also indicated that the heat transfer rate will increase with increasing sound pressure at the sound frequency of 20,000 cycles/sec when the temperature difference, ΔT, remains constant. Temperature difference means the surface temperature of the platinum wire of the test section minus the bulk temperature of its surrounding water. It should be noticed that

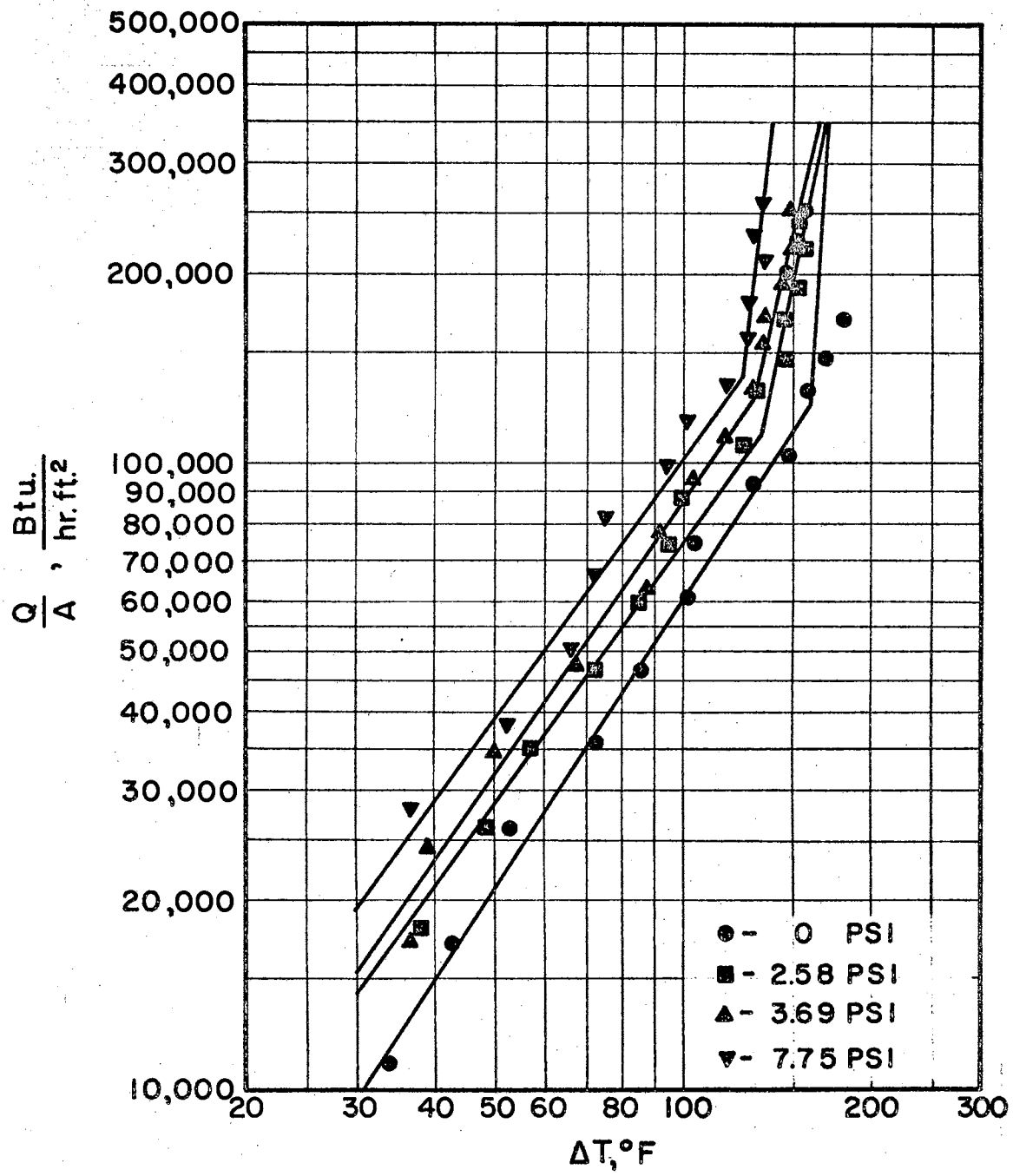

Figure 14. Heat Transfer Rate Versus the Temperature Difference for Various Sound Pressures, I.

the bulk temperature of the water in this case could not be maintained constant during all experiments because some of the acoustical energy was converted into thermal energy and thus increased the bulk temperature of water. The sound pressure referred to in this report is the average peak-to-peak value. Three readings along the platinum wire of the test section were recorded for each acoustical energy input. The average value of these three readings was reported in this thesis. Some of the photographs recording the sound pressures for various acoustical power inputs are reproduced and shown in Figure 15 and Figure 16. It is seen in these photographs that the wave patterns in the water in the vicinity of the test section are complicated and the frequencies of these waves are very close to 20,000 cycles/sec. The method of calculation for the surface temperature of the platinum wire of the test section, the heat transfer rate and coefficient is presented in Appendix E.

Figure 17 indicates that there exists a certain value of sound pressure beyond which the effects of sound waves on heat transfer rate become less pronounced in nucleate boiling region and the heat transfer rate would start to decrease in the free convective region. The value of sound pressure has been found to be 7.75 psi in the present setup when the bulk temperature of the water is around $85^{\circ}F$. It should be noticed in Figure 17 that only data points are presented for the two cases in which the sound pressures are 9.34 psi and 9.70 psi respectively. The dotted lines are reproduced from Figure 14 for comparison. Similarly the curves for heat transfer coefficient against the temperature difference are drawn and presented in Figure 18 and Figure 19. All of the curves correlating the experimental data in Figure 14, Figure 17, Figure 18,

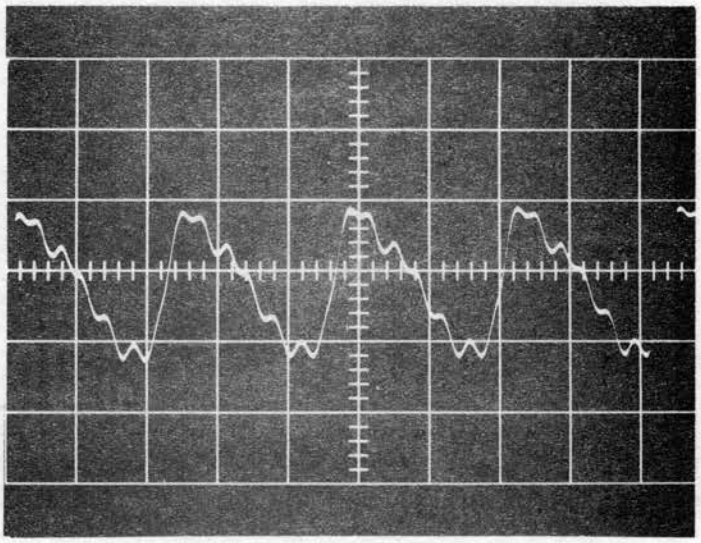

Figure 15 Sound Pressure Signals on the Oscilloscope Screen,
Vertical Scale: 1.24 psi/cm;
Horizontal Scale: 20 μ sec/cm

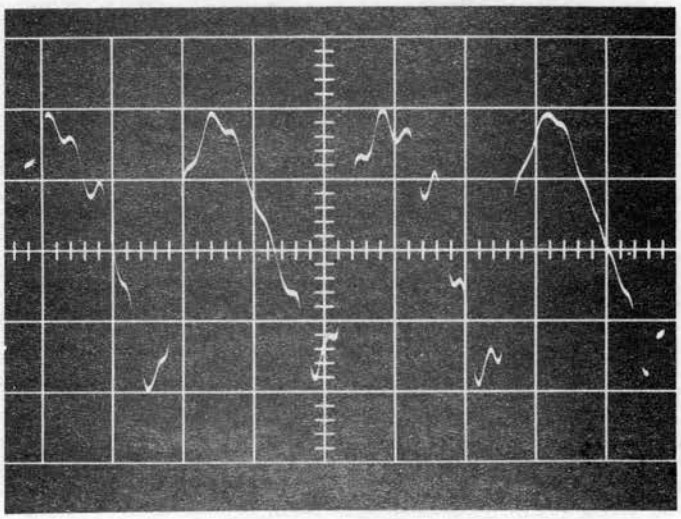

Figure 16 Sound Pressure Signals on the Oscilloscope Screen,
Vertical Scale: 2.48 psi/cm;
Horizontal Scale: 20 μ sec/cm

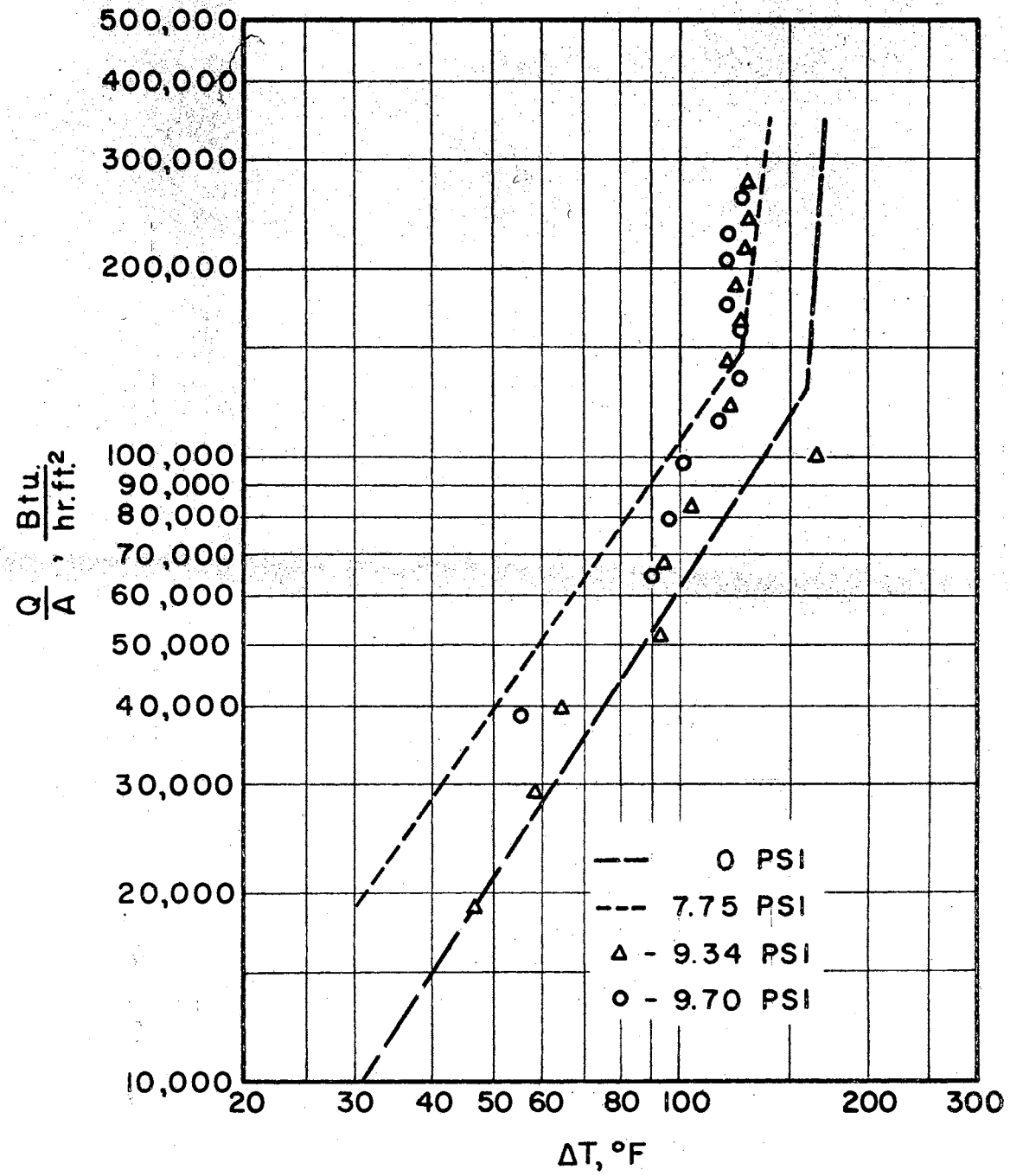

Figure 17. Heat Tranfer Rate Versus Temperature Difference for Various Sound Pressures, II.

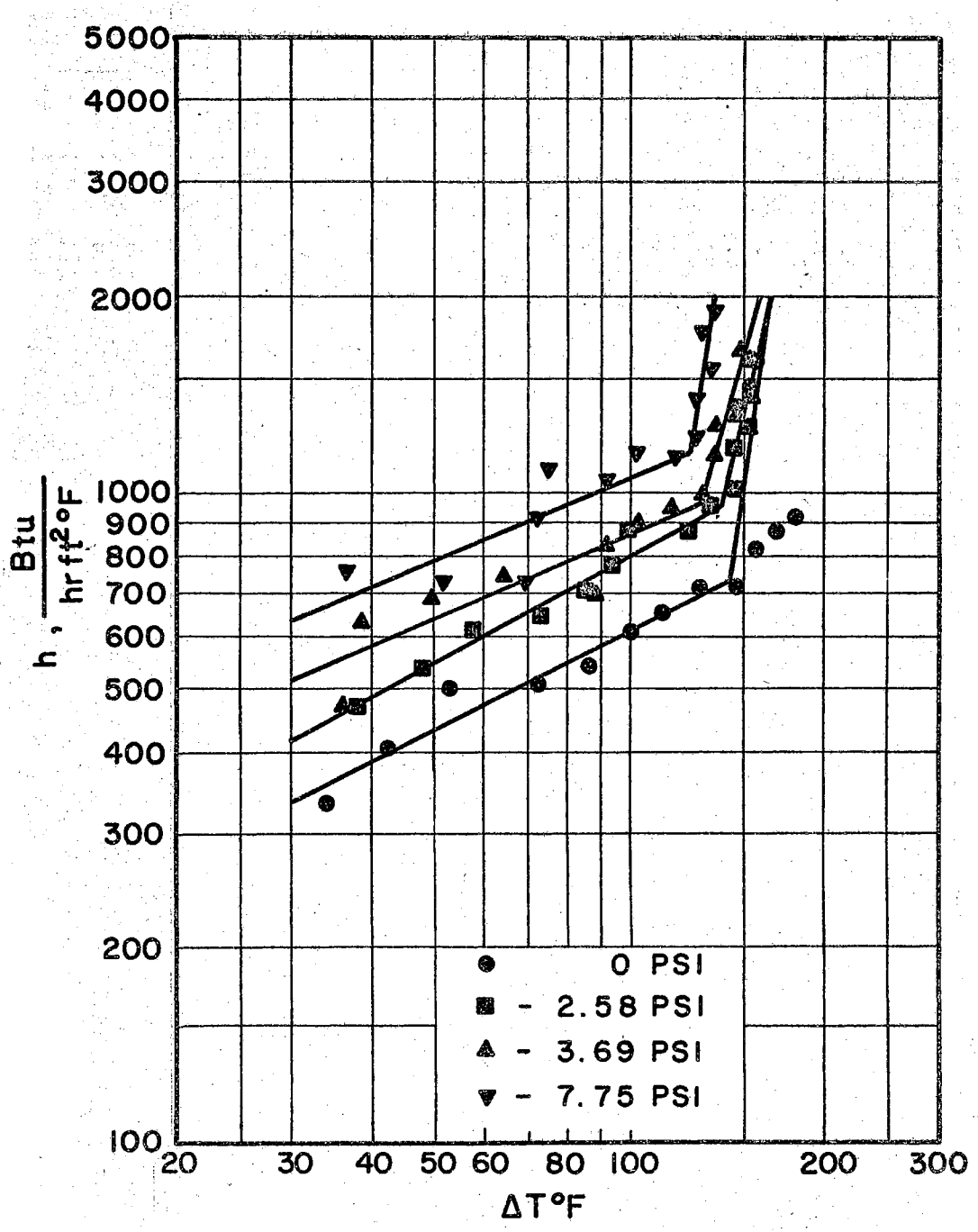

Figure 18. Heat Transfer Coefficient Versus Temperature Difference for Various Sound Pressures, I.

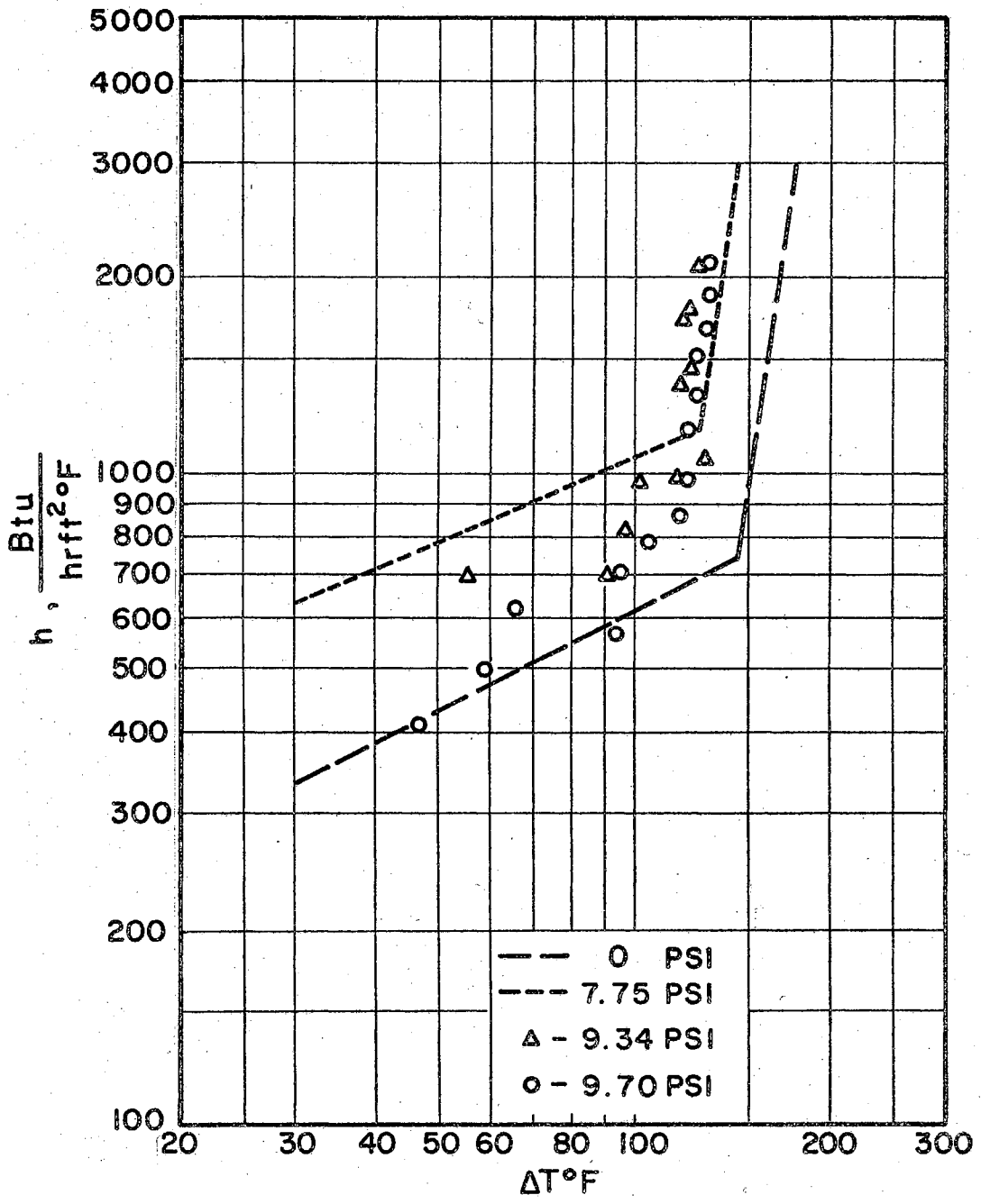

Figure 19. Heat Transfer Coefficient Versus Temperature Difference for Various Sound Pressures, II.

and Figure 19 are determined through the use of the least square method. Unfortunately, there is no other information available for comparison with the present results.

Figure 20 shows the relation between the heat flux and the sound pressure in the free convection region. It is seen that when the sound pressure increases in the vicinity of the test section the heat flux will increase for a given temperature difference. Sometimes, this increase is about 80% more than the amount of heat flux obtained in the absence of sound waves, such as shown in Figure 21. Figure 21 also indicates that the effects of sound waves on the heat flux is more pronounced with a small temperature difference.

It may be interesting to note that the incipient point of pool boiling is also affected in the sound field of 20,000 cycles per second. It is seen in Figure 22 that the surface temperature of the platinum wire of the test section at the incipient point of boiling will decrease as the sound pressure increases. That is, the presence of sound waves would make the nucleate boiling occur sooner. For example, in the absence of sound, the surface temperature of the test section is 240° F at the present experimental setup when the nucleate boiling occurs. However, in the presence of a sound field with a sound pressure of 7.75 psi and a sound frequency of 20,000 cycles/sec, the surface temperature in consideration is only about 213° F. As shown in Figure 22, the effects of sound waves on the incipient point of nucleate boiling will become less pronounced as the sound pressure increases.

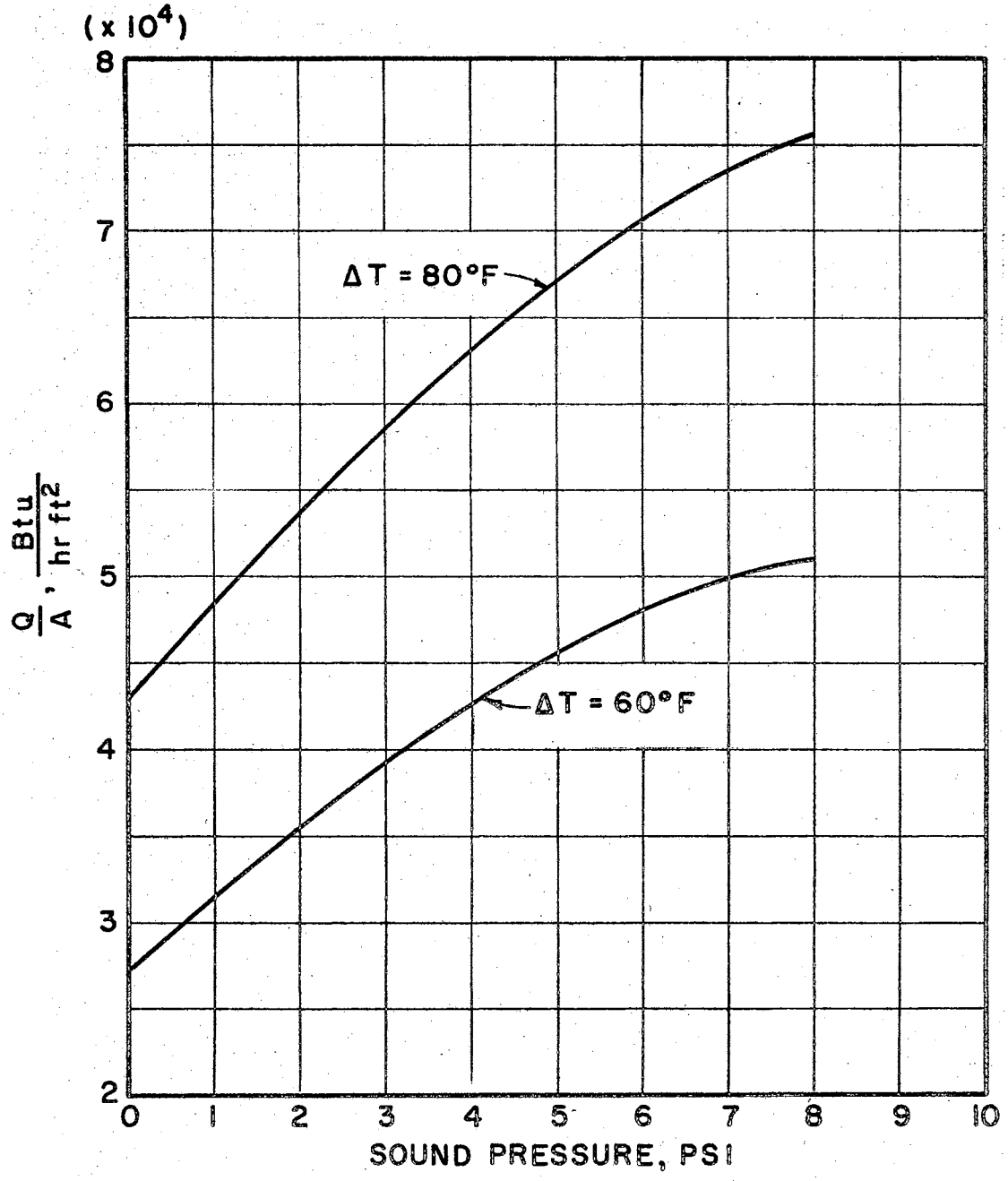

Figure 20. Heat Transfer Rate Versus Sound Pressure in Free Convection Region.

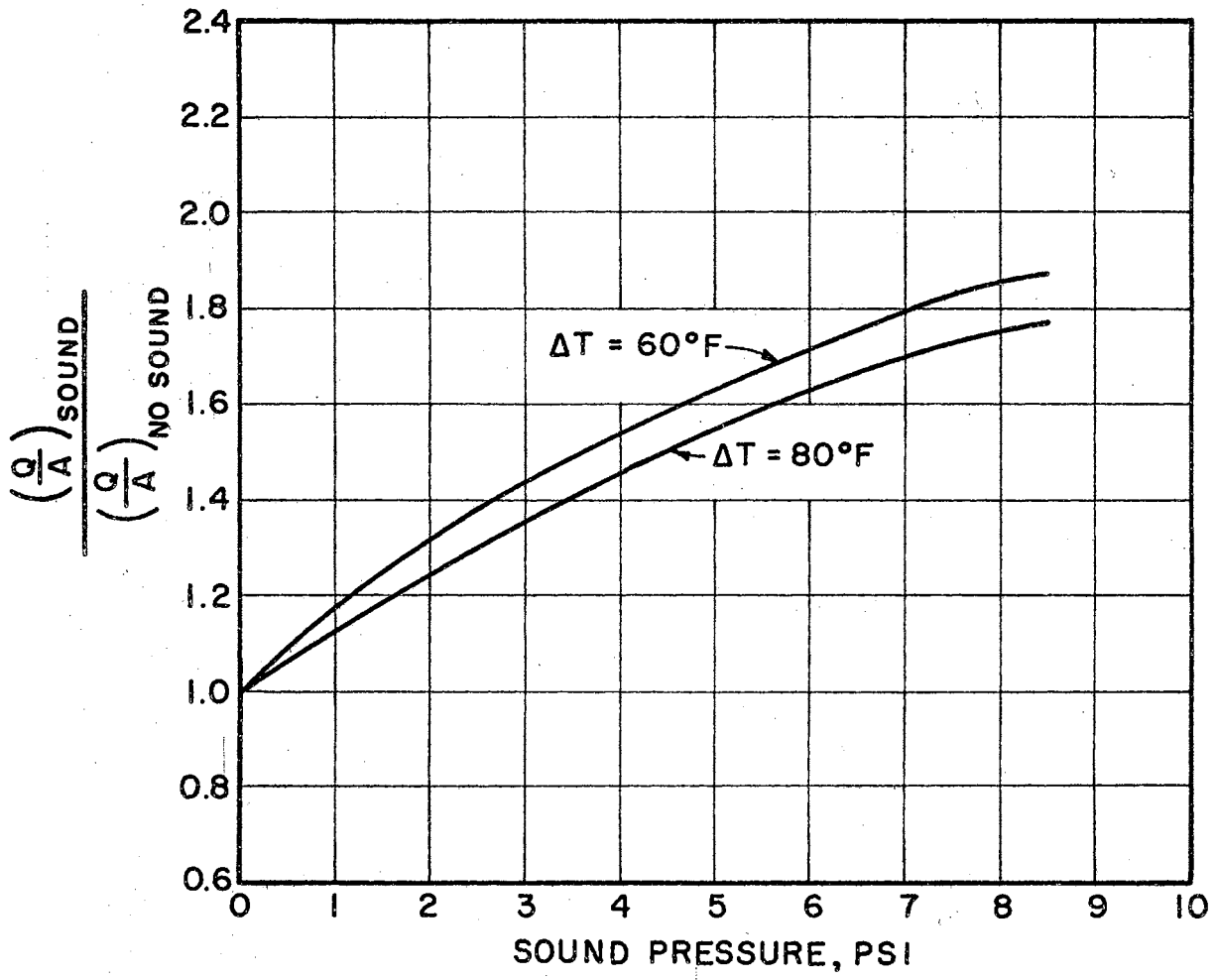

Figure 21. Ratio of Heat Transfer Rate with Sound to Heat Transfer Rate Without Sound Versus Sound Pressure in Free Convection Region.

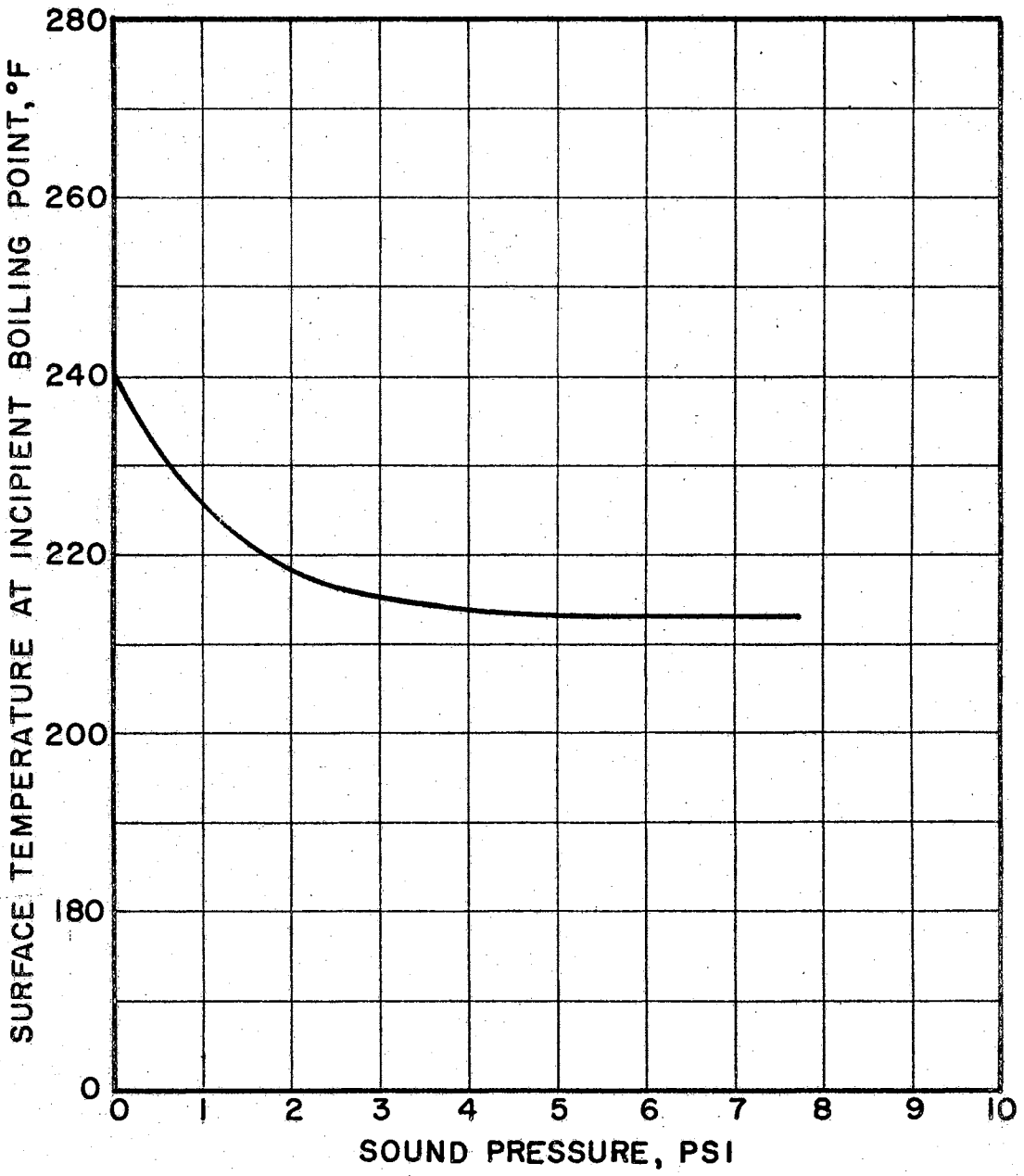

Figure 22. Effect of Sound Waves on the Incipient Point of Nucleate Boiling at One Atmospheric Pressure.

It should be noticed that the incipient points of nucleate boiling under various sound pressures presented here are determined by the intersection of the nucleate boiling line and free convection line on a log-log plot of heat transfer rate versus the temperature difference. All these incipient points of boiling are indicated in Figure 14 and located at the knees of the heat-flux curves for nucleate boiling. The incipient point of nucleate boiling defined in this way is the idealized point at which the boiling phenomenon becomes the predominant heat transfer mechanism. In the present apparatus, the surface temperature at the incipient boiling point has been found to be 240^{o}F under no influence of sound waves. This value is in close agreement with those obtained by some other researchers (41), (42), (43). Since no other information is available for the case in which the surface temperature in consideration is recorded under the influence of sound waves, the experimental results obtained in this investigation cannot be entirely checked at the present time.

In the present investigation, one of the important findings is that the surface temperature of the heating element can be reduced at a given heat flux through the use of sound waves. Based upon the experimental data, the curves for the surface temperature of the test section versus the heat flux have been plotted and are shown in Figure 23. Each of these curves were obtained under a certain sound pressure. It is seen that the cooling will increase both in free convection region and in nucleate boiling region as the sound pressure increases. For example, it is shown in Figure 24 that an increase in sound pressure would gradually reduce the surface temperature of the test section in the

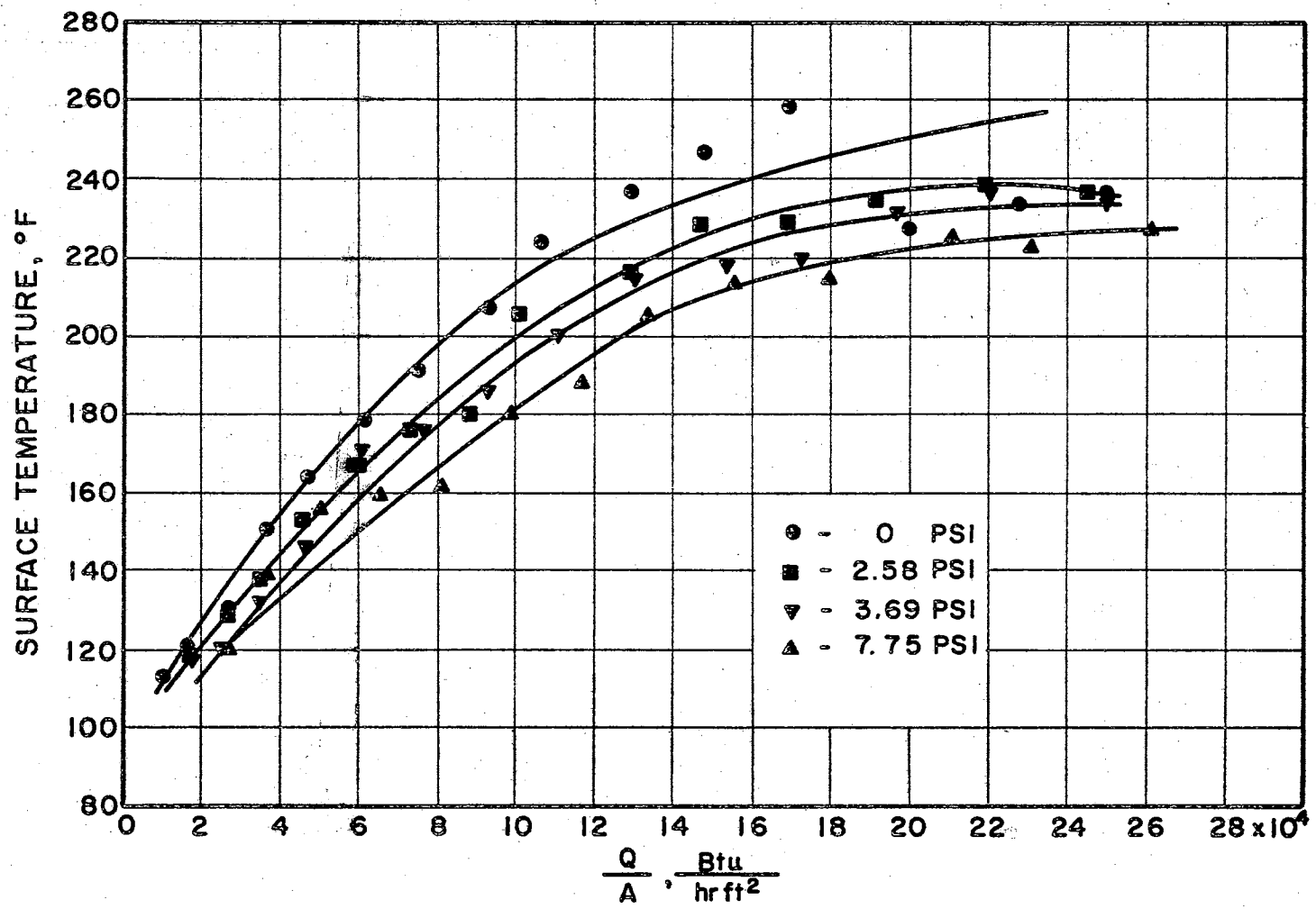

Figure 23. Surface Temperature of Test Section Versus the Heat Flux for Various Sound Pressures, I.

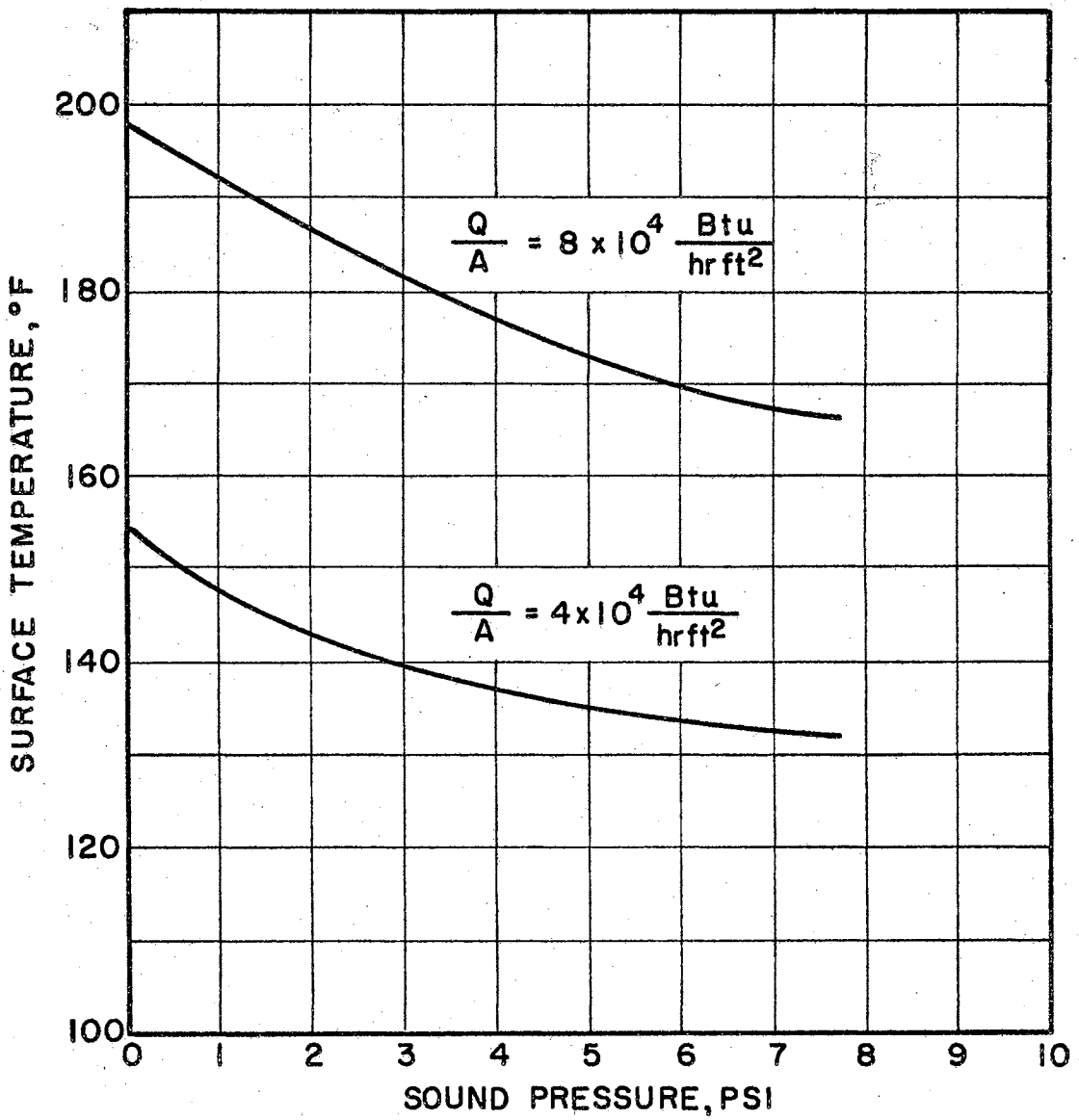

Figure 24. Effect of Sound Waves on the Surface Temperature of Test Section in Free Convection Region.

free convection region, even when the heat flux is maintained. Figure 25 indicates the similar effect of sound waves on the surface temperature of the test section in the nucleate boiling region.

It may be interesting to note that this acoustically-induced cooling effect on the heating surface cannot be continually increased by increasing the sound pressure. Figure 26 apparently shows that there exists a certain value of sound pressure beyond which the surface temperature of the test section will not be continuously reduced, but on the contrary, will start to go up. This value of sound pressure has been found to be approximately 7.75 psi in the present apparatus. It should be noticed in Figure 26 that the data points are only presented for the two cases in which the sound pressures are 9.34 psi and 9.70 psi, while the two dotted lines are reproduced from Figure 23 for comparison.

Some experiments were carried out for the water with the bulk temperature around 200°F in the present investigation. During these experiments the two submerged heaters were used to maintain this temperature of the water. It was found that the bulk temperature of the water was quite steady in this series of experiments, whether the sound waves were applied or not. As mentioned before, the data of experiments are tabulated and shown in Appendix D. Some results calculated from these data are also presented in the same appendix. It may be noticed that the method of calculation for the surface temperature of the test section, the heat transfer rate and coefficient is the same as that used in the case in which the bulk temperature of the water is around 85°F. When the bulk temperature of the water is maintained at 200°F, only the nucleate boiling phenomenon could be studied in the present experimental setup.

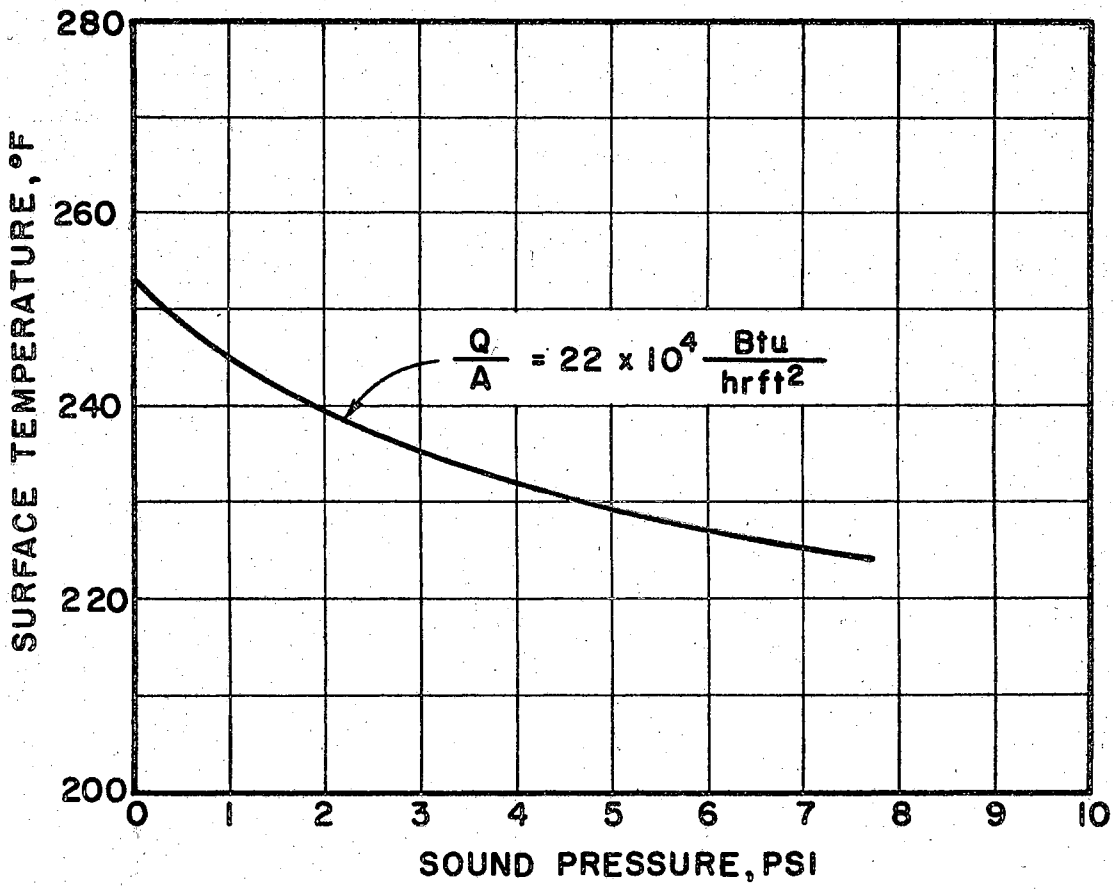

Figure 25. Effect of Sound Waves on the Surface Temperature of Test Section in Nucleate Boiling Region.

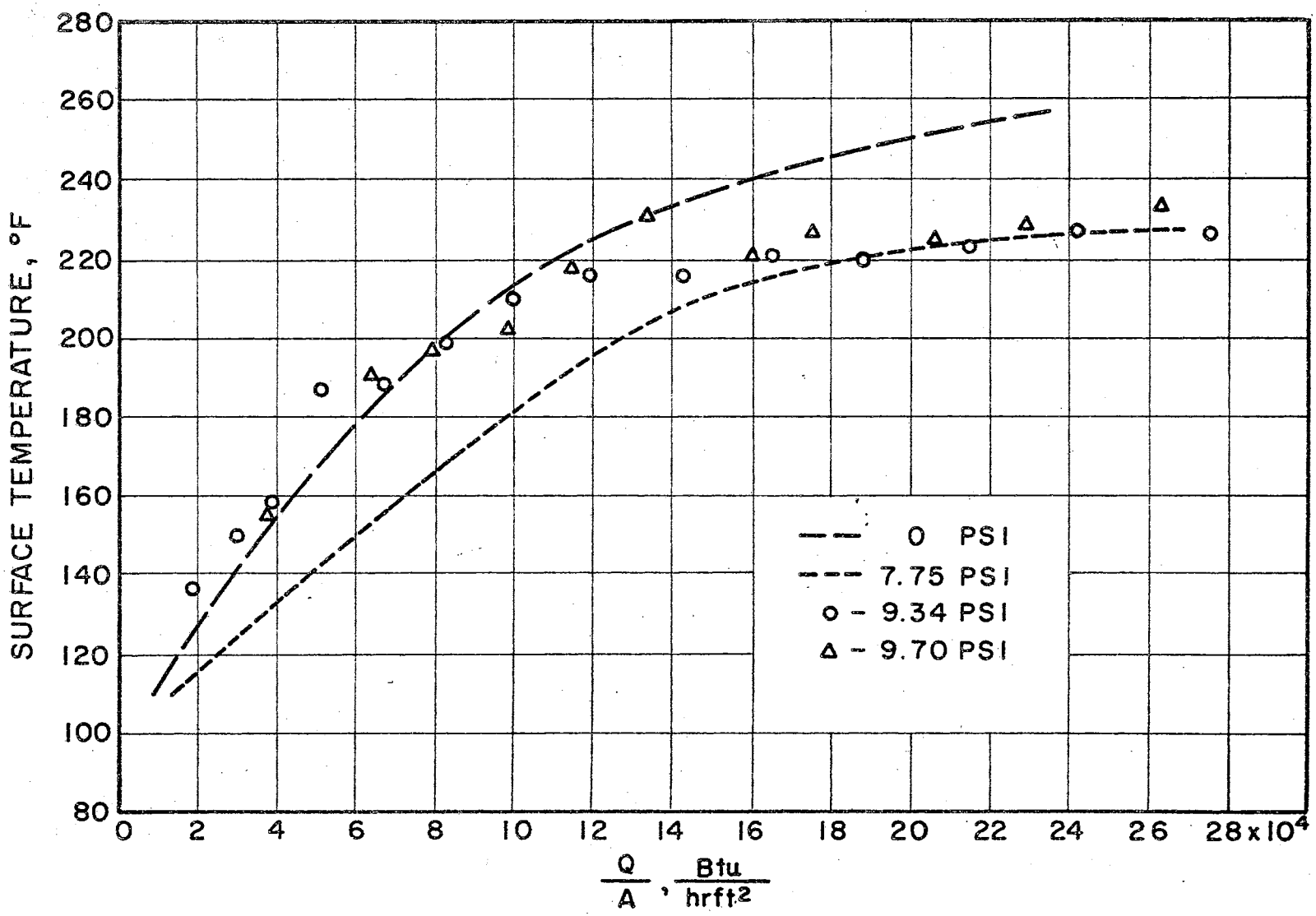

Figure 26. Surface Temperature of Test Section Versus the Heat Flux for Various Sound Pressures, II.

Figure 27 indicates that the heat flux from the test section varies with the temperature difference under various acoustical conditions. The frequency of sound waves applied in this series of experiments is fixed at 20,000 cycles/sec while the sound pressure in the vicinity of the platinum wire of the test section varies from zero psi to 6.25 psi. It is seen in Figure 27 that when the sound pressure in consideration is in the range of zero psi to 3.69 psi the heat flux in the nucleate boiling region can be increased by increasing the sound pressure even if the temperature difference remains constant. Since these curves shown in Figure 27 are not parallel to each other, it is expected that the effect of sound waves on the heat flux in nucleate boiling region will not be the same for various temperature differences. For example, it is seen in Figure 28 that when the sound pressure is maintained to be 3 psi in the vicinity of the test section, the ratio of heat flux from the test section under the influence of sound to the heat flux in the absence of sound is 2.28 at the temperature difference $70^{\circ}F$. However, the ratio in consideration is only 1.94 when the temperature difference changes to $80^{\circ}F$. A comparison between Figure 21 and Figure 28 indicates that the effect of sound waves on the heat flux in the nucleate boiling region is different from that in the free convection region. It seems that the presence of sound waves is more effective in increasing the heat flux in the nucleate boiling region than in the free convection region. Figure 28 also indicates that the heat flux in nucleate boiling region can be increased almost three times in the present apparatus through the use of sound waves.

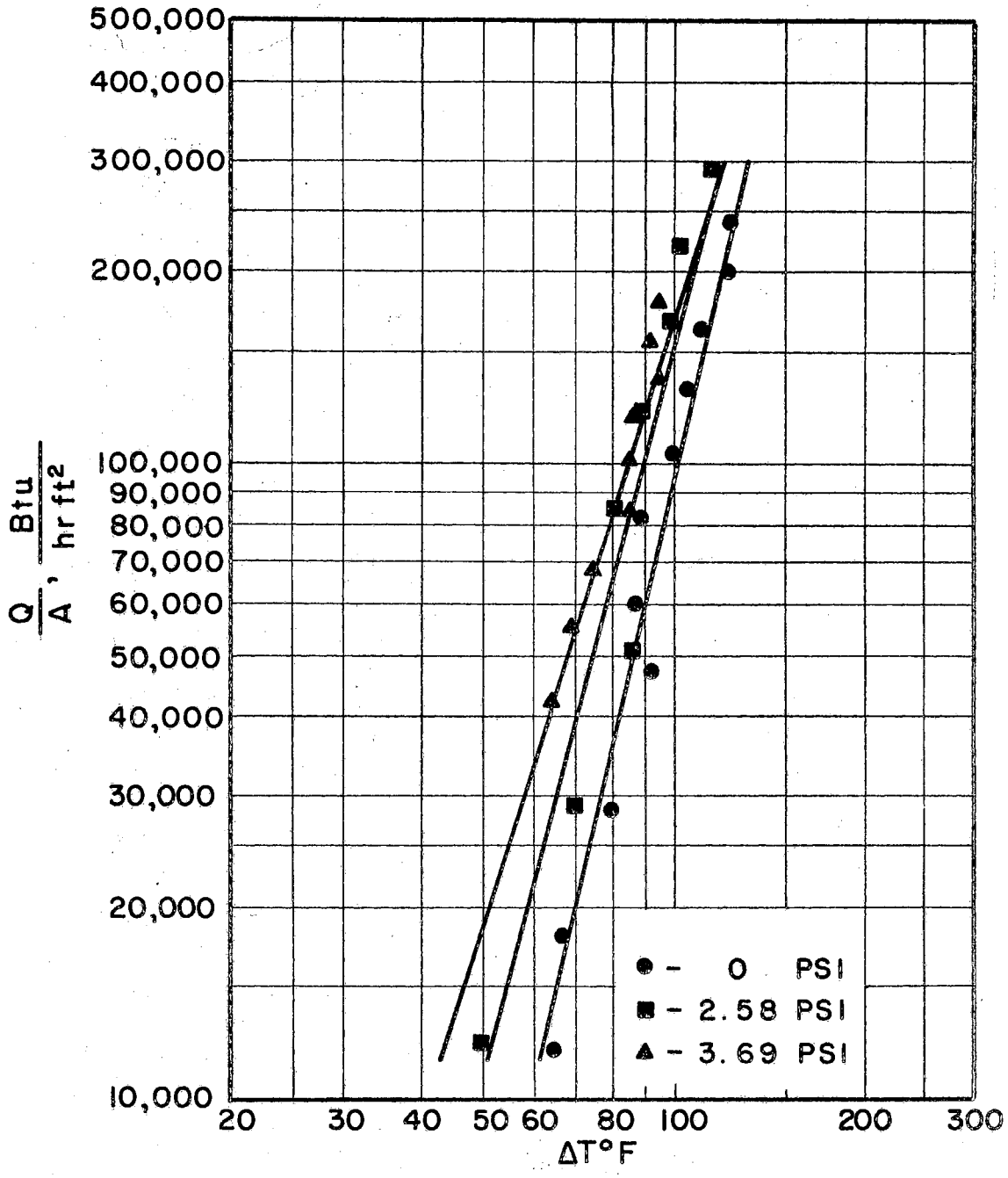

Figure 27. Heat Transfer Rate Versus Temperature Difference for Various Sound Pressures, I. (Bulk Temperature of Water ≐ 200°F).

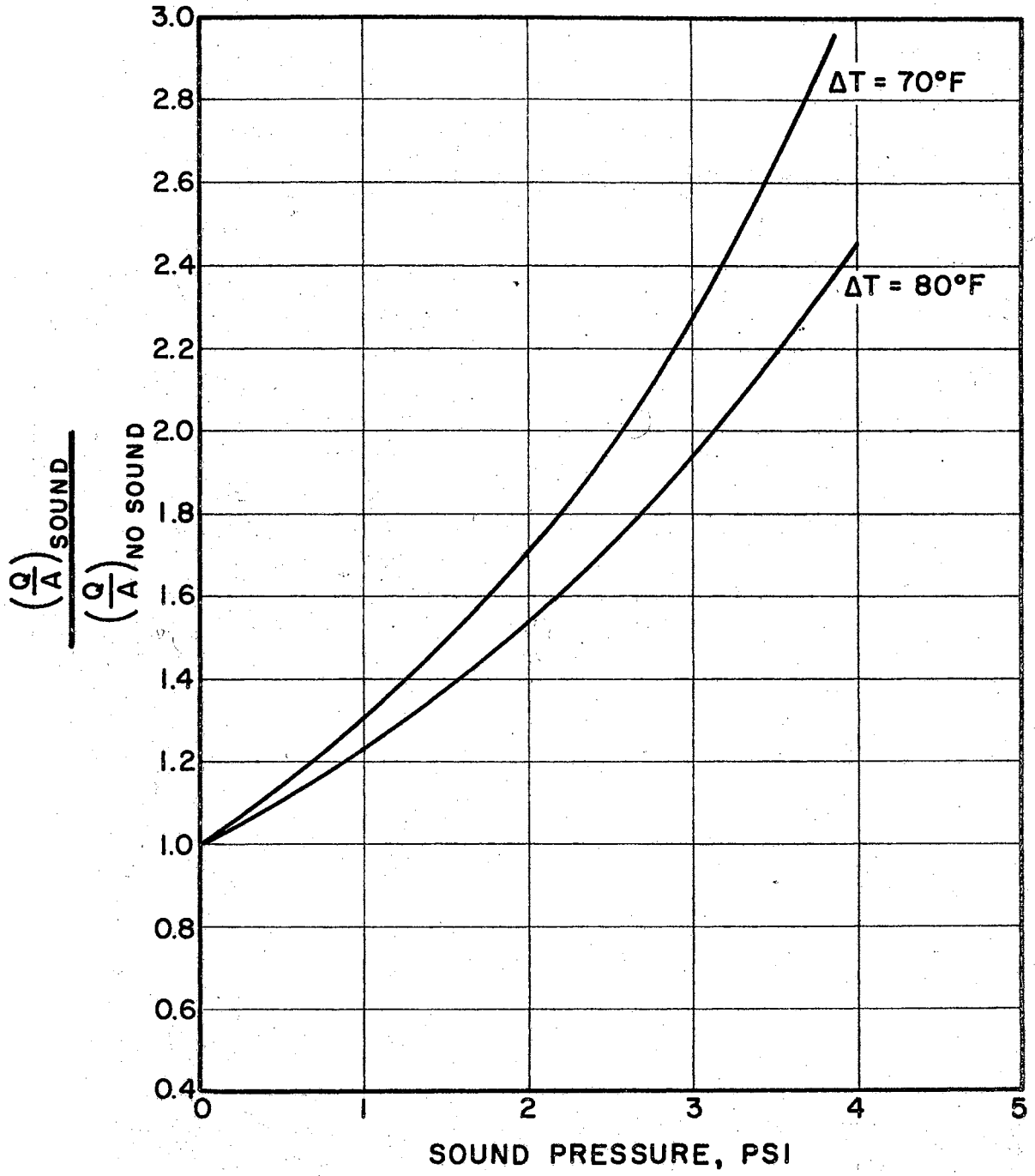

Figure 28. The Ratio of Heat Flux Under the Influence of Sound to the Heat Flux in the Absence of Sound vs the Sound Pressure in Nucleate Boiling Region.

Figure 29 shows the relation between the heat flux in the nucleate boiling region and the sound pressure at a constant sound frequency of 20,000 cycles/sec. It should be remembered that these results are only valid when the bulk temperature of the water is around 200°F in the present apparatus. It is seen that when the sound pressure increases in the vicinity of the test section, the heat flux will increase at a given temperature difference. However, the heat flux in the nucleate boiling region cannot be continuously increased by increasing the sound pressure at a constant sound frequency. It was indicated in the experiments that when the sound pressure was increased beyond 3.69 psi in the vicinity of the test section, the effect of sound waves on the heat flux in the nucleate boiling region became more complicated than was expected. Figure 30 shows that when the sound pressure is equal to 6.25 psi not all of the data points representing the values of heat flux at various temperature differences under this acoustical condition are above the dotted line which is determined for the sound pressure 3.69 psi. It seems that there are two sections in the range of present experiments: One section in which the heat fluxes are generally greater for the sound pressure 6.25 psi than the corresponding values for the sound pressure 3.69 psi. In another section, on the contrary, the heat fluxes will decrease as the sound pressure increases to 6.25 psi from the value 3.69 psi. It may be noticed that these two dotted lines shown in Figure 30 are just reproduced from Figure 27 for comparison. For completeness, the curves for heat transfer coefficient versus the temperature difference are plotted and presented in Figure 31 and Figure 32. All these curves correlating the experimental data in

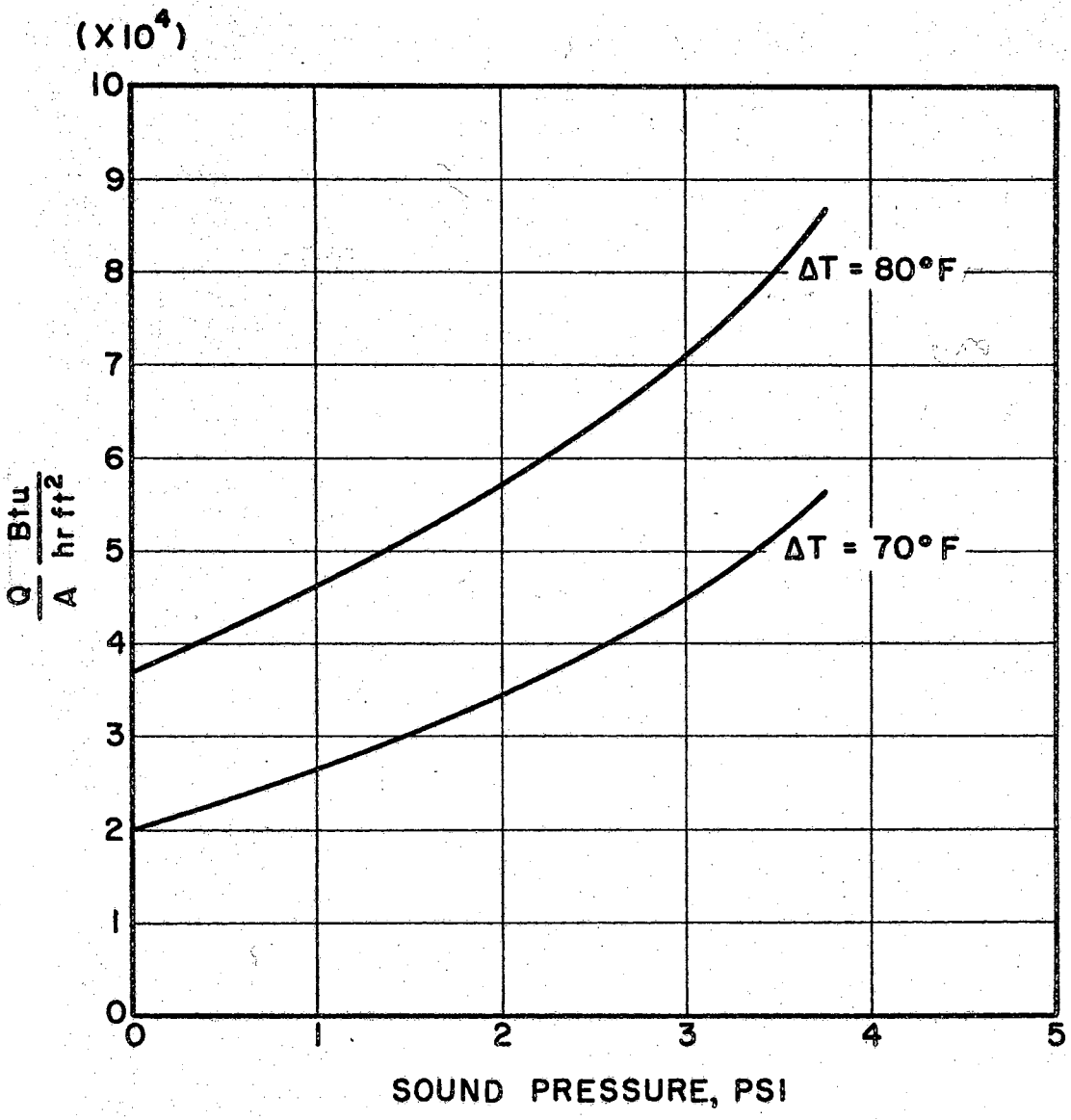

Figure 29. Heat Transfer Rate Versus Sound Pressure in Nucleate Boiling Region. (Bulk Temperature of Water ≐ 200°F).

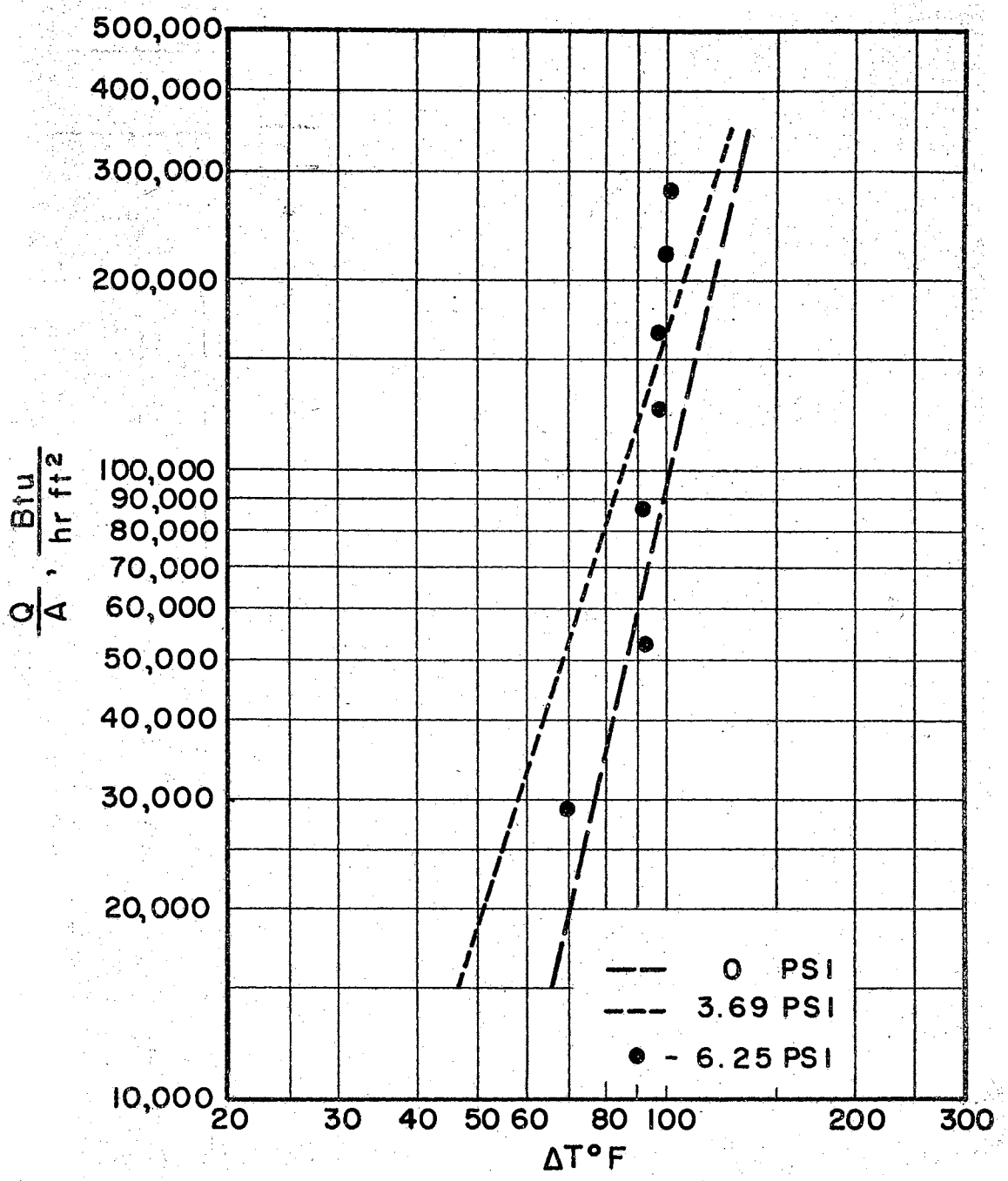

Figure 30. Heat Transfer Rate Versus Temperature Difference for Various Sound Pressures, II. (Bulk Temperature of Water ≐ 200°F).

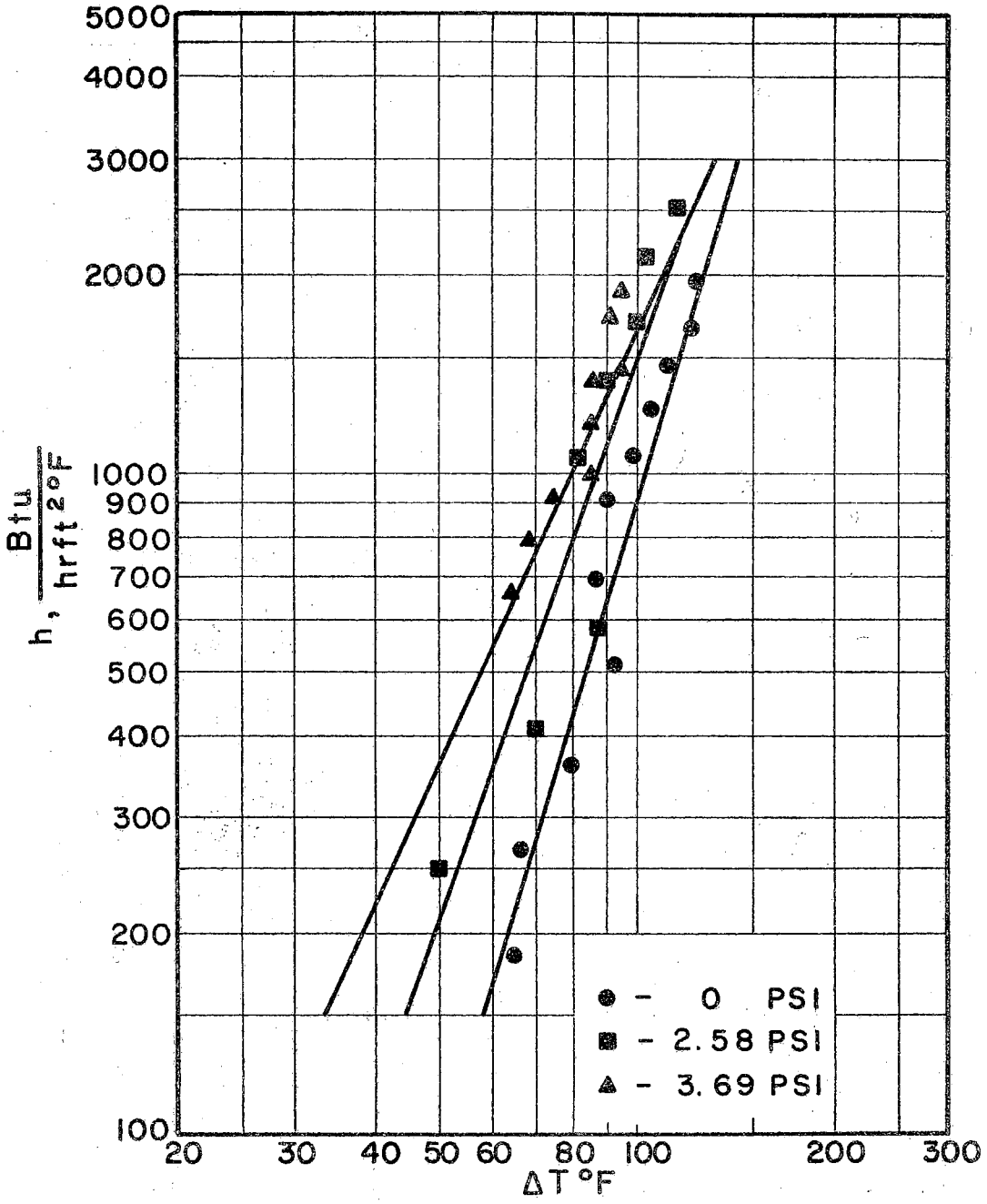

Figure 31. Heat Transfer Coefficient Versus Temperature Difference for Various Sound Pressures, I. (Bulk Temperature of Water = 200°F).

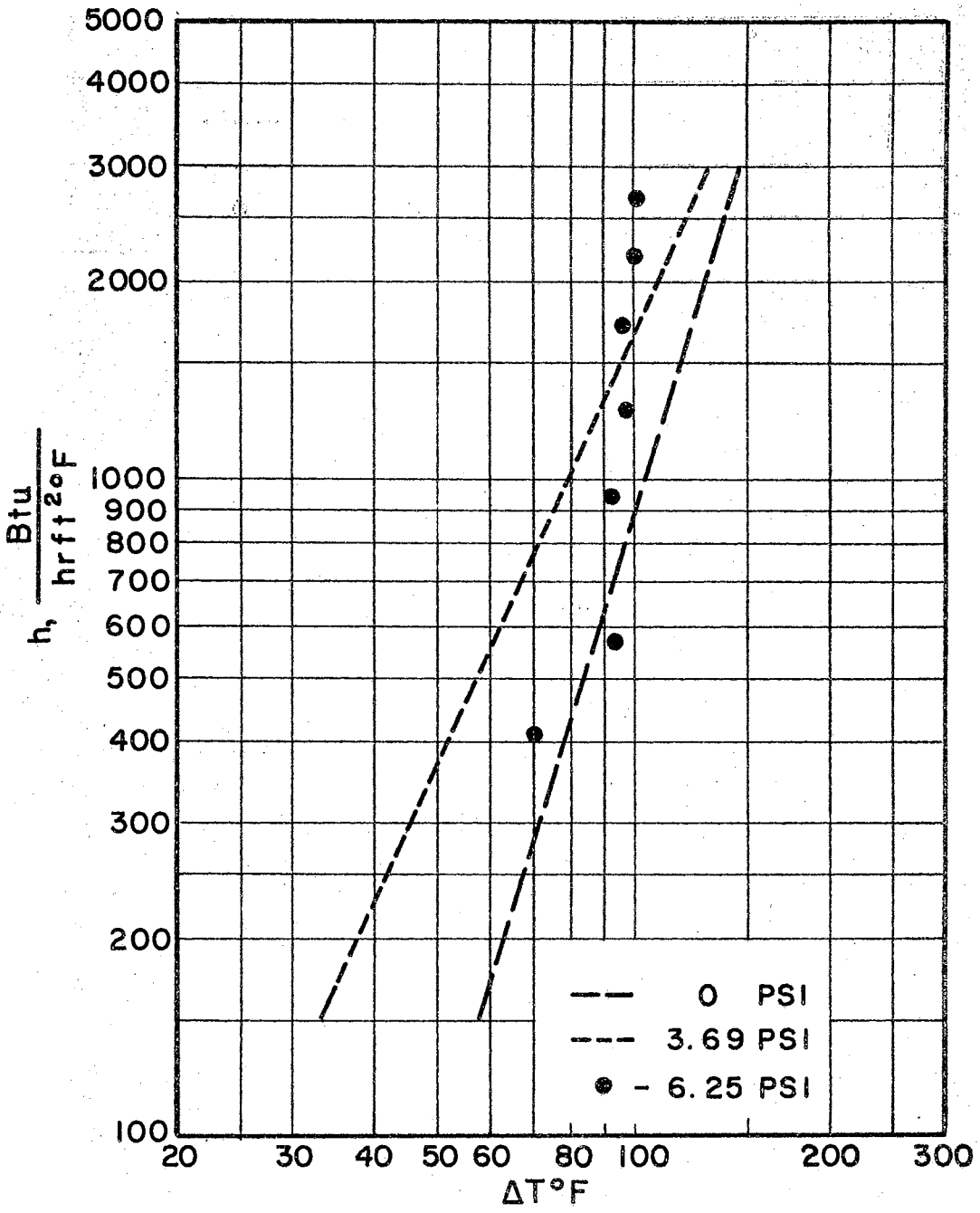

Figure 32. Heat Transfer Coefficient Versus Temperature Difference for Various Sound Pressures, II. (Bulk Temperature of Water 200°F).

Figure 27, Figure 30, Figure 31, and Figure 32 are determined through the use of the least square method.

In the experiments in which the bulk temperature of the water was maintained in about 200°F, it was found that the surface temperature of the test section could be reduced at a given heat flux through the application of sound waves. The experimental results are presented in Figure 33 and Figure 34. In Figure 33, each of these curves correlating the experimental data was obtained under a certain sound pressure. It should be noticed in Figure 34 that no curve is used to correlate the data points obtained for the sound pressure 6.25 psi, while the two dotted lines are reproduced from Figure 33 for comparison. It is seen that the acoustical cooling on the test section will increase as the sound pressure increases within a certain range. This range of sound pressure has been found to be approximately zero to 3.69 psi in the present apparatus. When the sound pressure is beyond the upper limit, the surface temperature of the test section, on the contrary, will not continuously decrease as indicated in Figure 34.

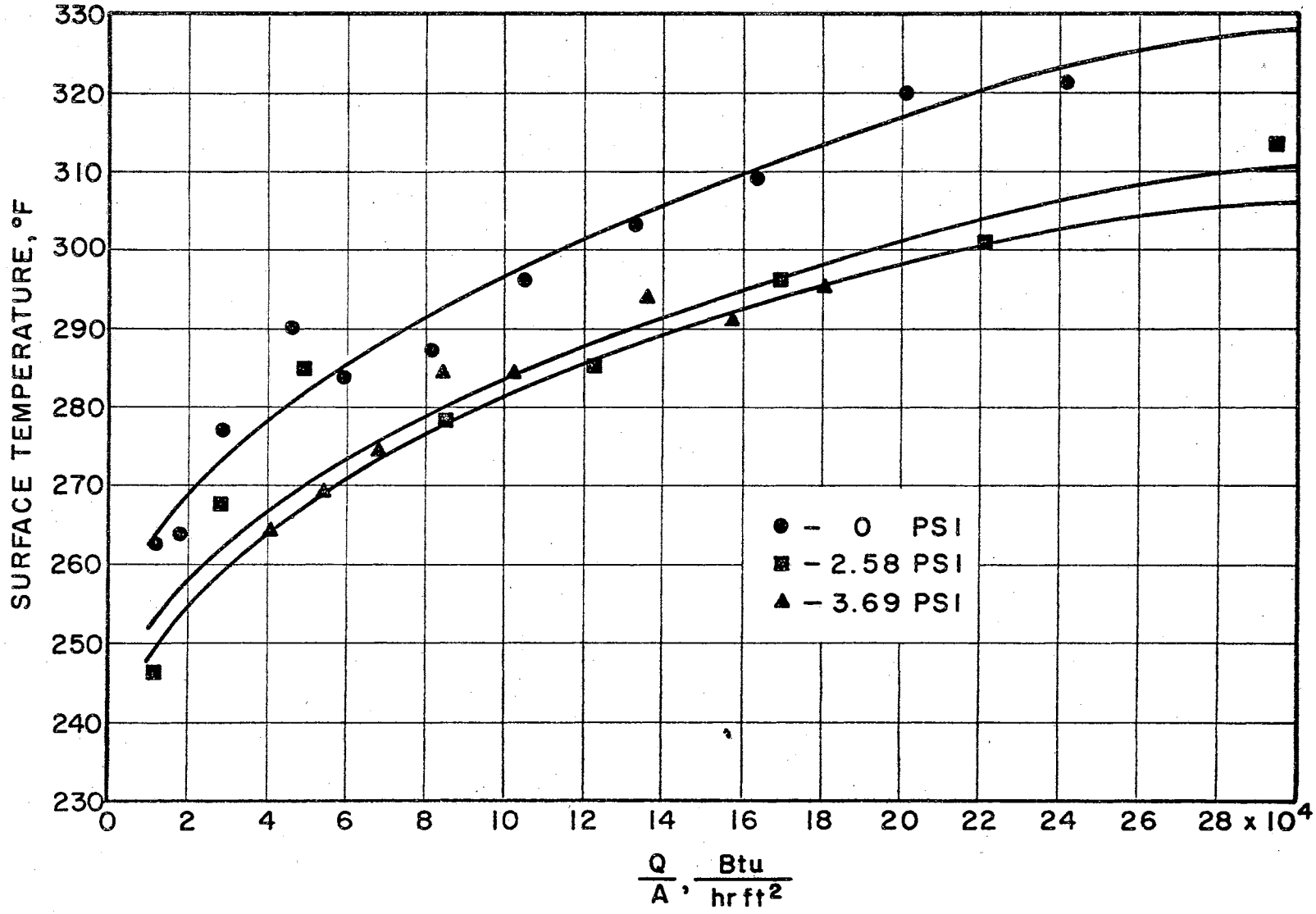

Figure 33. Surface Temperature of Test Section Versus the Heat Flux for Various Sound Pressure, I. (Bulk Temperature of Water Approximately Equals 200°F).

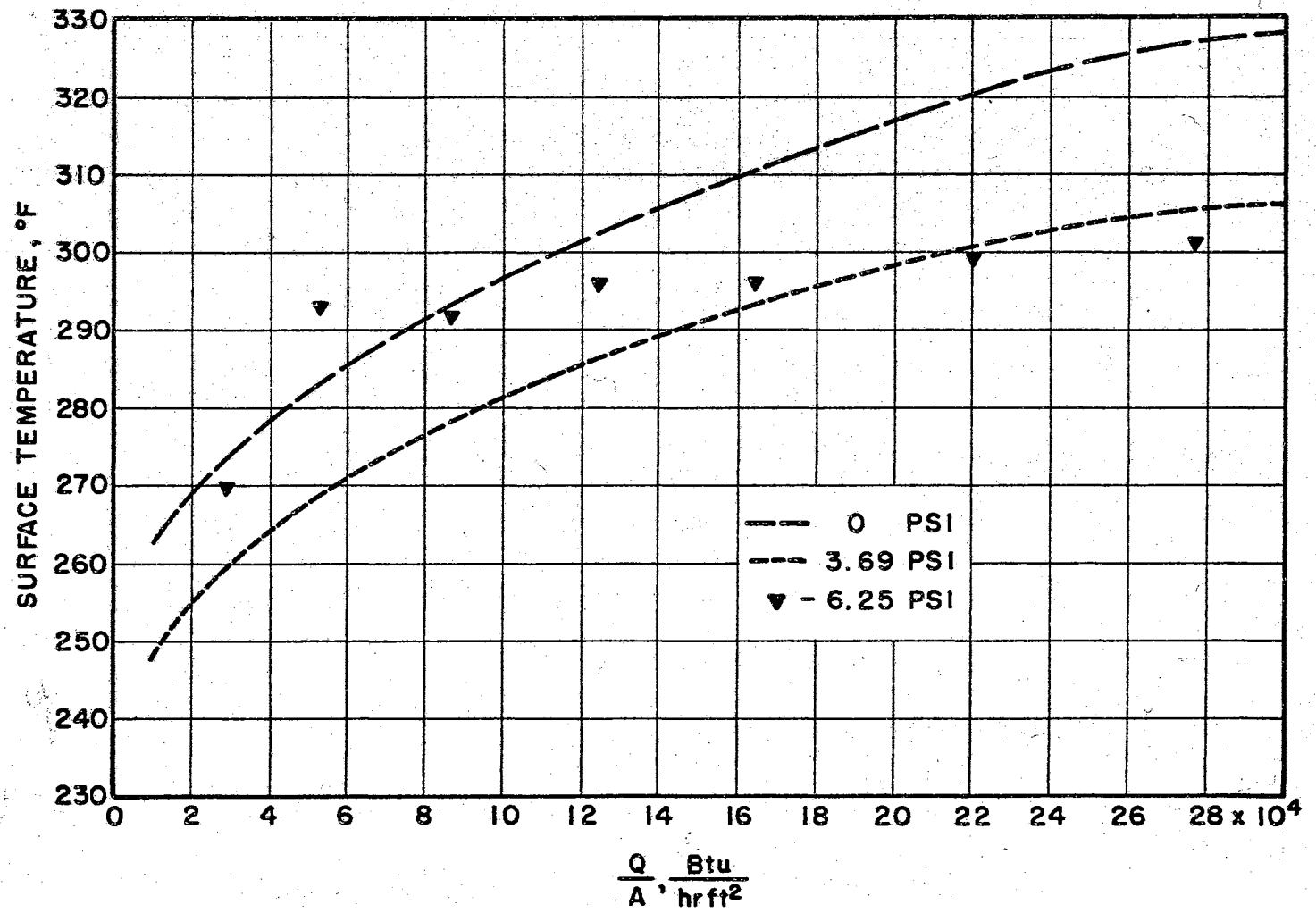

Figure 34. Surface Temperature of Test Section Versus the Heat Flux for Various Sound Pressure, II. (Bulk Temperature of Water Approximately Equals 200°F).

CHAPTER VII

DISCUSSION

There are many published works as mentioned in Chapter II, indicating that the agitation or micron convection induced by the growth and collapse of vapor bubbles is mainly responsible for the high heat transfer coefficient in the nucleate boiling region. This agitation mechanism is especially true for the low heat-flux region in nucleate boiling. It, therefore, is expected that the heat transfer coefficient will increase if this agitation can be intensified by some means.

The results of experiments conducted for the present investigation indicate clearly that the presence of sound waves can increase the heat transfer rate at a given temperature difference, both in the free convection region and in the nucleate boiling region. These results also indicate that the heat transfer rate can be increased by increasing the sound pressure at the sound frequency of 20,000 cycles/sec. even when the temperature difference remains constant. In other words, it can be said that the surface temperature of the heating surface can be gradually reduced at a given heat flux when the sound pressure is increased at a constant frequency of 20,000 cycles/sec. This phenomenon can be explained by the agitation mechanism. That is, when the sound waves are impressed on the vicinity of the test section, they will create a micro-scaled stirring motion in the water which surrounds the test section. Then

this stirring motion in the water will intensify the agitation which has been already induced by vapor bubbles. It is found that this stirring motion created in the presence of sound waves will increase as the sound pressure increases at a constant frequency. It is these combined agitations which are responsible for the increase in the heat transfer rate under the influence of sound waves.

The results of analytical work, which has been shown in Chapter III, indicate that when the sound waves are impressed in the vicinity of a vapor bubble growing in a superheated liquid the bubble growth rate will fluctuate in such a manner as shown in Figure 2. Then these fluctuations of the bubble growth rate will induce a strong stirring motion in the vicinity of the vapor bubble. The analytical calculations also show that the degree of these stirrings depends upon the sound pressure, when the sound frequency remains constant. It is also seen in these analyses that even when the vapor bubble ceases to grow in a liquid the vapor bubble still experiences a volume pulsation under the influence of sound waves. That is, the volume of the vapor bubble changes periodically in the sound field, even though the mean volume of the vapor bubble remains unaltered. It is shown that this volume pulsation, which will obviously induce a strong agitation in the liquid, has an amplitude proportional to the sound pressure. In the analytical part of this thesis, the equation for the resonant radius of a vapor bubble is derived and shown as Equation (53). It has been found that the resonant radius of a vapor bubble in the sound field of 20,000 cycles/sec is much smaller than that of a vapor bubble departing from a heating surface under no influence of sound waves. The latter value is determined through the use of Fritz's equation

shown as Equation (54). Therefore, it can be expected that the radius of a vapor bubble departing from the heating surface under the influence of sound waves would be smaller than that in the absence of sound. This reduction of radius of the vapor bubble departing from the heating surface implies that higher agitation in the vicinity of the heating section can be expected under the influence of sound waves.

There is no doubt that the analyses presented in Chapter III are simple and based on several assumptions. However, the results of these analyses have furnished a solid basis on which a mechanism is proposed to explain the experimental results. In summary, this proposed mechanism is that when the sound waves are impressed in the vicinity of the test section a micro-scaled stirring motion is created in the water surrounding the test section and intensifies the agitation already induced by the vapor bubbles. These stirring motions, which will intensify as the sound pressure increases, are responsible for an increase of heat transfer rate in nucleate boiling region when the sound waves are applied.

The sound frequency may play an important part in affecting the nucleate boiling heat transfer. This has been indicated in the analytical part of this thesis. However, no experiment has been carried out to give more information in this respect because the present apparatus was designed to operate only at the sound frequency of 20,000 cycles/sec.

It is generally known that the nucleate boiling region can be divided into two parts. (11) (15) The first is called the region of isolated bubbles where no interference among the bubbles would occur. This part corresponds to the low heat-flux region in nucleate boiling. However, in the second part, which corresponds to the high heat-flux region,

the mutual influence among the bubbles becomes significant. For the present investigation, the experiments have been carried out only in the low heat-flux region and the analytical work has been based upon the assumption that the interference among the bubbles can be neglected. Therefore, the mechanism proposed to explain the experimental results may not be valid in the high heat-flux region of nucleate boiling. This is especially true when the heat flux approaches the critical value in the nucleate boiling region.

It also has been found in the experiments that the incipient point of nucleate boiling is affected in the presence of sound waves. As the sound pressure increases at the sound frequency of 20,000 cycles/sec, the surface temperature of the heating surface at the incipient point of nucleate boiling will decrease. Obviously, this can be related to the presence of the acoustically-induced agitation in the vicinity of the test section. The higher the agitation in the water, the lower the surface temperature required to start the boiling on the heating surface. However, there was no attempt to determine the surface temperature of the test section when the first vapor bubble appears on it. The point of incipient boiling is defined by the method discussed in the last chapter.

One of the important experimental findings in the present investigation is quite interesting and unexpected. That is, there is a certain sound pressure level above which the effects of sound waves on the nucleate boiling heat transfer will be different. These experimental findings have been reported in detail in Chapter VI. This phenomenon can be explained as follows: when the sound waves are generated and propagate

through the water, they will induce a degassing process in the water if the sound pressure is high enough. As the sound pressure is increased beyond a certain value, the degassing process induced by the sound waves becomes so vigorous that the platinum wire of the test section is partly surrounded by an unstable gas-vapor film. This gas-vapor film appeared to be unstable. This idea of the unstable gas-vapor film surrounding the platinum wire of the test section is based upon many observations during the experiments. It is believed that this film is responsible for the fact that the surface temperature of the test section will start to go up at a given heat flux, if the sound pressure is greater than a certain value. As far as the heat transfer rate is concerned, the sound waves have two different effects on it at that time. One is to continuously increase the acoustically induced agitation in the vicinity of the heating surface, while the other is to create an unstable gas-vapor film surrounding the heating surface. Depending upon the balance of these two effects, the heat transfer rate may continue to increase or start to decrease. It is indicated in the experimental results that the value of sound pressure beyond which this critical phenomenon will occur is at least determined by the following factors: the bulk temperature of water, gas content in water, the frequency of the sound waves, and the range of heat flux.

In the present investigation, the author has also tried to determine whether there exists a minimum value of sound pressure below which the sound waves of 20,000 cycles/sec would have no effect on the heat transfer rate. The experimental finding is that the heat transfer rate in the nucleate boiling region will be immediately affected in the presence

of sound waves at the sound frequency of 20,000 cycles/sec. The minimum value of the sound pressure in consideration seems not to exist in the present apparatus.

Finally, it should be pointed out that the application of sound waves in the area of the nucleate boiling heat transfer is a complicated matter. Many factors have to be taken into account before the increase in the heat transfer rate due to the presence of sound waves can be insured. Obviously, the sound pressure is one of the important variables when the sound frequency is fixed. The optimum value of the sound pressure may be different for each different sound frequency. When the sound pressure is fixed, it is believed that there may also exist an optimum value of sound frequency. Undoubtedly, the choices of the sound pressure and frequency are closely related to the bulk temperature and properties of the fluid and the range of the heat flux which is desired. It is also believed that the orientation of the heating surface in a sound field may have a role in affecting the heat transfer rate. Not less important than the above factors, the economic consideration should be taken into account when this application is considered for industrial use.

CHAPTER VIII

CONCLUSIONS AND RECOMMENDATIONS

The following conclusions are made as a result of the present study:

(1) The heat transfer rates are affected both in the free convection region and in the nucleate boiling region when sound waves are impressed in the vicinity of a heating surface. The amount of increase in the heat transfer rate due to the presence of the sound waves is significant and worthy of this present investigation. For example, in the nucleate boiling region with the bulk temperature of water approximately 200°F, the heat transfer rate can be increased to almost three times as much as that obtained under no influence of sound.

(2) At the constant sound frequency of 20,000 cycles/sec, the heat transfer rate can be increased by increasing the sound pressure in the vicinity of the heating surface, even when the temperature difference between the heating surface and its surrounding water remains constant. This statement is valid only for a certain range of sound pressure. The sound waves are more effective in the nucleate boiling region than in the free convection region. Also the effects of sound waves on the heat transfer rate are different for various temperature differences.

(3) The presence of sound waves has an induced cooling effect on the heating surface. That is, the surface temperature of the heating

surface at the constant heat flux can be reduced to some extent under the influence of sound waves. It has been found in experiments that as the sound pressure in the vicinity of the heating surface increases at the sound frequency of 20,000 cycles/sec, the surface temperature in consideration will decrease. However, this statement is valid only for a certain range of sound pressure.

(4) Based upon the analytical results obtained in the present investigation, a mechanism has been proposed and used to qualitatively explain the effects of sound waves on the nucleate boiling heat transfer. This proposed mechanism is summarized as follows: when the sound waves are impressed on the vicinity of the heating surface, a micro-scaled stirring motion is created in the water surrounding the heating surface. Then, these stirring motions will intensify the agitation induced by the vapor bubbles. It has been found that these stirring motions will increase as the sound pressure increases at a certain sound frequency. It is these stirring motions which are responsible for the fact that the heat transfer rate in the nucleate boiling region can be increased by increasing the sound pressure.

(5) It has been found in experiments that there exists a certain value of sound pressure beyond which the sound waves of 20,000 cycles/sec have a different effect on the nucleate boiling heat transfer. That is, when the sound pressure is increased beyond a certain value, the surface temperature of the heating surface will not continuously be reduced, but on the contrary, will start to increase. Also, the heat transfer rate will not continuously increase in the nucleate boiling region as it would be in the low sound pressure, i.e., below the critical value

of sound pressure. These phenomenon may be contributed by an existence of the unstable gas-vapor film which results from an acoustically-induced degassing process in water and which surrounds the platinum wire of the test section. In the present experimental setup, the critical sound pressure has been found to be approximately 7.75 psi for the bulk temperature of water around 85°F, or approximately 3.69 psi for the bulk temperature of water around 200°F.

(6) The incipient point of nucleate boiling is affected in a sound field. It has been found in experiments that when the sound pressure increases at the constant sound frequency of 20,000 cycles/sec the surface temperature of the heating section required to start the nucleate boiling will decrease.

The following recommendations are made for the future work in this field:

(1) The future work should be directed toward the fundamental aspects of the present problem. Since the vapor bubble would play an important part in the nucleate boiling heat transfer, it becomes necessary to have a better understanding of the history of a vapor bubble under the influence of sound. Studies need to be made of the bubble formation in liquids or on the heating surface for various acoustical conditions. A study needs to be made of the motion of a vapor bubble in the liquid in a sound field. Also, some experiments need to be carried out to provide the information about the growth of a vapor bubble in the liquid for various acoustical conditions.

(2) Since the sound frequency is one of the important variables in the present study, it would represent a new progress if some experiments

are carried out to determine the effect of the sound frequency on the nucleate boiling heat transfer. It is very possible that the orientation of the heating surface in a sound field may play a role in affecting the heat transfer rate; therefore, some work should be done to provide more information in this respect.

(3) The future work should also be directed toward the practical aspects of the present study. It appears that some investigations need to be carried out on a fluid-flow system with surface boiling in a sound field. In addition to the water used as the boiling liquid, some other fluids of different properties should be used in experiments for various acoustical conditions. It is also interesting and of practical significance to have the information about the effect of sound waves on the nucleate boiling in high-pressure systems.

BIBLIOGRAPHY

1. Isakoff, S. E., "Effect of an Ultrasonic Field on Boiling Heat Transfer - Exploratory Investigation," 1956 Heat Transfer and Fluid Mechanics Institute, Stanford University Press, Stanford, California, 1956.

2. Nukiyama, S., "The Maximum and Minimum Values of the Heat Q Transmitted From Metal to Boiling Water Under Atmospheric Pressure," Journal of Society of Mechanical Engineers, Japan, Vol. 37, June 1934.

3. Westwater, J. W., "Boiling of Liquids," Advances in Chemical Engineering, (T. B. Drew and J. W. Hoopers, Jr., Editors) Academic Press Inc., 1956.

4. Jakob, M., Heat Transfer, Vol. I, John Wiley and Sons, Inc., 1959.

5. Rohsenow, N. W. and J. A. Clark, "A Study of the Mechanism of Boiling Heat Transfer," Trans. ASME, Vol. 73, p. 609, 1951.

6. Gunther, F. C. and F. Kreith, "Photographic Study of Bubble Formation in Heat Transfer to Subcooled Water," 1949 Heat Transfer and Fluid Mechanics Institute, published by University of California, p. 113, 1949.

7. Bankoff, S. G., W. J. Colaham, and D. R. Bartz (editors), Summary of Conference on Bubble Dynamics and Boiling Heat Transfer Held at the Jet Propulsion Laboratory June 14 and 15, 1956, Jet Propulsion Laboratory Memo No. 20-137, California Institute of Technology, 1956.

8. Forster, H. K. and R. Grief, "Heat Transfer to Boiling Liquids - Mechanism and Correlations," Journal of Heat Transfer ASME, February, 1959.

9. Edward, D. K., "The Role of Interface Mass Tansfer," M.S. Thesis, University of California, Berkeley, California, 1956.

10. Sabersky, R. H. and H. E. Mulligan, "On the Relationship Between Fluid Friction and Heat Transfer in Nucleate Boiling," Jet Propulsion, Vol. 25, p. 9, January, 1955.

11. Zuber, N., "Hydrodynamic Aspects of Boiling Heat Transfer," Ph.D. Thesis, University of California, Los Angeles, California, June 1959.

12. Zmola, P. C., "Investigation of the Mechanism of Boiling in Liquids, Ph.D. Thesis, Purdue University, 1950.

13. Westwater, J. W. and J. G. Santangelo, "Photographic Study of Boiling," Industrial Engineering Chemistry, Vol. 47, p. 1605, August, 1955.

14. Westwater, J. W., "Boiling Heat Transfer," American Scientist, Vol. 47, p. 427, 1959.

15. Tien, C. L., "A Hydrodynamic Model for Nucleate Pool Boiling," International Journal Heat and Mass Transfers, Vol. 5, p. 533, 1962.

16. Rohsenow, W. M., "A Method of Correlating Heat Transfer Data for Surface Boiling of Liquids," Trans. ASME, Vol. 74, p. 969, 1952.

17. Forster, H. K. and N. Zuber, "Growth of a Vapor Bubble in a Superheated Liquid," Journal of Applied Physics, Vol. 25, p. 474, 1954.

18. Plesset, M. S. and S. A. Zwick, "The Growth of Vapor Bubbles in Superheated Liquids," Journal of Applied Physics, Vol. 25, p. 493, 1954.

19. Levy, S., "Generalized Correlation of Boiling Heat Transfer," Journal of Heat Transfer, ASME, p. 37, February 1957.

20. Chang, Y. P. and N. W. Snyder, "Heat Transfer in Saturated Boiling," Chemical Engineering Progress Symposium Series, Vol. 55, No. 29, 1960.

21. Cichelli, M. T. and C. F. Bonilla, "Heat Transfer to Liquid Boiling Under Pressure," Trans. A.I.Ch.E., Vol. 41, p. 755, 1945.

22. Bonilla, C. F. and J. S. Busch, "Pool-Boiling Heat Transfer with Mercury," Chemical Engineering Progress Symposium Series, Vol. 53, No. 20, 1957.

23. Nishikawa, K. and K. Yamagata, "On the Correlation of Nucleate Boiling Heat Transfer," International Journal Heat and Mass Transfer, Vol. I., p. 219, 1960.

24. Hara, T., "The Mechanism of Nucleate Boiling Heat Transfer," International Journal Heat and Mass Transfer, Vol. VI., p. 959, 1963.

25. Kurihara, H. M. and J. E. Meyers, "The Effect of Superheat and Surface Roughness on Boiling Coefficients," Journal A.I.Ch.E., Vol. VI, p. 83, 1960.

26. Lienhard, J. H., "A Semi-Rational Nucleate Boiling Heat Flux Correlation," International Journal Heat and Mass Transfer, Vol. VI, p. 215, 1963.

27. Benjamin, J. E. and J. W. Westwater, "Bubble Growth in Nucleate Boiling of a Binary Mixture," International Heat Transfer Conference, Part I, published by University of Colorado, Boulder, Colorado, p. 212, 1961.

28. Fand, R. M. and J. Kaye, "The Effect of High Intensity Stationary and Progressive Sound Fields on Free Convection from a Horizontal Cylinder," ASTIA Document No. AD 209532, March 1959.

29. Fand, R. M. and E. M. Feeble, "A Comparison of the Influence of Mechanical and Acoustical Vibration on Free Convection from a Horizontal Cylinder," Aeronautical Research Laboratory No. 148, Part II, December 1961.

30. Fand, R. M., "On the Mechanism of Interaction Between Vibration and Heat Transfer," Aeronautical Research Laboratory No. 148, Part IV, December 1961.

31. Westervelt, P. J., "The Effects of Sound Waves on Heat Transfer," Journal Acoustical Society of America, Vol. 32, No. 3, p. 337, 1960.

32. Sprott, A. L., J. P. Holman, and F. L. Durand, "An Experimental Study of the Effects of Strong Progressive Sound Fields on Free Convection Heat Transfer from a Horizontal Cylinder," Paper No. 60-HT-19, Presented at ASME-A.I.Ch.E. Heat Transfer Conference, Buffalo, New York, August 1960.

33. Holman, J. P., "The Mechanism of Sound Field Effects on Heat Transfer," Journal of Heat Transfer, Trans. ASME, Vol. 82, p. 393, 1960.

34. Fand, R. M. and J. Kaye, "The Influence of Vertical Vibration on Heat Transfer by Free Convection from a Horizontal Cylinder," International Heat Transfer Conference, Part II, Boulder, Colorado, p. 490, 1961.

35. Chang, Y. P., "A Theoretical Analysis of Heat Transfer in Natural Convection and in Boiling," Trans. ASME, Vol. 79, p. 1501, 1957.

36. Fand, R. M., J. Roos, P. Cheng, and J. Kaye, "The Local Heat Transfer Coefficient Around a Heated Horizontal Cylinder in an Intense Sound Field," Aeronautical Research Laboratory No. 148, Part III, December 1961.

37. Kovalenko, V. F., "An Experimental Investigation of the Vibration Effect on Heat Transfer in the Process of Boiling, Teploenerpartika, No. 5, p. 76.

38. Romie, F. E., "Experimental Investigation of the Effect of Ultrasonic Vibration on Burnout Heat Flux with Boiling Water," Atomic Energy Commission, ATL. A 113, December 1960.

39. Fritz, W., "Berechnung des Maximalvolumens von Dampfblasen," Phys. Zeitsch., Vol. 36, p. 379, 1935.

40. Osborne, M. F. M. and F. H. Holland, "The Acoustical Concomitants of Cavitation and Boiling, Produced by a Hot Wire," Journal of Acoustical Society of America, Vol. 19, p. 13, January 1947.

41. Rinaldo, P. M., "Effect of Diameter on Boiling Outside Tubes," M.S. Thesis, MIT, 1947.

42. Addoms, J. M., "Heat Transfer at High Rates to Water Boiling Outside Cylinders," Sc.D. Thesis, MIT, 1948.

43. Vos, A. S. and S. J. D. von Stralen, "Heat Transfer to Boiling Water - Methylethylketone Mixtures," Chemical Engineering Science, Vol. 5, p. 50, 1956.

APPENDIX A

DETERMINATION OF AN EXACT SOLUTION TO EQUATION (24)

The equation in consideration is expressed as follows:

$$\frac{\partial^2 T}{\partial x^2} = \frac{1}{\alpha} \frac{\partial T}{\partial \theta} \tag{A-1}$$

with the boundary and initial conditions,

$$T(x,0) = T_i \tag{A-2}$$

$$T(0,\theta) = g(P_o) \tag{A-3}$$

$$T(\infty,0) = T_i \tag{A-4}$$

where $T = t - t_s$ and the origin of coordinates is at the vapor bubble surface. Let

$$\xi = \frac{x}{2(\alpha\theta)^{\frac{1}{2}}}$$

Equation (A-1) and its boundary and initial conditions become respectively

$$\frac{d^2 T}{d\xi^2} + 2\xi \frac{dT}{d\xi} = 0 \tag{A-5}$$

$$T(\xi) = T_i \quad \text{at } \xi = \infty \tag{A-6}$$

$$T(\xi) = g(P_o) \quad \text{at } \xi = 0 \tag{A-7}$$

Equation (A-5) can be solved when it is multiplied by an integrating factor e^{ξ^2}. That is,

$$e^{\xi^2}\left(\frac{d^2T}{d\xi^2} + 2\xi \frac{dT}{d\xi}\right) = 0$$

or

$$\frac{d}{d\xi}\left(e^{\xi^2} \frac{dT}{d\xi}\right) = 0 \tag{A-8}$$

Integrating Equation (A-8) would give

$$e^{\xi^2} \frac{dT}{d\xi} = C_1 \tag{A-9}$$

where C_1 is an integration constant.

After another integration, Equation (A-9) becomes

$$\int_o^T dT = C_1 \int_o^\xi e^{-\xi^2} d\xi \tag{A-10}$$

A combination of Equation (A-7) and Equation (A-10) would give

$$T(\xi) - g(P_o) = C_1 \frac{\sqrt{\pi}}{2} \text{ erf } (\xi) \tag{A-11}$$

The constant, C_1, can be determined through the use of Equation (A-6). That is,

$$T_i - g(P_o) = C_1 \frac{\sqrt{\pi}}{2}$$

then

$$C_1 = \frac{2}{\sqrt{\pi}} \left[T_i - g(P_o) \right] \qquad \text{(A-12)}$$

A combination of Equation (A-11) and Equation (A-12) will give the solution to Equation (A-1) as follows:

$$T(\xi) = T_i \text{ erf } (\xi) + g(P_o) \text{ erfc } (\xi) \qquad \text{(A-13)}$$

Equation (A-13) can be also written as

$$T(x,\theta) = T_i \text{ erf } \left(\frac{x}{2(\alpha\theta)^{\frac{1}{2}}} \right) + g(P_o) \text{ erfc } \left(\frac{x}{2(\alpha\theta)^{\frac{1}{2}}} \right) \qquad \text{(A-14)}$$

APPENDIX B

DATA OF FRESH WATER

Chlorine Residual	0.52 PPM
Fluoride	1.01 PPM
Hardness	18.1 PPM
Silica	3.6 PPM
Iron	0.0 PPM
Calcium	37 PPM
Magnesium	12 PPM
Potassium	25 PPM
Sulphate	24 PPM
Chloride	39 PPM
Nitrate	0.8 PPM
Dissolved Solids	218 PPM
Sodium	27 %
Specific Conductance at 25 C.	390 Micromhos.
Caliform Bacteria	0/144
PH	7.8
Turbidity	0.06

APPENDIX C

LIST OF EQUIPMENT

Item	Manufacturer	Serial No.
DC Vacuum Tube Meter Model 412A	Hewlett Packard Co.	42,410,376
DC Vacuum Tube Meter Model 412A	Hewlett Packard Co.	00403250
Oscilloscope Type 535A	Tektronix Inc.	028712
Oscillotron Model K5	Coleman Inc.	1333
Periscope Model K5	Coleman Inc.	220
Oscilloscope Record Camera Model 150	Wollensak Co.	Polaroid D51282
Plating Rectifier	Electro. Tech. Equipment Co.	
Heater (W-1500,V-230)	General Electric	2D281
Heater (W-9000,V-240)	Edwin L. Weigand Co.	Cal. No. MTS 390A
Portable Shunt	Simpson Co.	Port. No. 6707
Quartz Pressure Transducer Model 601	Kistler Co.	3346
Charge Amplifier Model No. 568	Kistler Co.	SIN 133
Ultrasonic Generator Model No. 200CD	International Ultrasonics Inc.	

APPENDIX D

EXPERIMENTAL DATA AND CALCULATED RESULTS

TABLE I

EXPERIMENTAL DATA AND CALCULATED RESULTS FOR TEST NUMBER 1

Water Level in the Tank	6 1/2 inches	Room Temperature	74° F
Length of the Platinum Wire of Test Section	6 5/8 inches	Sound Pressure	0 psi
Distance from the Water Surface to the Test Section	4 7/8 inches	Sound Frequency	0 cycles/sec

Run No.	Voltage Drop Across the Test Section	Voltage Drop Across the Portable Shunt x 10^{+3}	Bulk Temp. of Water °F	Temp. at the Heating Surface °F	Temperature Difference ΔT °F	Heat Transfer Rate $\frac{Btu}{hr, ft^2}$	Heat Transfer Coefficient $\frac{Btu}{hr, ft^2\ °F}$
1	1.53	5.00	78	112.0	34.0	11286	331.1
2	1.92	6.19	78	120.7	42.7	17535	409.8
3	2.39	7.59	78	130.5	52.5	26764	508.9
4	2.83	8.72	78	150.7	72.7	36409	500.7
5	3.25	9.81	78	164.7	86.7	47039	542.1
6	3.75	11.10	78	178.3	100.3	61414	611.7
7	4.20	12.20	78	191.7	113.7	75600	664.6
8	4.71	13.40	78	207.3	129.3	93119	719.7
9	5.05	14.10	80	227.1	147.1	106065	720.8
10	5.64	15.50	80	238.3	158.3	130219	822.6
11	6.05	16.40	80	248.1	168.1	147796	879.1
12	6.55	17.40	80	262.8	182.8	169767	928.6
13	6.95	19.40	80	227.3	147.3	200840	1363.2
14	7.45	20.60	80	233.9	153.9	228606	1484.8
15	7.85	21.60	80	237.4	157.4	252573	1604.3

TABLE II

EXPERIMENTAL DATA AND CALCULATED RESULTS FOR TEST NUMBER 2

Water Level in the Tank	6 1/2 inches	Room Temperature	74° F
Length of the Platinum Wire of Test Section	6 5/8 inches	Sound Pressure	2.58 psi
Distance from the Water Surface to the Test Section	4 7/8 inches	Sound Frequency	20,000 cycles/sec

Run No.	Voltage Drop Across the Test Section	Voltage Drop Across the Portable Shunt x 10^{-3}	Bulk Temp. of Water °F	Temp. at the Heating Surface °F	Temperature Difference ΔT °F	Heat Transfer Rate $\frac{Btu}{hr, ft^2}$	Heat Transfer Coefficient $\frac{Btu}{hr, ft^2\ °F}$
1	1.94	6.28	80	118.1	38.1	17975	471.1
2	2.36	7.51	81	129.2	48.2	26149	541.9
3	2.78	8.72	81	138.7	57.7	35766	619.4
4	3.21	9.85	81	153.4	72.4	46650	643.5
5	3.69	11.10	81	167.1	86.1	60431	701.8
6	4.11	12.20	81	176.3	95.3	73980	775.7
7	4.51	13.30	81	180.9	99.9	88499	885.5
8	5.09	14.50	82	206.4	124.4	108893	874.9
9	5.59	15.70	82	216.0	134.0	129487	965.6
10	6.02	16.60	82	228.7	146.7	147441	1004.3
11	6.45	17.80	82	228.1	146.1	169392	1158.8
12	6.91	18.90	82	234.3	152.3	192687	1264.4
13	7.39	20.10	82	238.2	156.2	219156	1402.2
14	7.81	21.30	82	236.2	154.2	245440	1590.7

TABLE III

EXPERIMENTAL DATA AND CALCULATED RESULTS FOR TEST NUMBER 3

Water Level in the Tank	6 1/2 inches	Room Temperature	74° F
Length of the Platinum Wire of Test Section	6 5/8 inches	Sound Pressure	3.69 psi
Distance from the Water Surface to the Test Section	4 7/8 inches	Sound Frequency	20,000 cycles/sec

Run No.	Voltage Drop Across the Test Section	Voltage Drop Across the Portable Shunt x 10^{-3}	Bulk Temp. of Water °F	Temp. at the Heating Surface °F	Temperature Difference ΔT °F	Heat Transfer Rate $\frac{Btu}{hr, ft^2}$	Heat Transfer Coefficient $\frac{Btu}{hr, ft^2\ °F}$
1	1.91	6.18	82	718.4	36.4	17415	477.7
2	2.28	7.35	82	120.8	38.8	24725	636.9
3	2.72	8.61	83	132.7	49.7	34553	695.1
4	3.22	9.98	83	146.7	63.7	47413	744.1
5	3.75	11.20	83	172.0	89.0	61967	695.5
6	4.21	12.50	83	176.1	93.1	77643	833.3
7	4.65	13.60	83	186.8	103.8	93305	898.8
8	5.12	14.70	83	200.0	117.0	111045	948.4
9	5.61	15.80	84	214.0	130.1	130778	1004.5
10	6.11	17.10	84	218.4	134.4	154153	1146.4
11	6.49	18.10	84	220.8	136.8	173315	1266.6
12	6.96	19.10	85	232.0	147.0	196136	1333.8
13	7.41	20.20	86	236.6	150.6	220843	1465.6
14	7.86	21.50	86	234.1	148.1	249330	1682.5

TABLE IV

EXPERIMENTAL DATA AND CALCULATED RESULTS FOR TEST NUMBER 4

Water Level in the Tank	6 1/2 inches	Room Temperature	74° F
Length of the Platinum Wire of Test Section	6 5/8 inches	Sound Pressure	7.75 psi
Distance from the Water Surface to the Test Section	4 7/8 inches	Sound Frequency	20,000 cycles/sec

Run No.	Voltage Drop Across the Test Section	Voltage Drop Across the Portable Shunt x 10^{+3}	Bulk Temp. of Water °F	Temp. at the Heating Surface °F	Temperature Difference ΔT °F	Heat Transfer Rate $\frac{Btu}{hr, ft^2}$	Heat Transfer Coefficient $\frac{Btu}{hr, ft^2\ °F}$
1	2.43	7.80	87	123.5	36.5	27965	764.1
2	2.88	9.01	88	140.4	52.4	38285	729.4
3	3.34	10.20	88	156.7	68.7	50264	731.2
4	3.85	11.70	88	160.0	72.0	66460	922.3
5	4.30	13.00	88	163.5	75.5	82475	1091.2
6	4.79	14.10	88	182.2	94.2	99648	1057.8
7	5.22	15.20	88	189.8	101.8	117065	1148.9
8	5.65	16.10	88	206.1	118.1	134211	1135.5
9	6.15	17.30	88	214.9	126.9	156976	1236.6
10	6.59	18.50	90	216.8	126.8	180011	1419.6
11	7.19	19.90	91	226.0	135.0	211104	1563.3
12	7.52	20.90	92	223.0	131.0	231888	1769.0
13	8.01	22.10	93	228.0	135.0	261179	1933.0

TABLE V

EXPERIMENTAL DATA AND CALCULATED RESULTS FOR TEST NUMBER 5

Water Level in the Tank	6 1/2 inches	Room Temperature	74° F
Length of the Platinum Wire of Test Section	6 5/8 inches	Sound Pressure	9.34 psi
Distance from the Water Surface to the Test Section	4 7/8 inches	Sound Frequency	20,000 cycles/sec

Run No.	Voltage Drop Across the Test Section	Voltage Drop Across the Portable Shunt x 10^{+3}	Bulk Temp. of Water °F	Temp. at the Heating Surface °F	Temperature Difference ΔT °F	Heat Transfer Rate $\frac{Btu}{hr, ft^2}$	Heat Transfer Coefficient $\frac{Btu}{hr, ft^2\ °F}$
1	2.04	6.40	92	138.6	46.6	19263	412.7
2	2.53	7.80	92	150.3	58.3	29115	499.0
3	2.97	9.05	94	158.2	64.2	39656	616.9
4	3.49	10.20	94	187.4	93.4	52521	562.2
5	3.98	11.60	94	189.3	95.3	68117	714.3
6	4.42	12.70	94	199.5	105.5	82821	784.3
7	4.91	13.90	94	210.7	116.7	100695	862.6
8	5.38	15.10	95	216.5	121.5	119859	985.8
9	5.88	16.50	96	216.6	120.6	143144	1186.3
10	6.35	17.70	96	221.2	125.2	165829	1324.2
11	6.77	18.90	96	220.1	124.0	188784	1521.3
12	7.25	20.10	96	224.8	128.8	215005	1668.7
13	7.71	21.30	97	227.2	130.2	242297	1860.4
14	8.21	22.70	97	226.5	129.5	274969	2122.1

TABLE VI

EXPERIMENTAL DATA AND CALCULATED RESULTS FOR TEST NUMBER 6

Water Level in the Tank	6 1/2 inches	Room Temperature	74^{o} F
Length of the Platinum Wire of Test Section	6 5/8 inches	Sound Pressure	9.7 psi
Distance from the Water Surface to the Test Section	4 7/8 inches	Sound Frequency	20,000 cycles/sec

Run No.	Voltage Drop Across the Test Section	Voltage Drop Across the Portable Shunt x 10^{+3}	Bulk Temp. of Water ^{o}F	Temp. at the Heating Surface ^{o}F	Temperature Difference ΔT ^{o}F	Heat Transfer Rate $\frac{Btu}{hr, ft^2}$	Heat Transfer Coefficient $\frac{Btu}{hr, ft^2\ ^{o}F}$
1	2.93	8.95	101	156.6	55.6	38690	695.7
2	3.89	11.30	101	191.7	90.7	64854	714.6
3	4.34	12.50	101	197.8	96.8	80041	826.2
4	4.82	13.80	102	203.0	101.0	98138	970.8
5	5.29	14.80	102	218.7	116.7	115513	988.9
6	5.75	15.80	104	231.2	127.2	134041	1053.0
7	6.25	17.40	105	222.0	117.0	160451	1370.3
8	6.55	18.10	106	227.2	121.2	174918	1442.8
9	7.11	19.70	106	225.2	119.2	206657	1732.4
10	7.51	20.70	107	228.8	121.8	229363	1882.0
11	8.08	22.10	108	234.2	126.2	263462	2087.5

TABLE VII

EXPERIMENTAL DATA AND CALCULATED RESULTS FOR TEST NUMBER 7

Water Level in the Tank	6 1/4 inches	Room Temperature	80^{o} F
Length of the Platinum Wire of Test Section	6 7/32 inches	Sound Pressure	0 psi
Distance from the Water Surface to the Test Section	4 1/2 inches	Sound Frequency	0 cycles/sec

Run No.	Voltage Drop Across the Test Section	Voltage Drop Across the Portable Shunt x 10^{+3}	Bulk Temp. of Water ^{o}F	Temp. at the Heating Surface ^{o}F	Temperature Difference ΔT ^{o}F	Heat Transfer Rate $\frac{Btu}{hr, ft^2}$	Heat Transfer Coefficient $\frac{Btu}{hr, ft^2\ ^{o}F}$
1	1.66	4.65	198	263.1	65.1	12130	186.2
2	2.02	5.65	198	264.2	66.2	17935	270.8
3	2.58	7.09	198	277.2	79.2	28745	362.5
4	3.34	9.02	198	290.4	92.4	47343	512.3
5	3.75	10.20	198	284.9	86.9	60109	691.4
6	4.39	11.90	198	287.4	89.4	82095	917.6
7	5.00	13.40	198	296.1	98.1	105289	1073.2
8	5.65	15.00	198	303.3	105.3	133183	1264.7
9	6.30	16.60	198	309.0	111.0	164345	1479.4
10	7.05	18.30	198	320.7	122.7	202745	1651.4
11	7.71	20.00	198	321.1	123.1	242322	1967.0

TABLE VIII

EXPERIMENTAL DATA AND CALCULATED RESULTS FOR TEST NUMBER 8

Water Level in the Tank	6 1/4 inches	Room Temperature	80° F
Length of the Platinum Wire of Test Section	6 7/32 inches	Sound Pressure	2.58 psi
Distance from the Water Surface to the Test Section	4 1/2 inches	Sound Frequency	20,000 cycles/sec

Run No.	Voltage Drop Across the Test Section	Voltage Drop Across the Portable Shunt x 10^{+3}	Bulk Temp. of Water °F	Temp. at the Heating Surface °F	Temperature Difference ΔT °F	Heat Transfer Rate $\frac{Btu}{hr, ft^2}$	Heat Transfer Coefficient $\frac{Btu}{hr, ft^2\ °F}$
1	1.66	4.75	198	247.6	49.6	12391	249.5
2	2.57	7.15	198	268.1	70.1	28876	411.7
3	3.45	9.38	198	285.2	87.2	50834	582.6
4	4.49	12.30	198	279.4	81.5	86788	1064.9
5	5.38	14.60	198	286.5	88.5	123437	1394.6
6	6.35	17.00	198	296.7	98.7	169641	1717.9
7	7.29	19.40	198	301.2	103.2	222248	2153.0
8	8.49	22.20	198	314.7	116.7	296190	2537.3

TABLE IX

EXPERIMENTAL DATA AND CALCULATED RESULTS FOR TEST NUMBER 9

Water Level in the Tank	6 1/2 inches	Room Temperature	82° F
Length of the Platinum Wire of Test Section	7 inches	Sound Pressure	3.69 psi
Distance from the Water Surface to the Test Section	4 3/8 inches	Sound Frequency	20,000 cycles/sec

Run No.	Voltage Drop Across the Test Section	Voltage Drop Across the Portable Shunt x 10^{+3}	Bulk Temp. of Water °F	Temp. at the Heating Surface °F	Temperature Difference ΔT °F	Heat Transfer Rate $\frac{Btu}{hr, ft^2}$	Heat Transfer Coefficient $\frac{Btu}{hr, ft^2\ °F}$
1	3.50	8.70	200	264.0	64.0	42519	663.9
2	4.01	9.90	200	269.0	69.0	55434	802.9
3	4.49	11.00	200	274.7	74.7	68967	922.9
4	5.01	12.10	200	285.4	85.4	84649	991.0
5	5.55	13.40	200	285.5	85.5	103848	1213.1
6	6.01	14.50	200	286.1	86.1	121687	1413.1
7	6.41	15.30	200	294.2	94.2	136946	1453.1
8	6.89	16.50	200	291.6	91.6	158747	1731.8
9	7.39	17.60	200	295.8	95.8	181618	1895.2

TABLE X

EXPERIMENTAL DATA AND CALCULATED RESULTS FOR TEST NUMBER 10

Water Level in the Tank	7 inches	Room Temperature	80° F
Length of the Platinum Wire of Test Section	6 1/4 inches	Sound Pressure	6.25 psi
Distance from the Water Surface to the Test Section	5 1/2 inches	Sound Frequency	20,000 cycles/sec

Run No.	Voltage Drop Across the Test Section	Voltage Drop Across the Portable Shunt x 10^{+3}	Bulk Temp. of Water °F	Temp. at the Heating Surface °F	Temperature Difference ΔT °F	Heat Transfer Rate $\frac{Btu}{hr, ft^2}$	Heat Transfer Coefficient $\frac{Btu}{hr, ft^2\ °F}$
1	2.59	7.15	200	270.3	70.3	28961	411.9
2	3.55	9.50	200	293.6	93.6	52743	562.9
3	4.55	12.20	200	292.0	92.0	86814	942.6
4	5.48	14.60	200	296.8	96.8	125127	1291.4
5	6.30	16.80	200	296.0	96.0	165527	1722.8
6	7.31	19.40	200	299.6	99.6	221788	2226.2
7	8.20	21.70	200	301.6	101.6	278287	2736.8

APPENDIX E

METHOD OF COMPUTATION

The heat transfer rates, $\frac{Q}{A}$, is calculated by the following equation:

$$\frac{Q}{A} = \frac{3.412\ E \cdot I}{\pi D_w L} \tag{E-1}$$

where E is the voltage drop across the platinum wire of the test section and I is the direct current through the platinum wire. This direct current, I, is calculated by the following equation:

$$I = 500\ E_s \tag{E-2}$$

where E_s is the voltage drop across the portable shunt.

The heat transfer coefficient, h, is calculated by the equation:

$$h = \frac{Q/A}{t_w - t_b} \tag{E-3}$$

where the surface temperature of the heating surface, t_w, is estimated by the equation which has been derived and is shown in the Appendix F. In experiments, only the average temperature of the heating surface in the across section was measured.

APPENDIX F

DERIVATION OF THE RELATION BETWEEN THE SURFACE TEMPERATURE OF THE PLATINUM WIRE AND THE CORRESPONDING AVERAGE TEMPERATURE IN THE CROSS SECTION

When the direct currents pass through the platinum wire of the test section which is submerged in the water, the temperature of the wire will not be uniform in the cross section. Therefore, it becomes necessary to derive a relation between the average temperature in the cross section and the corresponding surface temperature.

For this problem, the differential equation for heat conduction with heat sources is expressed as follows:

$$\frac{d^2T}{dr^2} + \frac{1}{r}\frac{dT}{dr} + \frac{q'''}{K} = 0 \qquad \text{(F-1)}$$

The boundary conditions are:

$$T = T_o \quad \text{at } r = r_o \qquad \text{(F-2)}$$

$$\frac{dT}{dr} = 0 \quad \text{at } r = 0 \qquad \text{(F-3)}$$

For simplicity, it is assumed that the heat source, q''', is independent of time and temperature and has a unit Btu/ft^3 hr. Let

$$\xi = \ln(r) \qquad \text{(F-4)}$$

then Equation (F-1) can be written as

$$\frac{d^2T}{d\xi^2} = \frac{-q'''}{K} e^{2\xi} \tag{F-5}$$

The general solution to Equation (F-5) can be shown as

$$T(\xi) = \frac{-q'''}{4K} e^{2\xi} + C_1\xi + C_2 \tag{F-6}$$

where C_1 and C_2 are the integration constants.

With Equation (F-4), Equation (F-6) can be written as

$$T(r) = \frac{-q'''}{4K} r^2 + C_1 \ln(r) + C_2 \tag{F-7}$$

The two integration constants, C_1 and C_2, are determined by the use of the boundary conditions shown as Equation (F-2) and Equation (F-3). Therefore, these constants are shown as

$$C_1 = 0 \tag{F-8}$$

$$C_2 = T_o + \frac{q''' r_o^2}{4K} \tag{F-9}$$

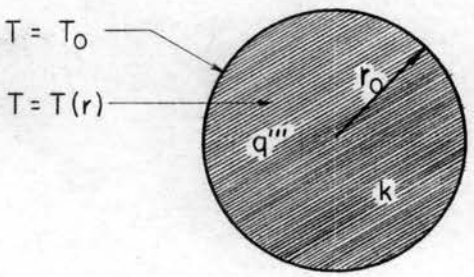

Thus, the temperature distribution in the cross section of the platinum wire can be shown as

$$T(r) = T_o + \frac{q'''}{4K} (r_o^2 - r^2) \qquad \text{(F-10)}$$

The average temperature in the cross section of the platinum wire is calculated by the following equation

$$\bar{T} = \frac{1}{r_o} \int_o^{r_o} T(r)\, dr \qquad \text{(F-11)}$$

That is

$$\bar{T} = \frac{1}{r_o} \int_o^{r_o} \left[T_o + \frac{q'''}{4K} (r_o^2 - r^2) \right] dr \qquad \text{(F-12)}$$

Therefore, the relation between the surface temperature of the platinum wire and the corresponding average temperature in the cross section is indicated as

$$T_o = \bar{T} - \frac{q''' r_o^2}{6K} \qquad \text{(F-13)}$$

where

$$q''' = \frac{3.412\ E \cdot I}{L \cdot \frac{\pi D_w^2}{4}} \qquad \text{(F-14)}$$

APPENDIX G

NOMENCLATURE

Symbols

a	Amplitude of Wave, ft
A	Area, ft^2
C	Constant
C_ℓ	Specific Heat of Liquid, Btu per lb ^oF
D_w	Diameter of Platinum Wire, ft
E	Voltage Drop Across the Test Section, Volt.
E_s	Voltage Drop Across the Portable Shunt, Volt.
f	Frequency of Vibration or Sound Frequency, cycles/sec.
f_f	Foamability
f_p	Pressure Factor
g	Acceleration of Gravity, ft per sec^2
g_c	Dimensional Constant, lbs mass ft per lb force hr^2
h	Heat Transfer Coefficient, Btu per hr ft^2 ^oF
I	Direct Currents, Amp
K	Thermal Conductivity of Liquid, Btu per hr ft ^oF
L	Length of the Platinum Wire of the Test Section, ft
n	Number of Nucleation Sites per Unit Area

P	Pressure, psi
ΔP	Pressure Difference Corresponding to the Superheat in Liquid, psi
P_o	Sound Pressure or Amplitude of Sound Pressure, psi
P_ℓ	Pressure in the Liquid, lbs per ft^2
P_v	Pressure in the Vapor, lbs per ft^2
P_a	Atmospheric Pressure, lbs per ft^2
P_{vm}	Pressure in the Vapor Bubble at $R = R_m$, lbs per ft^2
q	Heat Transfer Rate, Btu per hr ft^2
θ	Heat Flow, Btu per hr
q'''	Heat Source in the Platinum Wire, Btu per hr ft^3
r	Ratio of Specific Heat
r_o	Radius of the Platinum Wire, ft
R	Radius of a Vapor Bubble, ft
R_m	Mean Radius of a Vapor Bubble, ft
R_d	Radius of the Vapor Bubble Departing from the Heating Surface, ft
R_n	Resonant Radius of a Vapor Bubble, ft
t	Temperature, ^oF
t_s	Saturation Temperature, ^oF
t_v	Temperature of Vapor, ^oF
t_i	Initial Temperature in the Liquid, ^oF
t_w	Surface Temperature of the Heating Section, ^oF
t_o	Amplitude of Temperature Fluctuation in the Vapor Bubble in a Sound Field, ^oF

t_b	Bulk Temperature of the Liquid, ^oF
$\bar{T}$	Average Temperature in the Cross Section of the Heating Surface, ^oF
ΔT	Superheat, or $\Delta T = t_w - t_b$, ^oF
V	Volume of a Vapor Bubble, ft^3
V_m	Mean Volume of a Vapor Bubble, ft^3
v	Volume Pulsation, i.e., $v = V - V_m$, ft^3
x	Distance
α	Thermal Diffusivity of Liquid, ft^2 per hr
λ	Latent Heat, Btu per lbm
θ	Time, sec or hr
μ_ℓ	Dynamic Viscosity of the Liquid, lbs per ft hr
ν	Kinematic Viscosity, ft^2 per hr
ϵ	Eddy Thermal Diffusivity ft^2 per hr
ρ_ℓ	Density of Liquid, lbm per ft^3
ρ_v	Density of Vapor, lbm per ft^3
σ	Surface Tension of Liquid, lbs per ft
Φ	Contact Angles, Degree
ω	Angular Frequency, Radius per sec
ω_m	Natural Angular Frequency for a Vapor Bubble of Radius, R_m, radius per sec
ω_n	Natural Angular Frequency, Radius per sec
$\dot{v}$	i.e., $\frac{dv}{d\theta}$, ft^3 per sec
$\dot{R}_m$	$(\frac{dR}{d\theta})$ at $R = R_m$, ft per sec

$(\frac{dT}{dx})_{x=0}$	Temperature Gradient in the Liquid at the Vapor Bubble Surface, ^{o}F per ft
$(\frac{dR}{d\theta})$	Growth Rate of a Vapor Bubble, ft per sec
Pr	Prandtl Number
$f(P_o)$	A Function for the Pressure Fluctuation in Liquid
$g(P_o)$	A Function for the Temperature Fluctuation in Vapor

VITA

Kam Wu Li

Candidate for the Degree of

Doctor of Philosophy

Thesis: AN INVESTIGATION OF ACOUSTICAL EFFECTS ON THE LOW HEAT-FLUX REGION OF NUCLEATE POOL BOILING

Major Field: Mechanical Engineering

Biographical:

Personal Data: Born in Canton, China, February 16, 1934, the son of Mr. and Mrs. Yan-Chung Lee.

Education: Attended Chu Hai College (Hong Kong) and received the Bachelor of Science degree, with a major in Mechanical Engineering in June 1957; attended Colorado State University in September 1959, and received the Master of Mechanical Engineering degree in June 1961; completed the requirement for the Doctor of Philosophy degree in January 1965.

Professional Experience: Practiced in Hong Kong Power plant for three summers (1954, 1955 and 1956); teaching assistant in Chu Hai College from September 1957 to September 1958. Research Assistant in Mechanical Engineering at Oklahoma State University from September 1961 to January 1965.

Professional Organization: The writer is a member of the American Association for the Advancement of Science, and the following honorary organizations: Pi Tau Sigma and Kappa Mu Epsilon.